Identification and Characterization of a Membrane Binding, Amphipathic α-Helical Domain of CTP: Phosphocholine Cytidylyltransferase

by

Joanne E. Johnson

B.Sc. (Hon.) Simon Fraser University, 1990

Thesis submitted in partial fulfillment of the requirements

for the degree of Doctor of Philosophy

in the Department of Chemistry and

Institute of Molecular Biology and Biochemistry

SIMON FRASER UNIVERSITY

December 1995

APPROVAL

Name: Joanne E. Johnson

Degree: Ph.D.

Title of thesis: Identification and Characterization of a Membrane Binding, Amphipathic α-Helical Domain of CTP: Phosphocholine Cytidylyltransferase

Examining Committee:

Chair: Dr. D. Sen

Dr. R. B. Cornell (Associate Professor)
Senior Supervisor

Dr. R. J. Cushley (Professor)
Committee Member

Dr. R. H. Hill (Associate Professor)
Committee Member

Internal Examiner: Dr. T. J. Borgford
(Associate Professor)

External Examiner: Dr. R. O. Ryan
(Associate Professor
Biochemistry Department
University of Edmonton)

Date Approved: Dec 13/95

PARTIAL COPYRIGHT LICENSE

I hereby grant to Simon Fraser University the right to lend my thesis, project or extended essay (the title of which is shown below) to users of the Simon Fraser University Library, and to make partial or single copies only for such users or in response to a request from the library of any other university, or other educational institution, on its own behalf or for one of its users. I further agree that permission for multiple copying of this work for scholarly purposes may be granted by me or the Dean of Graduate Studies. It is understood that copying or publication of this work for financial gain shall not be allowed without my written permission.

Title of Thesis/Project/Extended Essay

Identification and Characterization of a Membrane Binding, Amphipathic α-Helical Domain of CTP: Phosphocholine Cytidylyltransferase

Author:

(signature)

Joanne Johnson

(name)

Dec 13/95

(date)

ABSTRACT

CTP:phosphocholine cytidylyltransferase (CT), which catalyses a key regulatory step in the biosynthesis of phosphatidylcholine in mammalian systems, is regulated by reversible binding to membranes. A region in the protein is predicted to form an amphipathic α-helix which has been proposed to be involved in the lipid interactions. Various approaches were taken to identify and characterize the membrane-binding domain of CT: (I) While the yeast and rat CT's share a large central region of homology, the yeast protein lacks the putative amphipathic helical domain. The activation of rat-liver CT and yeast CT by lipid vesicles was compared. Unlike rat-liver CT, the yeast CT was not affected by non-anionic lipids and its activation by anionic lipids occurred at an optimum lipid concentration about 10 fold lower than for the rat CT, above which the activity declined. Thus, we concluded that yeast CT is activated by a different mechanism than is rat CT. (II) We obtained four synthetic peptides corresponding to portions of the amphipathic α-helix of CT. All four peptides converted from random coil in dilute buffer to >60% α-helix in the presence of anionic membranes, as assessed by circular dichroism. In the presence of anionic lipid vesicles, a tryptophan on these peptides was relatively inaccessible to the aqueous quencher iodide, but was quenched effectively by the lipid phase quencher 9,10-dibromophosphatidylcholine. These results suggest a role in membrane binding for the region represented by these peptides, and suggest that binding is induced by stabilization of an α-helical conformation. (III) The hydrophobic photoreactive radiolabelled probe 3-(trifluoromethyl)-3-(*m*-[^{125}I]iodophenyl)diazirine ([^{125}I]TID) partitions into the membrane core, and upon irradiation, labels embedded regions of proteins. CT that was bound to phosphatidylcholine/oleic acid vesicles containing [^{125}I]TID became covalently labelled upon irradiation. Chymotrypsin digestion of [^{125}I]TID-labelled CT revealed that only fragments containing the amphipathic helix

contained significant label. A 62-residue synthetic peptide corresponding to the amphipathic helical domain of CT also becomes labelled by [^{125}I]TID in the presence of lipid vesicles. Thus, all results obtained indicate a membrane-binding mechanism for cytidylyltransferase involving the intercalation of the amphipathic α-helix region into the acyl chain core of the activating membrane.

Dedication

For my mother

Acknowledgements

I would like to thank my supervisor, Rosemary Cornell. Rose: what can I say! For six years of guidance through this research project, for your thorough proof-reading of this thesis, and most of all, for your tremendous enthusiasm for science. You have been a great inspiration, and I couldn't have had a better supervisor.

To my labmates, Dallas and Becky: thank you for your support, friendship, and for putting up with me over the past few months! Dallas, thanks for your great editing skills. Becky, thank you for helping me obtain a place to go when this is all done. I really appreciate everything!!

Many thanks to Gabe Kalmar, for his endless willingness to help with any question or problem that arose over the past six years.

Thanks to the many members of the Borgford lab, the Richards lab, the Cushley lab and the Kalmar lab for providing an environment where exchange of ideas (and reagents) was encouraged.

Thanks to my "off-the-hill" friends and family, for your encouragement and support, and for trying to understand exactly what I was doing up here. Special thanks to Melissa, for making me smile; to Jim and Enis, for the ham-soup; to my Dad, who never set limits (and who can now pronounce cytidylyltransferase!). Finally, thanks to Joe and Norm, for being my "home". After ten years up on the hill, you can kinda get your head in the clouds. Thanks for keeping me down on earth.

TABLE OF CONTENTS

LIST OF FIGURES

LIST OF TABLES

ABBREVIATIONS

APS	Ammonium persulfate
ATP	adenosine 5'-triphosphate
ADP	adenosine 5'-diphosphate
BHA2	Bromelain-released fragment of hemagglutinin
BSA	Bovine serum albumin
CD	Circular dichroism
CDP	Cytidine 5'-diphosphate
CHO	Chinese hamster ovary
CL	Cardiolipin
CTP	Cytidine 5'-triphosphate
CT	CTP:phosphocholine cytidylyltransferase
DAG	Diacylglycerol
DEAE	*O*-(diethylaminoethyl)-
DMEM	Dulbecco's modified Eagle medium
DOPG	Dioleoyl-phosphatidylglycerol
DPPC	Dipalmitoyl-phosphatidylcholine
DTT	Dithiothreitol
EDTA	Ethylenediaminetetraacetic acid
FCS	Fetal calf serum
HEPES	(N-[2-Hydroxyethyl)piperazine-N'-[2-ethanesulfonic acid])
HPLC	High performance liquid chromatography
lysoPC	Lysophosphatidylcholine
MG	Mono-acylglycerol
OA	Oleic acid

OH	Oleyl alcohol
PAGE	Polyacrylamide gel electrophoresis
PA	Phosphatidic acid
PBS	Phosphate-buffered saline
PC	Phosphatidylcholine
PE	Phosphatidylethanolamine
PG	Phosphatidylglycerol
PI	Phosphatidylinositol
PS	Phosphatidylserine
PPi	Pyrophosphate
6,7-dibromo PC	1-palmitoyl, 2-stearoyl-6,7-phosphatidylcholine
9,10-dibromo PC	1-palmitoyl, 2-stearoyl-9,10-phosphatidylcholine
11,12-dibromo PC	1-palmitoyl, 2-stearoyl-11,12-phosphatidylcholine
PMSF	Phenylmethylsulfonyl fluoride
PVDF	Poly(vinylidine difluoride)
SDS	Sodium dodecyl sulfate
Sph	Sphingosine
SOPC	1-stearoyl, 2-oleoyl-phosphatidylcholine
TD	buffer: 25 mM Tris, pH 7.5, 140 mM NaCl, 5 mM KCl, 0.5 mM Na_2HPO_4)
TEMED	N,N,N',N',-tetramethylenediamine
TFE	Trifluoroethanol
TID	3-(trifluoromethyl)-3-(*m*-[^{125}I]iodophenyl)diazirine
TLC	Thin layer chromatography
TPA	12-O-Tetradecanoyl-phorbol-13-acetate
Tris	Tris (hydroxymethyl) methylamine

TS	buffer: 25 mM Tris, pH 7.5, 140 mM NaCl, 5 mM KCl, 0.5 mM Na_2HPO_4, 1 mM $MgCl_2$, 1 mM $CaCl_2$
TUA	11-[4-[3-(trifluoromethyl)diazirinyl]phenyl]-[2^{3}H]-undecanoic acid
UV	Ultra violet
[Θ]	mean residue molar ellipticity

CHAPTER ONE: INTRODUCTION

1.1 Phosphatidylcholine in Mammalian systems

Phosphatidylcholine (PC) is the major phospholipid present in mammalian membranes, and is also a main component of serum lipoproteins and lung surfactant. In recent years, a key role for PC has been demonstrated in the formation of lipid second messengers in the signalling pathway of many growth factors and hormones. Due to its obvious importance, the regulation of cellular PC metabolism has been of much interest.

PC is the major phospholipid of biological membranes

Biological membranes are a collection of proteins embedded in a bilayer structure composed of many types of lipid. Phospholipids play an important role in forming the basic bilayer structure. In most cases, PC is the predominant phospholipid. For example, in the red blood cell, 40 to 60 % of the phospholipids in each subcellular membrane are composed of PC. (Gennis, 1989). The presence of PC appears to be critical, as there are no known diseases relating to a defect in cellular PC levels or metabolism. Interestingly, PC is absent in most prokaryotic organisms.

PC is the phospholipid component of serum lipoproteins

Lipids such as cholesterol which are water insoluble are transported through blood in a lipoprotein complex. In the complex, a neutral lipid core of triglycerides and cholesterol-ester is solubilized by an outer monolayer of phospholipids and protein. PC is the main (~70%) phospholipid component

forming the outer monolayer. Minor components include sphingomyelin (10-15%), lysoPC (2-5%), phosphatidylethanolamine (PE; ~3%) and anionic phospholipids (~5%) (Kostner, 1981). Liver cells are the major site for assembly of lipoprotein particles, and thus are responsible for PC synthesis above that needed for subcellular membranes. Blood levels of certain types of cholesterol-containing lipoproteins have been correlated with the risk of athlerosclerosis (Brown & Goldstein, 1983).

PC is the phospholipid component of lung surfactant

Surfactant is a protein/lipid mixture secreted by lung cells which reduces surface tension at the air : liquid interface by spreading in a phospholipid monolayer on the cell surface. The major component is PC (~70%), of which about half is the saturated species dipalmitoyl-PC. Phosphatidylglycerol (PG) is the major anionic lipid component (~10%), while phosphatidylethanolamine (PE), phosphatidylinositol (PI), sphingomyelin and cholesterol are present in small amounts. The protein component accounts for only about 10% of the mass (Yu *et al.*, 1983; Possmayer, 1989). Surfactant production begins in the lung of the fetus just before birth. Its presence is crucial to newborns to prevent respiratory distress syndrome, a common condition in premature births (Fulmer & Crystal, 1976).

PC is involved in signal transduction

PC breakdown is important in the generation of lipid second messengers, which function in the transduction of intracellular signals for cell growth and regulation in response to extracellular stimuli (Exton, 1990; 1994). In the past decade, diacylglycerol formed by the breakdown of phospholipids has been

recognized as an important second messenger. It has been found to activate a key cell regulatory protein, protein kinase C. Initial studies demonstrated the importance of phosphatidylinositol-4,5,-bisphosphate hydrolysis in producing diacylglycerol upon cell stimulation. It is now apparent that a major source for diacylglycerol involved in signal transduction is PC (Exton, 1990; 1994). Thus, upon stimulation by certain growth factors, cellular PC is broken down by activated phospholipases. As diacylglycerol is a direct substrate, PC biosynthesis may be a mechanism to attenuate the diacylglycerol signal (Pelech and Vance, 1989).

PC hydrolysis can also produce arachidonic acid, the immediate precursor for the biosynthesis of the intercellular signalling molecules, prostaglandins. Arachidonic acid is a fatty acid that is esterified to the *sn*-2 carbon of the glycerol backbone of PC, and can be released by hydrolysis with an activated phospholipase A_2.

1.2 PC metabolism in mammalian systems

1.2.1 PC synthesis via the CDP-choline pathway

While there are a number of possible pathways for the synthesis of PC in animal cells, the key pathway is via CDP-choline, elucidated by Kennedy (reviewed 1989). This pathway is utilized exclusively for *de novo* PC synthesis in all tissues examined, with the exception of liver cells in which the methylation pathway also functions (Section 1.2.2). A mutation in the CDP-choline pathway in chinese hamster ovary (CHO) cells caused growth arrest and a large decrease in the cellular PC levels at the non-permissive temperature, demonstrating this

route as the primary PC source (Esko and Raetz, 1980).

The substrates and enzymes of this biosynthetic pathway are outlined in Figure 1.1. In the first step of the pathway, choline taken up by the cell is quickly phosphorylated with ATP by the enzyme *choline kinase* to form phosphocholine. *CTP:phosphocholine cytidylyltransferase* then catalyzes the transfer of a cytidyl-group to phosphocholine to produce CDP-choline and pyrophosphate. The activated choline is then transferred from CDP-choline to diacylglycerol by *cholinephosphotransferase* to form the end product, PC. An interesting feature of this pathway is the involvement of both soluble (choline, phosphocholine, CDP-choline) and membrane-associated (diacylglycerol) substrates in the synthesis of the membrane phospholipid. As a result, the enzymes in the pathway are also both soluble (choline kinase) and membrane-embedded (cholinephosphotransferase). The medial step in the pathway is carried out by cytidylyltransferase, which can be found at both sites in the cell.

1.2.2 Other pathways for PC synthesis

A second major route for the synthesis of PC involves methylation of the head group of PE. PE-N-methyltransferase catalyzes three successive transfers of a methyl group from the donor, S-adenosylmethionine, to PE and the intermediates monomethyl- and dimethyl-PE to form PC (Fig. 1.1). This biosynthetic route is active only in liver, where it accounts for only 20 to 40 % of PC synthesis (Ridgeway, 1989).

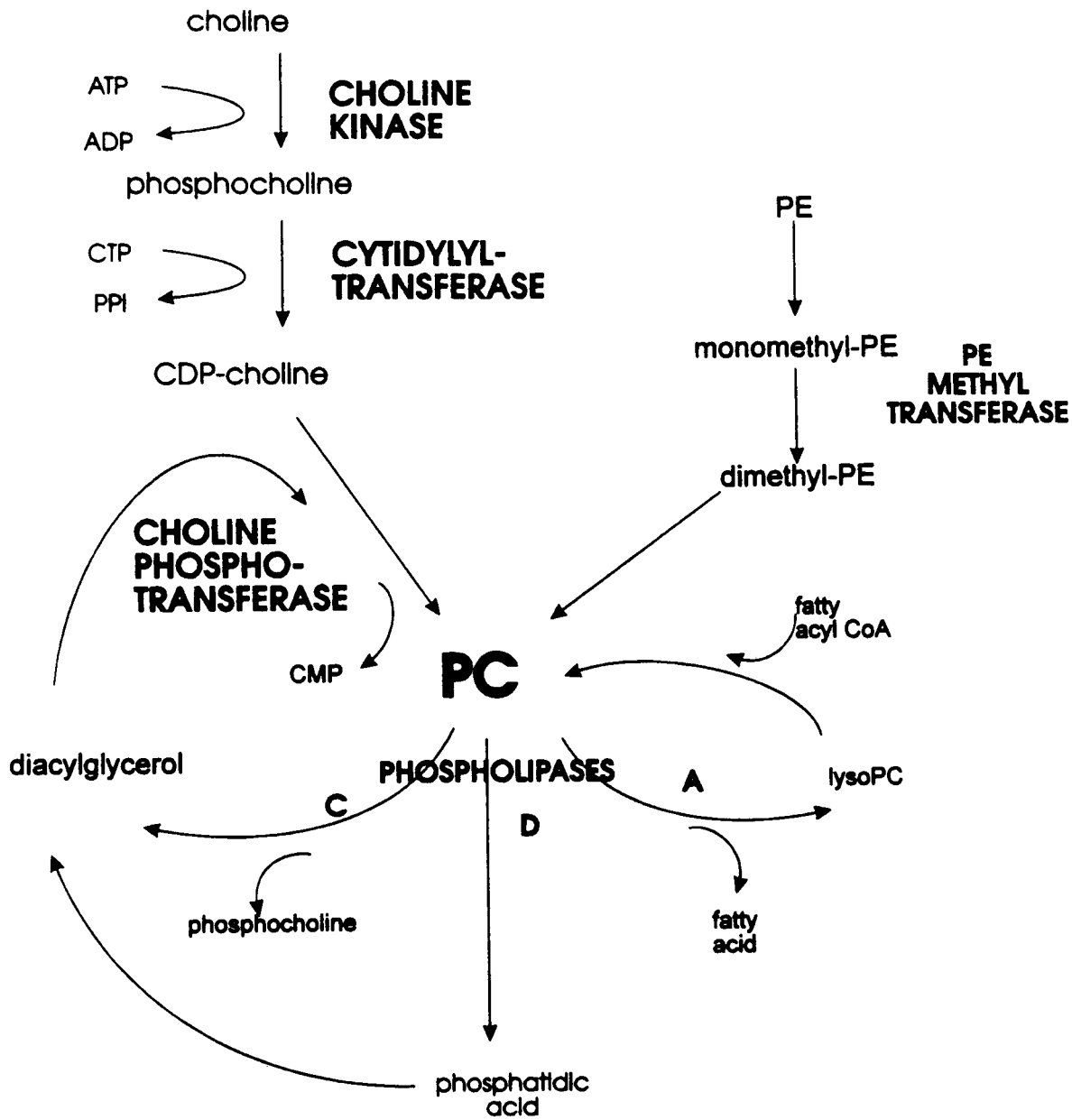

Figure 1.1: PC metabolic pathway.

Lysophosphatidylcholine (lysoPC) is a breakdown product of PC which can be converted to PC upon addition of a fatty acyl chain (fatty acyl-CoA) by an acyltransferase. This acylation reaction is part of a deacylation/reacylation cycle that functions to control the fatty acid composition of PC (Choy & Arthur; 1989). Cells lacking a functional CDP-choline pathway (Esko *et al.*, 1982) or starved for choline (Tercé *et al.*, 1994) are able to survive in the presence of lysoPC.

1.2.3 PC catabolism

PC is broken down in the cell by a group of enzymes known as phospholipases (Roberts & Dennis, 1989). Numerous sites on the PC molecule are subject to hydrolysis, and phospholipases are grouped according to the site hydrolysed and products formed (Fig. 1.1). Phospholipase A hydrolyses the fatty acyl bond, producing free fatty acid and lysoPC, which can be further degraded by a lysophospholipase A to a free fatty acid and glycerol phosphocholine. Phospholipase A1 and A2 hydrolyze the acyl chain at the *sn*-1 and *sn*-2 positions respectively of the phospholipid. Phospholipase C hydrolyses the glycerophosphate bond of PC, releasing diacylglycerol and phosphocholine. Phospholipase D hydrolyses the choline phosphate bond, releasing choline and phosphatidic acid. In unstimulated cells, the phospholipase A pathway appears to be the dominant basal catabolic route for PC (Morash *et al.*, 1988). All three phospholipases can be signal activated (Liscovitch, 1992; Exton, 1994).

1.2.4 Regulation of PC levels

The importance of PC in cells dictates a need for its levels to be well regulated. PC synthesis is required for progression of cells through the cell cycle (Tercé *et al.*, 1994). As cells grow, there is a requirement for increased membrane mass, and thus an increased supply of the main phospholipid. As PC is broken down by phospholipases, due to basal turnover or for production of lipid second messengers, there must be a mechanism whereby the pool of lipid is replaced. In some cell lines PC biosynthesis is necessary for functions other than membrane biogenesis, such as surfactant production by lung starting immediately before birth, and lipoprotein secretion by liver.

Coordinated regulation of PC metabolism has been demonstrated. Treatment of cells with an exogenous PC-specific phospholipase C greatly stimulated the biosynthesis of PC, demonstrating the presence of a regulatory mechanism for the cellular membrane composition (Kent 1979; Sleight & Kent, 1983a). The breakdown of PC by signal-activated phospholipases was coordinated to an increase in PC biosynthesis (Tronchère *et al.*, 1995). Conversely, artificial stimulation of the PC biosynthetic pathway by overexpression of a key enzyme resulted in a concurrent increase in PC breakdown, such that the overall cellular PC level was not greatly affected (Walkey *et al.*, 1994). Elucidation of the regulatory step in the PC biosynthetic pathway is central to understanding the control of cellular PC levels.

1.2.4.1 CTP:phosphocholine cytidylyltransferase is the key regulatory enzyme of the CDP-choline pathway

Over many years of study it has become apparent that the key regulatory step for PC biosynthesis is that catalyzed by CTP:phosphocholine cytidylyltransferase (CT). Choline supplementation of rat hepatocytes resulted in only a slight increase in PC synthesis, but a great accumulation of cellular phosphocholine, the substrate for CT (Sundler & Akesson, 1975). Radiolabelled choline taken up by HeLa cells rapidly accumulated in the form of phosphocholine (Vance *et al.*, 1980). As the radiolabel disappeared from this substrate, it was rapidly converted to PC with no accumulation of CDP-choline. In the same study, addition of poliovirus stimulated PC biosynthesis at the CT step by increasing turnover of phosphocholine to PC. CT was thus suggested as the rate-controlling reaction of PC synthesis (Vance & Choy, 1979). Similar analyses of choline metabolites in myoblasts (Cornell & Goldfine, 1983) and lung type II cells (Post, *et al.*, 1982) corroborate these results. Since this initial hypothesis, there has been abundant evidence that the modulation of CT activity correlates with changes in PC synthesis, stimulated by phospholipase C (Sleight & Kent, 1980; 1983 a & b; Wright *et al.*, 1985; Watkins & Kent, 1991; Slack *et al.*, 1991), fatty acids (Pelech *et al.*, 1983; Pelech *et al.*, 1984; Whitlon *et al.*, 1985; Aeberhard *et al*, 1986; Tronchere *et al.*, 1991; Wang *et al.*, 1993a) or other mechanisms (Paddon & Vance, 1980; Esko & Raetz, 1980; Weinhold *et al.*, 1981; Pelech *et al.*, 1981; Pritchard *et al.*, 1982; Lim *et al.*, 1983; Sleight & Kent, 1983c; Pelech *et al.*, 1984 ; Jamil *et al*, 1990; Hatch *et al.*, 1991; Utal *et al.*, 1991; Weinhold *et al.*, 1994; Walkey, *et al.*, 1994).

1.2.4.2 Regulation by other enzymes of the CDP-choline pathway

The reaction catalyzed by choline kinase commits cellular choline to the CDP-choline pathway, directing it away from alternate metabolism to betaine. Hence, this enzyme was a candidate for regulation. Choline destined for PC synthesis is rapidly converted to phosphocholine by choline kinase under most conditions. However, there are systems where changes in the PC synthesis rate correlated with changes in cellular choline kinase activity (Teegarden *et al.*, 1991; Kent, 1989). Gene induction and phosphorylation have been proposed to regulate choline kinase activity (Ishidate, 1989).

Cholinephosphotransferase appears to be regulated only by substrate availability, and has been proposed to serve as the rate-limiting step for PC synthesis only in such circumstances where the diacylglycerol supply is limiting (Lim *et al.*, 1986; Cornell, 1989a; Jamil *et al.*, 1992; Walkey *et al.*, 1994).

1.3 CTP:phosphocholine cytidylyltransferase

It has become clear that a major mechanism for activation of CT is its reversible association with membranes (Vance & Pelech, 1984). Purification of the rat-liver enzyme in 1986 and the subsequent cloning, in 1987, of a yeast CT gene and in 1990 of a rat CT cDNA have lead to the production of tools such as CT-directed antibodies, expression systems and the study of mutants. With these new technologies in hand, recent studies have shown phosphorylation and lipid-association to be involved in a complex regulation of CT. It is apparent that the key signals for CT activation are the properties and lipid composition of the target membrane. An understanding of the mechanism of membrane binding

and identification of the membrane binding domain of the protein are therefore central to the understanding of the regulation of the enzyme and PC metabolism.

1.3.1 The key regulatory event for CT is its association with cellular membranes

1.3.1.1 Initial Investigations of Lipid activation:

Initial characterization of CT in rat-liver homogenates revealed that storage of the enzyme, or incubation at 37 °C for a few hours, resulted in an increase in the enzymatic activity (Schneider, 1963). Extraction of the lipids from the solution with acetone/butanol abolished CT activity, which was returned by re-addition of the isolated lipid (Fiscus & Schneider, 1966). In the same study, analysis of the extracted lipid components revealed elevated levels of lysophospholipids, formed along with fatty acids from the breakdown of phospholipids. The necessity for an incubation period in order to produce activating lipids suggested that breakdown products, not the steady-state lipids themselves, were involved in this stimulation. Thus, a positive feedback mechanism for the stimulation of PC synthesis by its breakdown products was proposed (Fiscus & Schneider, 1966). A further study of rat-liver cytosolic CT suggested that the presence of lysoPE and fatty acids, produced from hydrolysis of PE by an endogenous phospholipase A upon incubation, could be responsible for CT activation (Choy & Vance, 1978).

Lipid stimulation of CT activity was also observed in lung extracts. CT in the soluble fraction of fetal rat lung was stimulated 10-fold by addition of a chloroform/methanol extract containing total lung lipids (Stern *et al.*, 1976).

Further investigation revealed that CT was activated ~6-fold by addition of pure anionic phospholipids PI, and PG, but was not affected by PC or PE, and only slightly affected at high concentrations by lysoPC (Stern *et al.*, 1976). The CT activity lost from rat lung extracts upon isopropyl ether extraction was restored by readdition of fatty acids (Feldman *et al.*, 1981).

Addition of lipids to soluble extracts of CT from rat-liver or lung not only activated the enzyme, but induced the formation of large CT-lipid aggregates, suggesting that CT was binding to a lipidic structure (Stern *et al.*, 1976; Choy *et al.*, 1979). Lipid induced aggregation of rat-liver cytosolic CT was stimulated *in vitro* by PC, and phospholipase C treatment (forming diacylglycerol from phospholipids), but not by cholesterol or lysophospholipids (Choy *et al.*, 1979). Fatty acids were effective at inducing aggregation of cytosolic CT from rat liver (Pelech *et al.*, 1983). Aggregation, and accompanying activation of CT from rat lung was induced by the anionic phospholipids PG, PI and cardiolipin, but not by PC alone, or lysoPC (Feldman *et al.*, 1978). Thus, selective activation of the enzymatic activity was accompanied by association of CT with lipids.

1.3.1.2 The Translocation Model

Early studies noted a bimodal distribution of CT in rat liver or lung homogenates, with a large percentage in the soluble and the remainder associated with membrane fractions (Schneider, 1963; Weinhold *et al.*, 1973). The subcellular distribution of CT in lung tissue varied with the developmental state: adult lung, with a higher CT activity, had a greater percent of microsomal CT than fetal lung (34% vs. 7%) (Stern *et al.*, 1976). A correlation between the activity and membrane association of CT in these systems was not perceived at

the time.

A model for CT regulation involving interconversion between membrane-bound and soluble forms was first proposed based on studies of PC biosynthesis in phospholipase C-treated myoblast cells (Sleight & Kent, 1980). In this model system, PC was hydrolyzed by addition of exogenous phospholipase C, stimulating the cells to increase PC synthesis in order to maintain membrane integrity (Kent, 1979). PC synthesis, monitored by incorporation of [^{3}H]choline, was stimulated at the step of CDP-choline formation. Total cellular CT activity measured *in vitro* was increased. A larger portion of the CT was associated with the membrane fraction in phospholipase C-treated cells (70%) than in control cells (30%). Membrane CT was fully active in the absence of added lipids, while soluble CT was inactive unless supplemented by lipids. Thus, a model was proposed in which soluble CT forms an inactive cellular reservoir, which can be recruited to the cellular membrane and activated when there is a requirement for increased PC biosynthesis.

Translocation of CT to membranes, resulting in an activation of the enzyme and increased PC biosynthesis, has been demonstrated in many cell types (*e.g.* CHO cells, HeLa cells, rat lung, rat hepatocytes), and has been promoted by such stimuli as addition of exogenous phospholipase C, (Section 1.3.1.4), fatty acids (Section 1.3.1.3), diacylglycerol (Section 1.3.1.4) and phorbol ester (Section 1.3.1.4). As well, physiologically relevant circumstances have been responsible for a change in the distribution of CT. In hepatocytes, inhibition of the methylation pathway for PC synthesis resulted in increased use of the CDP-choline pathway, and translocation of CT to the membrane (Pritchard *et al.*, 1982). Liver from rats fed a high cholesterol and cholate diet had an increased PC synthesis rate, increased cellular CT activity and a higher distribution of CT

on the membrane (Lim *et al.*, 1983). Shortly after birth, a stage of lung development at which PC synthesis is elevated, CT membrane activity is increased (Weinhold *et al.*, 1984). In hepatocytes starved for choline, thus unable to use the CDP-choline pathway, CT was located in the membrane fraction. Upon readdition of choline, PC synthesis was reinstated whereupon CT moved back to the soluble fraction (Yao *et al.*, 1990; Jamil *et al.*, 1990; Weinhold *et al.*, 1994). In all cases studied, with the exception of choline starvation in which there is a lack of substrate, CT translocation to membranes correlated with increased enzymatic activity and an increased rate of PC synthesis. In these studies, CT translocation was assessed by separation of soluble and particulate cell fractions after treatment of intact cells with the various agents. Two methods for separation have been employed: 1) centrifugation of cell homogenates, or 2) digitonin permeabilization. The distribution of enzyme has been assessed by monitoring activity in these fractions, or more recently, by CT mass determination by immunoblotting approaches (Utal *et al.*, 1991; Watkins & Kent, 1991; 1992; Wang *et al.*, 1993a). Moreover, changes in CT intracellular distribution have been directly visualized in fixed cells via immunolocalization using fluorescent-tagged anti-CT antibodies (Watkins & Kent, 1992; Wang *et al*, 1993a).

An *in vitro* translocation assay was developed which enabled easier analysis of the translocation phenomenon. Isolated cell extracts were incubated with various effectors *in vitro,* then separated into soluble and particulate fractions by ultracentrifugation in order to localize the CT activity (Pelech *et al.*, 1984b, Weinhold *et al.*, 1984). Translocation promotion by various lipid species was examined and compared directly, without interference by differential cellular uptake or potential secondary effects, in order to better understand the binding mechanism (Cornell & Vance 1987a). In this study, a variety of compounds with

differing head group and acyl chain length functioned as translocation activators. Membrane binding was inhibited by detergents but not high ionic strength suggesting an important role for hydrophobic interactions (Section 1.3.2.3).

Translocation of CT to membranes is reversible *in vivo*. CT returned from the membrane to the soluble fraction upon removal from cell culture media of the translocation stimulators oleic acid (Pelech *et al.*, 1984b; Houweling *et al*, 1994), phorbol ester (Pelech *et al*, 1984a), choline deficiency conditions (Yao *et al*, 1990; Jamil *et al.*, 1993), or phospholipase C (Sleight & Kent, 1983b; Wright *et al.*, 1985; Houweling *et al.*, 1994). *In vitro* translocation of CT is also readily reversible upon removal of oleic acid with bovine serum albumin (BSA) (Weinhold *et al.*, 1984; Cornell & Vance 1987a).

What are the cellular signal(s) that cause CT to translocate? There are many examples of translocation stimulators added exogenously to cells (see above). Although a phosphorylation mechanism was suggested to mediate these effects, it is apparent that a lipid signal is the main element responsible for CT translocation (Section 1.3.1.5). Two key potential activators of CT activity are free fatty acid levels (Section 1.3.1.3) and membrane diacylglycerol (Section 1.3.1.4). Both of these activators are formed from the breakdown products of PC, suggesting a positive feedback mechanism to maintain PC levels.

1.3.1.3 Fatty acids induce translocation

Translocation of CT can be promoted by addition of exogenous fatty acids. Fatty acids were the predominant species extracted from lung cytosol that, upon readdition, activated lipid-free cytosolic CT (Feldman *et al.*, 1981).

Treatment of cells with fatty acids stimulated PC synthesis and promoted CT translocation to membranes (Pelech *et al.*, 1983; 1984b; Whitlon *et al*, 1985; Aeberhard *et al.*, 1986; Cornell & Vance, 1987a; Wang *et al.*, 1993a; Houweling *et al.*, 1994). Translocation of CT *in vitro* correlated with the free fatty acid content of the membrane fraction (Weinhold *et al.*, 1984). While a selectivity for unsaturated over saturated fatty acids has been reported (Feldman *et al.*, 1981; Weinhold *et al.*, 1984; Pelech *et al.*, 1984b), *in vitro* studies demonstrated that both classes of fatty acid were effective translocation promoters (Cornell & Vance, 1987a). Differential solubility or effects of Ca^{+2} in the cell media, may be the source of apparent selectivity for unsaturated over saturated fatty acids in the cell culture systems.

A role for fatty acid stimulation has been postulated in a physiological situation (Weinhold *et al.*, 1984). Shortly after birth, PC synthesis increases in order to produce surfactant. The level of membrane-bound CT in rat lungs increased shortly after birth, with a coincident increase in free fatty acid levels. Thus, fatty acid levels may play an important role in regulation of CT in lungs of newborns.

Fatty acids are a good candidate for the regulation of PC synthesis. They are direct breakdown products of PC, resulting from hydrolysis by phospholipase A. Thus, their production can lead to a positive feedback mechanism for the resynthesis of PC.

1.3.1.4 Diacylglycerol induces translocation

Activation of CT by diacylglycerol was initially proposed due to the promotion of a CT-lipid aggregate by a phospholipase C treated extract

containing elevated diacylglycerol (Choy *et al.*, 1979). However, in the same study, exogenous diacylglycerol alone did not promote CT-lipid aggregation. Likewise, treatment of whole cells with phospholipase C increased the diacylglycerol content (Sleight & Kent, 1980), but the observation that a diacylglycerol suspension did not activate cytosolic CT prompted the conclusion that a transient decrease in PC levels triggered CT translocation in this system. Similar results were obtained with an *in vitro* translocation assay (Cornell & Vance; 1987a). Phospholipase C-treated membranes containing elevated diacylglycerol levels promoted CT binding *in vitro* while a suspension of diacylglycerol was ineffective. However, these authors noted that diacylglycerol alone does not form a stable membrane bilayer so addition of diacylglycerol in a suspension may not present an appropriate surface to activate CT. Diacylglycerol incorporated into sonicated PC vesicles was, in fact, capable of binding CT *in vitro* (Cornell & Vance, 1987b).

Diacylglycerol promoted CT translocation *in vivo*, independently of phospholipase C-treatment. Diacylglycerol containing short (8 carbon) fatty acyl chains, which is able to effectively enter the cell and become incorporated into subcellular membranes, promoted CT translocation in pituitary cells (Kolesnick & Hemer, 1990; Slack *et al.*, 1991). When added to neuroblastoma cells together with phospholipase C, this short-chain diacylglycerol caused no further increase in CT activity while oleic acid (Section 1.3.1.3) elevated CT activity. This implied a common mechanism of action for the phospholipase C and diacylglycerol, a mechanism not shared with oleic acid (Slack *et al.*, 1991).

Diacylglycerol levels are altered by phorbol esters, which affect CT translocation. 12-O-Tetradecanoyl-phorbol-13-acetate (TPA) is a potent tumor-promoting agent, producing many cell responses including a stimulation of PC

synthesis (Paddon & Vance, 1980) with a corresponding activation and translocation of CT (Pelech *et al*, 1984a). However, TPA had no direct effect on CT membrane binding *in vitro* (Cornell & Vance, 1987a; Kolesnick & Hemer, 1990). Protein kinase C is activated by tumor-promoting phorbol esters such as TPA, suggesting a phosphorylation regulatory mechanism (see Section 1.3.1.5). However, no change in the *in vivo* phosphorylation level of CT was observed after treatment of HeLa cells with TPA (Watkins *et al.*, 1990). Treatment of pituitary cells with short-chain diacylglycerol produced a similar effect as TPA (Kolesnick & Hemer, 1990). TPA treatment of HeLa cells caused an elevation in cellular diacylglycerol levels which correlated to CT activation and translocation (Utal *et al.*, 1991). These results demonstrate that the key trigger for TPA-induced membrane binding was mediated by the lipid signal, diacylglycerol.

Diacylglycerol is an ideal candidate for a physiological regulator of CT activity and PC synthesis. Diacylglycerol is a direct breakdown product of PC, via phospholipase C or the combined action of phospholipase D and phosphatidic acid phosphohydrolase, and could stimulate PC resynthesis via a positive feedback mechanism. Diacylglycerol is also a direct substrate for the resynthesis of PC, reacting with the CDP-choline formed by CT. Thus, elevated diacylglycerol levels would activate CT, leading to increased supply of CDP-choline. This process would enlarge both substrate pools for PC synthesis by choline phosphotransferase.

1.3.1.5 Role of phosphorylation in translocation

Covalent modification by phosphorylation is a regulatory mechanism for many cellular proteins. Protein kinases, which catalyze this reaction, are a group

of diverse and highly regulated enzymes that respond to various cellular signals by phosphorylating their specific target proteins. These proteins are dephosphorylated by separate enzymes, the protein phosphatases.

A phosphorylation/ dephosphorylation mode of regulation for CT was proposed on the basis of PC synthesis and CT activity modulation by protein kinase and phosphatase activators and inhibitors (Niles & Makarski, 1979; Pelech *et al.*, 1981; Pelech *et al.*, 1982). Protein phosphatase inhibitors NaF and okadaic acid decrease cellular CT activity and membrane binding (Hatch *et al.*, 1990; 1991). This suggested that phosphorylated CT, which would accumulate in the absence of active phosphatases, is more stable in its inactive, soluble form. Radiolabelled CT was isolated from cells grown in a [^{32}P]phosphate-containing media, directly demonstrating *in vivo* phosphorylation (Watkins & Kent, 1990). Okadaic acid treatment caused an increase in the ^{32}P-content of soluble CT, and a decrease in membrane-bound enzyme (Hatch *et al.*, 1992). Phosphorylation levels *in vivo* were affected by treatment with phospholipase C (Watkins & Kent, 1991), oleic acid (Wang *et al.*, 1993a; Houweling *et al.*, 1994) or choline deprivation (Weinhold *et al.*, 1994). CT phosphorylation levels varied with the cell cycle in concert with activity of the enzyme, resulting in cyclic changes in the PC biosynthetic rate (Jackowski, 1994). In these cases, soluble, highly-phosphorylated CT was induced to translocate to the membrane, where it was dephosphorylated. Thus, dephosphorylation was proposed to be an important event in the membrane binding of CT.

Dephosphorylation is not an essential trigger for membrane binding. In choline-deprived Hep G2 cells, dephosphorylation of CT preceded membrane translocation (Weinhold *et al.*, 1994). However, dephosphorylation occurred subsequent to translocation induced by oleic acid in rat hepatocytes, suggesting

dephosphorylation is not a prerequisite for membrane binding (Houweling *et al.*, 1994). Purified CT (Section 1.3.2.5), which is highly phosphorylated (MacDonald & Kent, 1994), was activated and bound to membranes in the absence of kinases and phosphatases (Weinhold *et al.*, 1986; Feldman & Weinhold, 1987; Cornell 1991a & b), also implying that a dephosphorylation event is not essential for membrane binding. The phosphorylated sites on CT were mapped to 16 C-terminal serine residues (MacDonald & Kent, 1994). Deletion mutants or Ser-to-Ala mutants lacking all phosphorylation sites had lipid-interacting characteristics similar to wild-type CT (Cornell *et al.*, 1995; Wang & Kent, 1995a & b; Yang & Jackowski, 1995). Although the dephosphorylation event that occurs upon membrane binding *in vivo* is not the key trigger for membrane binding or activation of CT, it may function to destabilize the soluble form of the enzyme and thus enhance the lipid signalling.

The identity of the kinase(s) that regulate CT *in vivo* are not definitely known. Neither TPA stimulation of protein kinase C (Section 1.3.1.4), nor cAMP stimulation of protein kinase A (Jamil *et al.*, 1992) in cultured cells alter the phosphorylation state of CT. The sequence of CT (Kalmar *et al.*, 1990) contains consensus sites for casein kinase II and cdc2 kinase, which phosphorylate CT *in vitro* (Cornell *et al.*, 1995).

1.3.1.6 Subcellular site of translocation

Phospholipid synthesis is thought to occur on the endoplasmic reticulum membrane system (Vance *et al.*, 1977). Cholinephosphotransferase, the last enzyme in the main PC biosynthetic pathway, is an integral membrane protein localized predominantly in the endoplasmic reticulum, with possible traces in the

Golgi system (Cornell, 1989a; Vance & Vance, 1988). Upon fractionation of rat-liver or phospholipase C-treated Krebs II cells, membrane-bound CT colocalized with markers from the endoplasmic reticulum (Vance & Vance, 1988; Tercé *et al.*, 1988), with smaller amounts found in the Golgi system (Vance & Vance, 1988), consistent with the idea of PC synthesis occurring mainly in the endoplasmic reticulum. However, CT in phospholipase C-treated CHO cells did not consistently colocalize with either of these organelles under multiple cell fractionation conditions, but did colocalize with the nucleus (Morand & Kent, 1989). Development of CT-specific antibodies allowed the direct microscopic detection of the protein in fixed cells using a fluorescent-labelled antibody, a technique called immunolocalization. Membrane-bound CT in CHO cells that had been choline-starved or treated with phospholipase C, or HeLa cells treated with oleic acid, was immunolocalized to the nuclear envelope (Watkins & Kent, 1992; Wang *et al.*, 1993a). Immunolocalization in unstimulated cells localized soluble CT to the nucleus in CHO cells, HepG2 cells, murine fibroblast cell lines (NIH-3T3 and L-cells) and in rat liver slices (Wang *et al.*, 1993b). Expression of a rat-liver CT cDNA with a deletion of a N-terminal nuclear localization signal in a CT-defective CHO cell line resulted in localization to both the cytosol and nucleus, but had no effect on enzymatic activity or cellular PC biosynthesis (Wang *et al.*, 1995). The physiological significance of CT localization to the nucleus is not apparent.

1.3.1.7 Translocation as a common mechanism for protein regulation

CT is not the only enzyme to be regulated by a change in its subcellular distribution. The terms ambiquitous (Wilson, 1978) and amphitropic (Burn, 1988)

have been coined to describe a group of soluble enzymes that reversibly associate with membranes under the appropriate conditions. This regulatory mechanism has the advantage that the protein can change its distribution quickly and reversibly. Membrane association ultimately changes the activity of the protein, either by promoting a conformational change or by bringing the protein in close contact with its substrates or another regulatory protein. As these proteins often respond to levels of lipid activators, fluctuations in the membrane composition can play a key role in regulation.

Protein kinase C, which plays an important regulatory role in cell growth and differentiation, is a prominent example of a protein regulated by translocation to activating membranes. The soluble protein is activated by binding with great specificity to membranes containing phosphatidylserine and diacylglycerol (Newton, 1993). Binding promotes a conformational change which activates the protein (Orr *et al.*, 1992). Thus, an increase in diacylglycerol levels resulting from cell stimulation promotes the translocation of protein kinase C to membranes, where it is active and able to phosphorylate its many substrates.

Phospholipases and other lipases are generally soluble enzymes that are activated upon binding to membranes, where their substrates reside. As substrate concentration is varied, activity is greatly enhanced at the substrate concentrations where micelle or membrane formation occurs. This interfacial activation may be due to a high local concentration or specific orientation of the substrate occurring on the membrane, or may be the result of a conformational change occurring in the protein upon membrane binding. Binding and activity of phospholipases are greatly sensitive to properties of the lipid bilayer (Menashe, *et al.*, 1986; Rebecchi, *et al*, 1992; Rao, *et al.*, 1993).

Stimuli other than membrane composition causes some proteins to

translocate. Pyruvate oxidase binds and is activated by membranes in the presence of its substrate, pyruvate, and its cofactor, thiamine pyrophosphate (Grabau *et al.*, 1989). The affinity of synapsin I for synaptic vesicles appears to be regulated by phosphorylation (Scheiber *et al.*, 1986). Some proteins are localized to membranes via lipid modification. G proteins, Ras protein, and non-receptor tyrosine kinases, all of which are involved in signal transduction, are covalently linked to a myristoyl, prenyl or palmitoyl group which is thought to provide a membrane anchor. Palmitoylation is a reversible process, and enzymatic removal of the acyl chain can signal the protein to translocate to the cell cytosol, resulting in attenuation of signal transmission (Casey, 1995; Wedegaertner, *et al.*, 1995).

1.3.2 Mechanistic studies of the Membrane activation of CT

1.3.2.1 Purification of CT

The purification of CT has enabled significant advances in the investigation of the mechanism of CT membrane-binding and activation. *In vivo* studies have established the physiological role for the enzyme regulation. However, an isolated, well defined system is needed to elucidate the membrane interaction and activation mechanisms, and the identity of possible lipid activators. Investigations of activating lipid species in cell extracts could be misinterpreted due to the presence of endogenous lipid species or lipases capable of changing the apparent lipid composition.

Early attempts at CT purification produced an unstable enzyme that tended to aggregate (Choy & Vance, 1976) or was only partially pure (Choy *et*

al., 1977). The enzyme was purified to homogeneity from rat-liver cytosol by Weinhold *et al.* (1986). The key step in the protocol involved the binding of cytosolic CT to an excess of PC/oleic acid vesicles, and subsequent acid precipitation of the lipid-protein complex. After this stage, detergents were needed in the purification protocol and in the final column elution in order to stabilize the enzymatic activity. The purified enzyme contained traces of endogenous lipids (Cornell, 1991b). Removal of the detergent and endogenous lipid in the purified enzyme was achieved by DEAE Sepharose chromatography, but produced a highly unstable protein that aggregated (Cornell, 1989b) and quickly lost activity ($t_{1/2}$ of 1/2 hr) unless activating lipid was restored (Cornell, 1991b).

Purification of CT has led to many significant advances. It has allowed the mechanistic study of the enzyme in a controlled arena. Lipid vesicles or micelles of defined amounts and compositions have been utilized to investigate the selectivity and mechanism of CT activation (Feldman & Weinhold, 1987; Cornell, 1991a & b). A pure source of CT allowed the production of highly specific antibodies. This advance was important in the investigation of *in vivo* phosphorylation of CT (Section 1.3.1.5) and in the immunolocalization to the nucleus (Section 1.3.1.6). Protein sequence analysis of isolated CT segments allowed production of oligonucleotide probes, leading to the cloning and sequencing of CT cDNA from rat liver (Kalmar *et al.*, 1990). As a result of the cloning, techniques such as mutagenesis and overexpression were made possible, to enable dissection of the molecule's functional domains.

1.3.2.2 Lipid activators

CT is selective in its membrane interactions. The enzyme is not activated by PC vesicles alone, but requires the presence of certain lipid activators. Two classes of lipids appear to be the main activators for CT. Class I lipids are anionic phospholipids and fatty acids, and Class II lipids are neutral lipids with small polar head groups.

Class I: Anionic lipids

Fatty acids induce activation and translocation of CT *in vivo* (Section 1.3.1.3). In cell extracts, anionic phospholipids such as PI, PS, and PG were also effective at activating CT and causing translocation *in vitro* (Stern *et al.*, 1976; Choy & Vance, 1978; Choy *et al.*, 1979; Feldman *et al.*, 1981; Feldman *et al.*, 1985). While vesicles containing PC alone were ineffective at activating soluble CT, addition of oleic acid to the vesicles greatly stimulated activity. CT activation by oleic acid in the absence of any phospholipid was greatly reduced, demonstrating the requirement for a membrane structure. PG vesicles alone activated CT, and addition of oleic acid to PG vesicles did not increase this activity (Feldman *et al.*, 1985), suggesting the two lipids have a common mechanism of activation, via their negative charge.

Purified CT was activated by anionic lipid vesicles *in vitro,* but not by PC vesicles (zwitterionic) nor by oleic acid alone (Weinhold *et al.*, 1986; Feldman & Weinhold, 1987; Cornell, 1991a & b). CT activity was sensitive to the mole % of oleic acid or PG up to 60 mol% above which CT was not activated further (Feldman & Weinhold, 1987). CT activity could also be stimulated by Triton X-100 micelles containing anionic lipid (Cornell, 1991a). While an assortment of

anionic lipids were capable of maximally activating CT, the relative effectiveness was dependent on the charge of the lipid head group. For example, the mole % cardiolipin (charge -2) required for full CT activation was 2-fold lower than that required of PG, PI, and PS (charge -1). PG, PI and PS have different polar head groups, yet were all equally effective at activating CT. Cardiolipin and PG have a similar head group structure, yet differ in their charge and activation potency. Increasing the ionic strength increased the mole % PG needed to maximally activate CT. These results suggest that CT does not recognize a specific lipid head group structure, but responds to the surface charge density of the lipidic surface. Physical association of CT with the micelles containing anionic phospholipid demonstrated that the active form of CT is bound to a lipid structure (Cornell, 1991a).

Class II Neutral lipids with small polar head groups

Diacylglycerol induced translocation of CT *in vivo* (Section 1.3.1.4). As discussed (Section 1.3.1.4), diacylglycerol activated CT only when presented in a membrane environment. Monoacylglycerol and oleyl alcohol, like diacylglycerol, are uncharged and contain a small polar head group. These lipids promoted translocation of soluble CT *in vitro* (Cornell & Vance, 1987a). CT was physically associated with sonicated PC vesicles containing monoacylglycerol, oleyl alcohol or diacylglycerol *in vitro* (Cornell & Vance, 1987b).

Purified CT was activated by PC/diacylglycerol mixtures only when in vesicle form (Cornell, 1991a). Similar results were obtained with oleyl alcohol. CT was activated to the same extent by monoacylglycerol, oleyl alcohol or oleoyl-methyl ester (Johnson & Cornell, unpublished observation). Thus, there is not a strict specificity for diacylglycerol.

The requirement for a membrane structure for oleic acid and diacylglycerol activation suggests CT is not activated by direct binding of a monomer of activating lipid. Moreover, the lack of head-group specificity suggests CT does not possess a site designed to recognize a specific chemistry in an activator lipid molecule(s). Thus, lipid activators do not appear to directly activate CT, but their presence changes membrane properties which affects the CT-membrane interaction.

1.3.2.3 CT membrane binding involves both electrostatic interactions and membrane intercalation

The lipid bilayer is composed of a hydrophobic, acyl chain core with a polar surface composed of charged head groups. Proteins can interact electrostatically with the bilayer surface or embed themselves in the hydrophobic milieu. Peripheral membrane proteins, which interact exclusively with the membrane surface in an electrostatic manner, are diagnosed by their ability to be removed from the membrane in high pH or ionic strength media, conditions which do not disrupt the bilayer integrity. Proteins embedded in the hydrophobic membrane core are released only upon membrane disruption such as that caused by detergents.

The membrane binding of CT has both electrostatic and hydrophobic components. Lack of specificity in the response to class 1 anionic lipids, as well as the effect of ionic strength, suggested that CT responds to the negative surface charge on membrane (Cornell, 1991a). Lipids carrying a positive charge, for example sphingosine, antagonize the effect of anionic lipids, likely by neutralizing surface charge (Sohal & Cornell, 1990). These results imply

importance of a negative surface charge density on the membrane, and suggest a role for electrostatic interactions between CT and the membrane. However, once bound, high ionic strength media was insufficient to remove CT from membranes (Cornell & Vance, 1987a & b). Detergents dissociated CT from the membrane, suggesting hydrophobic rather than electrostatic interactions mediate the binding.

Involvement of both electrostatic and hydrophobic elements suggested a two step mechanism for CT binding in which anionic lipid vesicles promote electrostatic attraction of CT to the membrane surface, followed by penetration of a portion of the protein into the hydrophobic membrane core (Cornell, 1991b). A similar two-component model for membrane-interaction has been proposed for other membrane-interacting proteins such as melittin (Dufourcq & Faucon, 1977), synapsin (Benfenati *et al.*, 1989) and sec A (Ulbrandt *et al.*, 1992). A unifying feature of CT activators is the ability to disrupt membrane packing, and thus facilitate intercalation of a portion of the protein into the hydrophobic acyl chain core. CT activity was greatly diminished in the presence of gel-phase membranes, and anomalously enhanced at the gel-to-liquid crystalline phase transition (Cornell, 1991b). Small, highly curved vesicles were more potent than planar multilamellar vesicles (Cornell, 1991b). A correlation between CT membrane binding and the content of hexagonal phase-forming lipids in target membrane has been discussed (Cornell & Vance, 1987b; Jamil *et al.*, 1993). Bilayer phase and curvature, as well as the presence of class II lipids, influence membrane properties by disrupting the packing formation of the phospholipid lipid head groups and acyl chains of the membrane. The presence of anionic lipids in a membrane disrupts packing at the surface in addition to creating a negative surface charge. Phospholipases C and A_2 are examples of other

membrane-binding proteins sensitive to lipid packing (Menashe, *et al.*, 1986; Rao *et al.*, 1993). In order for the intercalation model to be feasible, there must exist a structural domain of CT that is stable in the hydrophobic membrane environment.

1.3.3 A model for the structural domains of CT

Determination of the amino acid sequence of mammalian CT enabled the formation of a model for domain structure and function. The first amino acid sequence was established for CT from rat-liver by Kalmar *et al.*, (1990) (Figure 1.2). The protein contained 367 amino acid residues, and had a calculated molecular weight of 41,720. The protein bound to vesicles or detergent micelles as a dimer (Cornell, 1989b). CT sequences have also been determined from mouse (Rutherford *et al.*, 1993), Chinese hamster ovary (CHO) cells (Sweitzer & Kent, 1994), and human (Kalmar *et al.*, 1994) sources. The four sequences are ~95 % identical, with most changes being conservative. On the basis of structural predictions and sequence homologies, a model has been proposed for the domain structure of CT (Fig. 1.3) (Kalmar *et al.*, 1990). The model for CT contains three distinct domains, one of which has been proposed to contain a structural element capable of hydrophobic membrane interactions.

MDAQSSAKVNSRKRRKEVPGPNGATEEDGIPSKVQRCAVGLRQPAPFSDE[50]

IEVDFSKPYVRVTMEEACRGTPCERPVRVYADGIFDLFHSGHARALMQAK[100]

NLFPNTYLIVGVCSDELTHNFKGFTVMNENERYDAVQHCRYVDEVVRNAP[150]

WTLTPEFLAEHRIDFVAHDDIPYSSAGSDDVYKHIKEAGMFAPTQRTEGI[200]

STSDIITRIVRDYDVYARRNLQRGYTAKELNVSF*INEKKYHLQERVDKVK*[250]

*KKVKDVEEKSKEFVQKVEEKSIDLIQKWEEKSREFIGSFLEMF*GPEGALK[300]

HMLKEGKGRMLQAISPKQSPSSSPTHERSPSPSFRWPFSGKTSPSSSPAS[350]

LSRCKAVTCDSEDEED[367]

Figure 1.2: Amino acid sequence of rat-liver CT.
Sequence dervived by Kalmar *et al.*, (1990) and revised by MacDonald and Kent (1993). Putative amphipathic helix is in italics. Tandem 11-mer repeats are underlined.

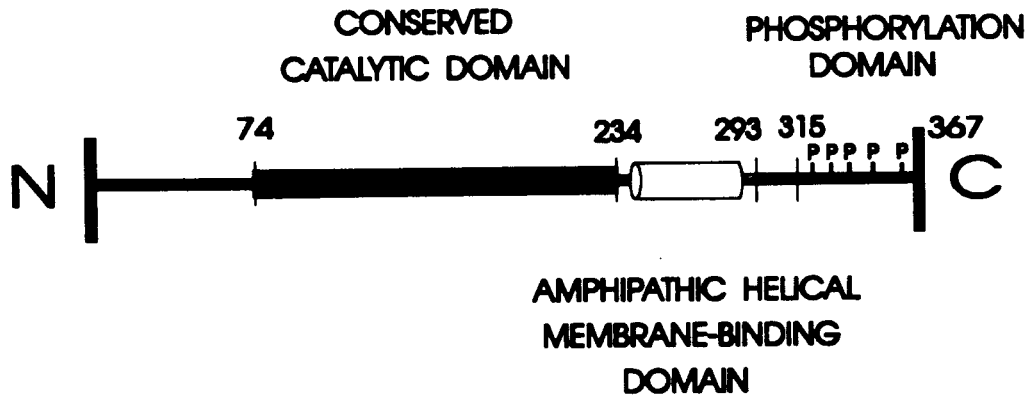

Figure 1.3: Domain Structure for mammalian CT.

1.3.3.1 Conserved catalytic domain

The N-terminal two-thirds of CT (residues 1 to 230) forms a discrete, protease insensitive domain (Craig *et al.*, 1994). This domain is homologous with yeast CT (Tsukagoshi *et al.*, 1987) and a related *B. subtilis* glycerol phosphate cytidylyltransferase (Mauel *et al.*, 1991; Park *et al.*, 1993). A single amino acid change in this region resulted in defective CTP binding (Veitch & Cornell, 1994), while deletion mutants composed of this domain alone are catalytically active (Wang & Kent, 1995b). Thus, the catalytic site is likely contained in this region.

1.3.3.2 Phosphorylation domain

The C-terminal 55 residues (315 to 367) contains many potential phosphorylation sites. The region is rich in serine-proline motifs that are potential substrates for cyclin dependent kinases, and contains potential sites for casein kinase II and glycogen synthase kinase II. This domain was highly phosphorylated *in vivo*, yet deletion mutants lacking this domain, although not phosphorylated, were fully active and capable of membrane binding (Section 1.3.1.5). Thus, this domain is not directly involved in catalysis or membrane binding, but may play a role in modulating these functions.

1.3.3.3 The proposed membrane binding domain containing a putative amphipathic α-helix

The region linking the catalytic and phosphorylation domain (residues 230 to 293) is predicted to be an extended helix (Garnier *et al.*, 1978; Chou & Fasman, 1978). The region contains an 11-residue motif repeated three times in tandem (Fig. 1.2). In the mouse gene, this region (residues 238 to 299) composes a separate exon (Rutherford, *et al.*, 1993), implying that it may function as a separate domain. When this putative helical sequence is presented as a helical wheel projection (Fig. 1.4) it is strikingly *amphipathic,* with a highly-charged polar face, and an opposing hydrophobic face.

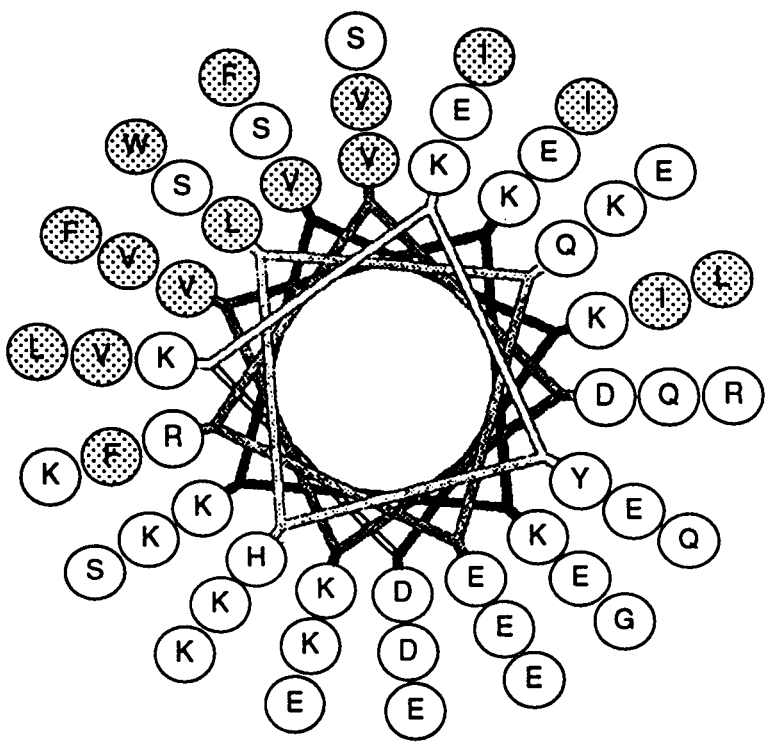

Figure 1.4:
Helical wheel representation of residues 238 to 291 of CT. Hydrophobic residues are shaded.

The amphipathic α-helix motif has been proposed to mediate lipid interactions of apolipoproteins (Segrest *et al.*, 1974), based on findings of increased helicity in apolipoprotein fragments upon membrane binding. These membrane-binding sequences formed helices with an asymmetric distribution of hydrophobic and polar amino acids, resulting in a large non-polar face, and an opposing polar face. This structure was proposed to bind to the phospholipid surface with the non-polar face interacting with the acyl chains of the membrane, and the polar residues interacting with the phospholipid head groups. Much physical evidence has accumulated to confirm the role of the amphipathic α-helix in the reversible binding of apolipoproteins (types A-I, A-II, C-II, C-III and E) to lipoprotein particles and PC membranes (Segrest *et al.*, 1990). The amphipathic α-helix has also been implicated in the membrane interactions of polypeptide hormones (Kaiser & Kezdy, 1984) and lytic peptides such as melittin (Terwilliger *et al.*, 1982).

As the sequence of CT contains no long stretches of hydrophobic amino acids, which would be indicative of a membrane spanning region, nor any consensus sites for the covalent attachment of a lipid anchor (myristoyl, palmitoyl or prenyl-group), the putative amphipathic helix region was proposed to mediate the membrane binding of CT (Kalmar *et al.*, 1990). In this model, the amphipathic α-helix would interact with the surface of activating membranes, its axis parallel to the membrane surface, which would enable its hydrophobic face to intercalate into the acyl chain core, and its polar residues to interact with the phospholipid head groups or a distinct region of the protein. This membrane binding would somehow facilitate activation of CT (Fig. 1.5).

In this study, various approaches have been taken to elucidate the role of the putative amphipathic α-helix in the CT-membrane interaction. In chapter two, the lipid regulation of rat-CT and yeast-CT were compared. Yeast-CT lacks the putative amphipathic α-helix region. In chapter three, spectroscopic techniques were utilized to investigate the secondary structure and membrane interactions of synthetic peptides corresponding in sequence to the putative amphipathic α-helix region of CT. These analyses proved the presence of a helical motif and suggested its role in membrane binding. In chapter four, hydrophobic photolabelling probes were utilized, in combination with proteolysis, to identify the amphipathic α-helix region as the key domain involved in the intercalation of CT into activating membranes.

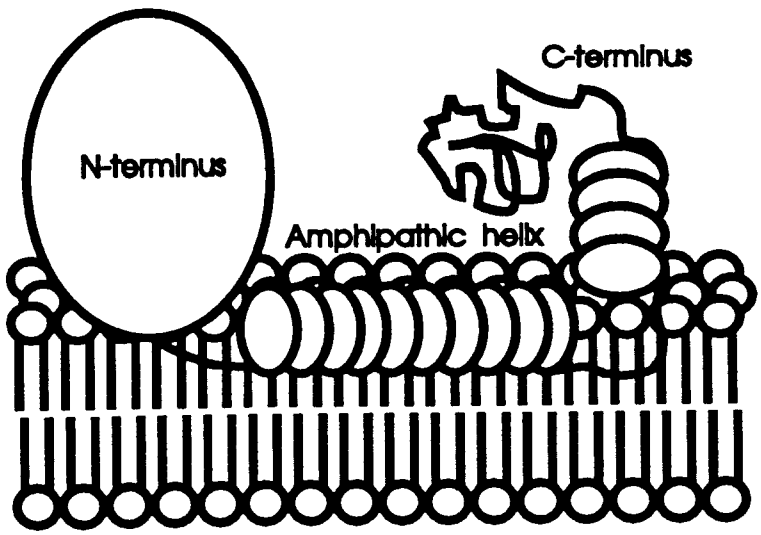

Figure 1.5: Model for membrane-bound CT.

CHAPTER TWO: COMPARISON OF THE LIPID INTERACTIONS OF RECOMBINANT YEAST-CT AND RAT-CT EXPRESSED IN COS CELLS

2.1 Introduction

CT regulation by translocation to membranes, and its importance in the regulation of PC synthesis, has been well characterized in mammalian systems (Chapter One). In yeast, PC synthesis proceeds via the CDP-choline pathway, or via the methylation of PE formed from PS decarboxylation or a CDP-ethanolamine pathway (Carman & Henry, 1989). Unlike most mammalian cells, yeast with a blocked CDP-choline pathway are able to utilize the alternate synthetic pathway to compensate (Nikawa *et al.*, 1983). Coordinate regulation of the alternate pathways is mediated by the availibity of the water-soluble substrates, choline and inositol. Choline supplementation, in the presence of inositol, represses the enzymes of the methylation pathway for PC synthesis (Carman & Henry, 1989), and induces the choline transporter and choline kinase activities (McMaster & Bell, 1994). Only at low exogenous choline concentrations did CT limit the rate of PC synthesis via the CDP-choline pathway (McMaster & Bell, 1994). The exact role of yeast-CT in regulation of PC synthesis is unclear.

CT from rat-liver and yeast sources has been cloned and sequenced (Kalmar, *et al.*, 1990; Tsukagoshi, *et al.*, 1987). A large central domain of the two proteins shares 65% identity at the amino acid level (Fig. 2.1). From the point of divergence at the C-terminal domain, the rat CT contains a putative amphipathic α-helix that has been implicated in membrane-binding (Section 1.3.3.3). The sequence of yeast-CT does not contain this putative amphipathic

α-helix.

The lipid activation and binding of recombinant rat-CT and yeast-CT has not been investigated. Therefore, the purpose of this study is three-fold.

- 1) To confirm that the previously unstudied recombinant rat CT, overexpressed in COS cells, has the same lipid activation and binding characteristics as the protein from the natural source.
- 2) To investigate the role lipids may play in modulating yeast-CT activity.
- 3) To investigate the importance of the putative amphipathic α-helix region in membrane binding, the lipid activation of rat-CT and yeast-CT was compared. If the putative amphipathic α-helix domain is involved in the membrane-interactions of rat-CT, yeast-CT which lacks this region would not be expected to respond to lipids in the same way.

In these studies, yeast-CT was modulated by lipids, but with characteristics different from rat-CT.

Figure 2.1: Comparison of yeast CT and rat CT protein sequences and domain models. A) Protein sequence comparison of rat liver (Kalmar *et al.*, 1990) and yeast (Tsukagoshi *et al.*, 1987) CTs. Asterisks indicate identical matches and dots indicate conservative changes. B) Domain model comparison of rat and yeast CTs.

A

```
RAT      MDAQSSAKVNSR----------------KRRKEVPGPNGATEEDGIPSK    33
YEAST    MANPTTGKSSIRAKLSNSSLSNLFKKNKNKRQREETEEQDNEDKDESKNQ    50
         *   .. *   *                 ** .*    .   . *

RAT      VQRCAVGL--RQPAPFSDEIE---VDFSKPYVRVTMEEACRG-----TPC    73
YEAST    DENKDTQLTPRKRRRLTKEFEEKEARYTNELPKELRKYRPKGFRFNLPPT   100
               *  *    .. *.*      .   .       .*      *

RAT      ERPVRVYADGIFDLFHSGHARALMQAKNLFPNTYLIVGVCSDELTHNFKG   123
YEAST    DRPIRIYADGVFDLFHLGHMKQLEQCKKAFPNVTLIVGVPSDKITHKLKG   150
         .**.*.****.***** ** . * * *  ***  ***** ** .** .**

RAT      FTVMNENERYDAVQHCRYVDEVVRNAPWTLTPEFLAEHRIDFVAHDDIPY   173
YEAST    LTVLTDKQRCETLTHCRWVDEVVPNAPWCVTPEFLLEHKIDHVAHDDIPY   200
         .**. . .* . . *** ***** **** ****** **.** ********

RAT      SSAGSDDVYKHIKEAGMFAPTQRTEGISTSDIITRIVRDYDVYARRNLQR   223
YEAST    VSADSDDIYKPIKEMGKFLTTQRTNGVSTSDIITKIIRDYDKYLMRNFAR   250
          ** ***.** *** * *  **** *.******.*.**** *  **. *

RAT      GYTAKELNVSFINEKKYHLQERVDKV----KKKVKDVEEKSKEF------   263
YEAST    GATRQELNVSWLKKNELEFKKHINEFRSYFKKNQTNLNNASRDLYFEVRE   300
         * *  *****..      .   .   .    **    .   *...

RAT      --VQKVEEKSI--DLI------QKWEEKSREFIGS---------------   288
YEAST    ILLKKTLGKKLYSKLIGNELKKQNQRQRKQNFLDDPFTRKLIREASPATE   350
           . *   * .   ••      •    .   *.

RAT      FLEMFGPEGALKHMLKEGKGRMLQAISPKQSPSSSPTHERSPSPSFRWPF   338
YEAST    FANEFTGENS-TAKSPDDNGNLFSQEDDEDTNSNNTNTNSDSDSN-----   394
         *   *  *         .  *  .        . *

RAT      SGKTSPSSSPASLSRCKAVT-CDISEDEED    367
YEAST    TNSTPPSEDDDDNDRLTLENLTQKKKQSAN    424
         .  * **        *
```

B

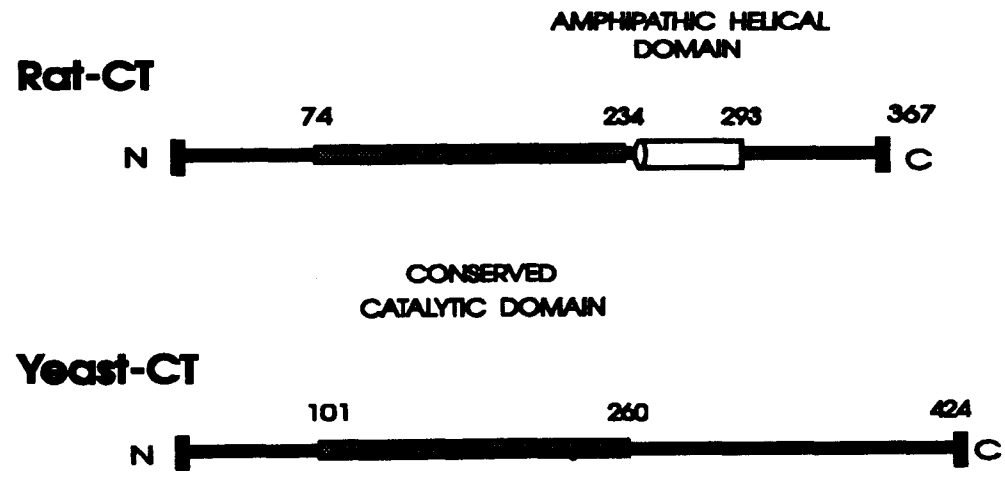

2.2 Experimental Procedures

2.2.1 Materials:

COS-1 cells and the pAX111 expression vector were gifts from Dr. Robert Kay (BC Cancer Research Center, Vancouver, BC). COS cells are derived from a monkey cell line, and have been engineered to support plasmid replication from a SV40 origin (Gluzman 1981). The pAX111 vector contains a human cytomegalovirus enhancer and promotor to drive transcription, and an SV40 origin of replication to drive rapid replication in COS cells (Kay & Humphries, 1991). The yeast-CT DNA was from Dr. S. Yamashita (Gunma University School of Medicine, Maebashi, Japan). The pAX111-rat-CT and pAX111-yeast-CT expression vectors were constructed by Dr. Gabe Kalmar as described (Johnson *et al.*, 1992). Phospholipids were from Avanti Polar Lipids (Alabaster, AL, USA). Sphingosine, oleic acid, mono-olein, oleyl alcohol, phospholipase C (from *B. cereus*) and choline kinase were from Sigma (St. Louis MO, USA). [^{3}H]choline chloride (80 Ci/mMol) was from New England Nuclear. Restriction enzymes and other DNA-modifying enzymes were from Pharmacia (Uppsala, Sweden) or BRL (Burlington, Ont.). Tissue-culture supplies were from Corning (Ithaca, NY, USA). Fetal-calf serum was from GIBCO/Life Technologies (Burlington, Ont.). Other chemicals were from Sigma or BDH (Vancouver, BC).

2.2.1.1 Preparation of *sn*-1,2,diacylglycerol

Diacylglycerol was prepared from egg PC by digestion with phospholipase C by the method of Myher & Kuksis (1979). Egg PC (1 mmol, 0.74 g) in diethyl ether was vigorously mixed, in a 2 phase system, with ~200 units phospholipase C (from *B. cereus*, obtained from Sigma) in 17.5 mM Tris, pH 7.4, 1 mM $CaCl_2$. After 20 hr, PC was completely converted to diacylglycerol, as analyzed by thin layer chromatography (TLC) (Section 2.2.3). The lipid was extracted three times with $CHCl_3$/MeOH (2:1) and dehydrated with excess Na_2SO_4. The solvent was removed with a rotary evaporator and by evaporation under N_2, and the resulting pure diacylglycerol was weighed, dissolved in $CHCl_3$ to 50 mM and stored at -20°C under N_2.

2.2.1.2 Preparation of [^{3}H]phosphocholine

[^{3}H]phosphocholine was prepared from [^{3}H]choline by reaction with choline kinase in the presence of ATP. 1 to 2 mCi [^{3}H]choline in ethanol was dried under nitrogen and reacted with 0.3 units choline kinase for 1 h at 37 °C in the presence of 0.1 M Tris pH 8.0, 10 mM ATP, 10 mM $MgCl_2$. [^{3}H]phosphocholine was separated from unreacted [^{3}H]choline on a Dowex ion exchange column: choline eluted with H_2O, phosphocholine eluted with 50 mM NaCl. Ca^{+2}-free phosphocholine (unlabelled) was added to give a final phosphocholine concentration of 10 to 15 mM and a specific activity of 10 to 15 Ci/mol.

2.2.2 Protein Quantitation

Protein was quantified by the method of Bradford (1976). Ovalbumin standards and protein samples were made to 100 µl. Coomassie Dye reagent (0.005% (w/v) Coomassie, 5% (v/v) Ethanol, 10% (v/v) H_3PO_4; filtered before use) was added, samples were incubated for 15 min at 37 °C, and the absorbance at 595 nm was measured. For a micro assay, 1 ml dye was added to proteins in the 0 to 25 µg range; for a macro assay, 3 ml dye reagent was added to proteins in the 0 to 100 µg range.

2.2.3 Phospholipid Analysis

Phospholipids in aqueous solution were extracted by the method of Bligh & Dyer (1959). To a 0.4 ml aqueous sample on ice was added 1.0 ml MeOH, 0.5 ml $CHCl_3$, 0.5 ml $CHCl_3$, and 0.5 ml H_20, vortexing after each addition. Samples were centrifuged at 2500 rpm for 5 min to encourage phase separation. The upper aqueous phase was removed, and the lower organic phase washed with 1.5 ml "theoretical upper phase" (MeOH:H_2O:$CHCl_3$, 48:47:3). This wash was repeated three times if aqueous samples were in phosphate buffer. The lower organic phase containing phospholipids was dried under nitrogen.

Phospholipid phosphate was quantified by the method of Bartlett (1959). Standards of Na_2HPO_4 in the range of 0 to 200 nmol phosphate were in a volume ≤20 µl. $HClO_4$ (0.5 ml) was added to dried lipid samples and standards, which were then incubated, covered, at 140 to 160 °C overnight. After samples had cooled, 4.4 ml ammonium molybdate (0.22% (w/v)), and 0.2 ml freshly made Fisk Subbarow solution (0.25% (w/v) 1-amino-2-napthyl-sulfonic acid, 0.5% (w/v)

Na_2SO_3, 15% (w/v) $NaHSO_3/Na_2S_2O_5$ in H_2O) were added with vortexing, and the samples boiled for 10 min. After cooling, absorbance at 820 nm was measured.

Lipid purity was analyzed by thin layer chromatography. Lipids (100 to 200 nmol) were separated on pre-run, activated, glass-backed silica plates. Phospholipids and fatty acids were separated in $CHCl_3$/ MeOH/ NH_3 (45:35:5 volume ratio), while neutral lipids such as diacylglycerol were separated in hexane /diethyl ether /acetic acid (60:40:1 volume ratio). Lipids were visualized with iodine vapour.

2.2.4 Preparation of sonicated vesicles

Lipids from $CHCl_3$ stocks were mixed in small round bottom flasks and the solvent evaporated under vacuum with a rotary evaporator for >10 min. Lipids were hydrated by vortexing in TE buffer (10 mM Tris, pH 7.4, 1 mM EDTA), unless otherwise specified. The resulting suspension was sonicated on ice (Branson sonicator with a fine probe operating at 80% power output) until the turbid solution was clear: 10 to 20 min for lipid dispersion containing anionic lipids, 20 to 45 min for vesicles containing PC with neutral lipids. The sonicated solution was spun at 20,000*g* for 5 min in a bench-top microfuge to remove any titanium debris from the sonicator probe. The resulting small, unilamellar vesicles containing PC alone or with neutral lipids were used the same day as preparation. Solutions containing anionic lipids were sometimes stored and used within a few days of preparation as they did not form any noticeable precipitate or become cloudy, and there was no noticeable difference in CT activation after one week of storage at 4 °C.

2.2.5 CT activity assay

The enzymatic activity of CT was analyzed by monitoring the incorporation of the radioactive substrate [^{3}H]phosphocholine into [^{3}H]CDP-choline. The solution, with a final volume of 50 μl, contained 20 mM Tris, pH 7.4, 87.5 mM NaCl, 12 mM $MgCl_2$, 3 mM CTP, 10 mM DTT, and variable amounts of lipid and enzyme. [^{3}H]phosphocholine (final concentration 1-2 mM) was added to start the reaction, which was incubated in a shaking 37 °C H_2O bath for 10 to 45 min, then quenched by addition of 30 μl MeOH/NH_3 (9:1). Samples were centrifuged at 20,000*g* for a few seconds, and a portion of the supernatant was spotted on a silica plastic-backed TLC plate (Merck # 5748) and developed in 0.6 % (w/v) NaCl /MeOH /NH_3 (5:5:1 volume ratio). The CDP-choline band was visualized with 0.02% (w/v in methanol) dichlorofluorescein under UV light, and the silica was scraped from the plate. [^{3}H]CDP-choline was quantified by liquid scintillation counting. Units of CT activity are nmol CDP-choline formed per minute.

2.2.6 Preparation of recombinant CT from COS cell culture

2.2.6.1 Maintaining COS cells:

COS cells were maintained as monolayers in Dulbecco Modified Eagle Medium (DMEM) with 5 % (v/v) Fetal Calf Serum (FCS) at 37 °C in 5% CO_2. When confluent, cells were released from plates by treatment with 0.05% (w/v) trypsin, 0.02% (w/v) EDTA in phosphate-buffered saline (PBS), diluted ten-fold with fresh media, and transferred to new plates. Cells were subcultured approximately every three days.

2.2.6.2 Transfection with Recombinant DNA

Cells (~1.5 x 10^6) were seeded on 10 cm plates 24 h prior to transfection with plasmid DNA. For transfection, cells were washed with TD (25 mM Tris, pH 7.5, 140 mM NaCl, 5 mM KCl, 0.5 mM Na_2HPO_4), then incubated with ~10 μg DNA in a TS solution (TD with 1 mM $MgCl_2$, 1 mM $CaCl_2$) with DEAE-Dextran (0.5 mg/ml) for 10 min at room temperature, then 40 min at 37 °C/ 5% CO_2. The DNA solution was removed, and cells were incubated with TS/20% (v/v) glycerol for 2 min, washed with TS and then with DMEM. Cells were treated with 100 μM chloroquine in DMEM / 5% FCS for 2.5 h at 37 °C/ 5% CO_2. Cells were rescued with DMEM/ 5% FCS, transferred to 15 cm dishes after 24 h, and allowed to grow at 37 °C/ 5% CO_2 until harvested.

2.2.6.3 Preparation of COS cell cytosolic extracts

Cells were harvested 72 h after DNA transfection using PBS/2.5 mM EDTA at 37 °C to release cells from dishes. Cells were pelleted at 1000*g* for 5 min and resuspended in 1.0 ml homogenization buffer (10 mM Tris pH 7.5, 1 mM EDTA, 3 mM $MgCl_2$, 1 mM PMSF, 2 mM DTT). All subsequent steps were performed at 4 °C. Cells were homogenized by 30 strokes of a Teflon/glass grinder. K_2HPO_4 was added from a 2 M, pH 7.4 stock in 5 aliquots, vortexing after each addition, to a final concentration of 0.2 M phosphate. The sample at this stage was termed the "homogenate".

For preparation of cytosol, the homogenate was centrifuged at 3000*g* for 5 min, and the supernatant centrifuged at 100,000*g* for 1 hr. The high speed supernatant was termed the "cytosol". The high speed pellet was resuspended

in homogenization buffer/0.2 M phosphate by sonication for 30 s with a low power sonicator (Fisher Sonic Dismembrator, model 300), and this suspension was termed the "microsomal fraction". These fractions were aliquoted and stored at -80 °C.

2.2.7 Assay for CT binding to Lipid-Enriched Microsomes:

Sonicated dispersions of oleic acid, SOPC, SOPC/diacylglycerol (2:1), or SOPC/sphingosine (1:1) were prepared as described (Section 2.2.4). Rat liver microsomes were prepared from a homogenized rat liver by ultracentrifugation, as described for COS cell microsomes (Section 2.2.6.3). Microsomes (0.25 mg protein, 130 nmol lipid) were enriched with lipids (400 nmol) by incubation with the sonicated lipid suspension at room temperature for 30 min. The samples were cooled to 4 °C and centrifuged for 1 h at 100,000*g*. The supernatant was removed and the pellet resuspended by sonication in homogenization buffer with 0.2 M phosphate. Under these conditions, the lipids sedimented in the "microsomal" pellet, except for a minor fraction of diacylglycerol, which floated on the top of the solution. To assay the membrane-binding of CT, 10 activity units (defined in Section 2.2.5; 0.15 - 0.25 mg protein) of COS cell cytosol containing expressed rat-CT or yeast-CT were added to the resuspended lipid-enriched microsomes. The mixture was incubated 5 min at 37 °C, cooled to 4 °C, and recentrifuged as above. The relative amounts of the added lipid found in the pellet and supernatant fractions were analyzed by extraction and TLC (Section 2.2.3). Both fractions were assayed for CT activity in the presence of an optimum concentration of PC/oleic acid (1:1) vesicles.

2.3 Results

2.3.1 Expression of Yeast-CT and Rat-CT in COS cells

Yeast-CT and rat-CT were expressed in COS cells. CT activity in cytosolic extracts from COS cells tranfected with the pAX111 vector alone was 2-3 units/mg protein when assayed in the presence of a saturating concentration of PC/oleic acid (1:1) vesicles (Table 2.1). Transfection with the yeast-CT or rat-CT clones resulted in an elevation to ~60 units/mg in COS-cell cytosolic extracts prepared 72 h after transfection (Table 2.1). Yeast-CT and rat-CT were subject to stimulation by lipids (Table 2.1). The activities in the presence or absence of PC/oleic acid (1:1) vesicles differed by factors of 8 (yeast-CT) or 25 (rat-CT). The intracellular distribution of CT activity in the cells transfected with yeast-CT, rat-CT or the vector alone was similar; 80-90% was found in the cytosolic fraction obtained by high-speed centrifugation. This distribution is similar to that found in rat liver (Section 1.3.1.2).

Table 2.1: CT specific activity in transfected COS cell cytosols

	Cytosolic CT Specific Activity	
Transfection	No lipid	+ PC/oleic acid
vector alone	0.4 ± 0.3	2.4 ± 0.7
rat-CT	2.4 ± 1.1	61 ± 14
yeast-CT	8 ± 4	64 ± 13

Cytosols were prepared from transfected COS cells as described in Section 2.2.6. CT activity was assayed in the presence of optimal concentration of egg PC/oleic acid (1:1) vesicles. Data are presented as activity units/mg of cytosolic protein (means ± S.D. of 3 - 6 separate transfections).

2.3.2 Effect of oleic acid and sphingosine

Sonicated unilamellar vesicles composed of egg PC and oleic acid (1:1; mol:mol) have been used as a standard for comparing the activation of purified rat liver CT by vesicles of different lipid compositions. PC/oleic acid vesicles stimulated yeast-CT and rat-CT activity up to 30-fold, whereas vesicles of egg PC alone had little effect (Fig. 2.2). The activation of yeast-CT, but not rat-CT, was decreased at lipid concentrations above 100 μM. In figure 2.2, the oleic acid content of the vesicles used was 50 mol%. The mole % of oleic acid in 1-stearoyl-2-oleoyl-PC (SOPC) vesicles was varied between 0 and 50 % (Fig. 2.3). Since yeast-CT was not stimulated at all by PC alone, the addition of oleic acid to the PC vesicles resulted in a more dramatic stimulation, compared to the oleic acid effects on rat CT. The activation of both CTs by oleic acid was completely blocked by incorporation of equimolar amounts of sphingosine into the vesicles (Fig. 2.4). This concentration of sphingosine should neutralize the negative charge of the fatty acid. Antagonism of anionic lipid activation by a cationic lipid suggests a role of the surface charge in the activation by oleic acid.

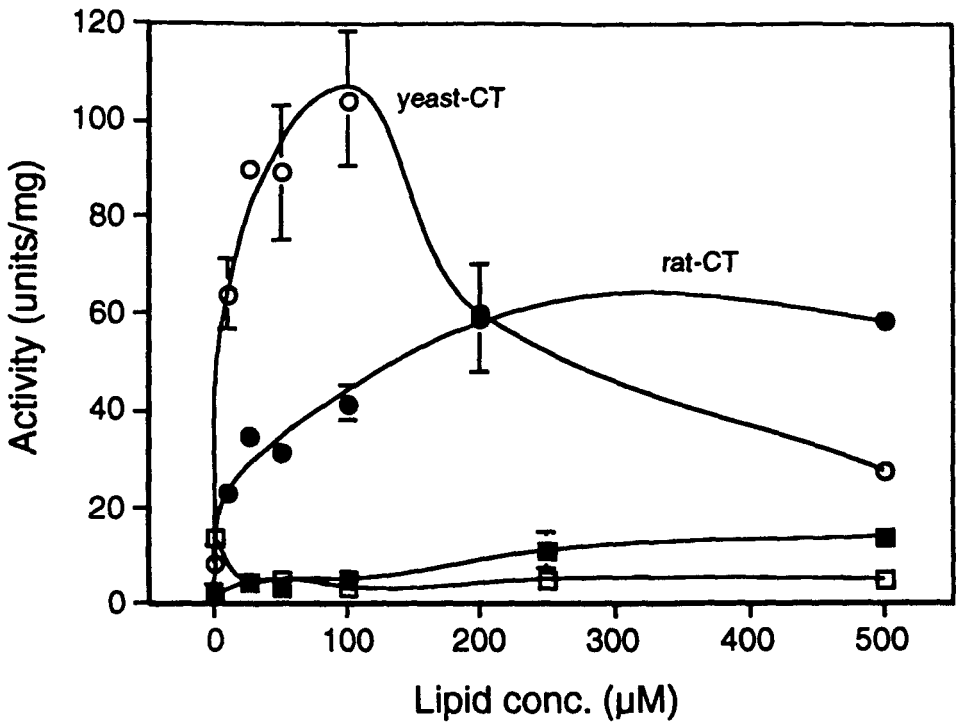

Figure 2.2: Dependence of CT activity on the concentration of egg PC/oleic acid or SOPC vesicles.

Cytosolic extracts from COS cells expressing rat-CT (closed symbols) or yeast-CT (open symbols) were assayed in the presence of the indicated concentration of egg PC/oleic acid (1:1, mol/mol, ●, ○) or SOPC vesicles (■ , □). Data are duplicate determinations of single experiments that were repeated three or four times with similar results.

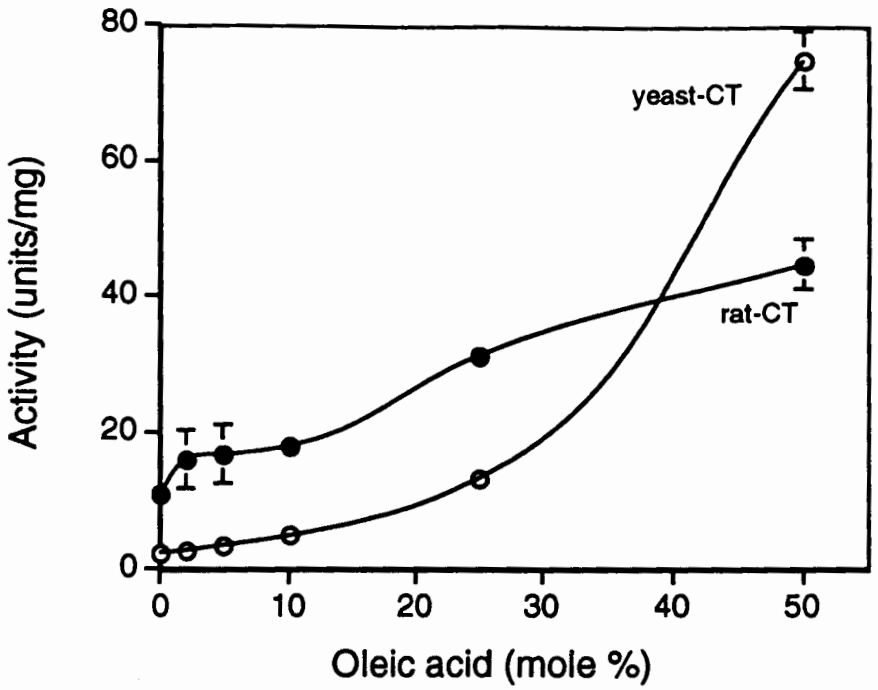

Figure 2.3: Dependence of CT activity on the mole % of oleic acid in SOPC vesicles.

Cytosolic extracts from COS cells expressing rat-CT (●) or yeast-CT (○) were assayed in the presence of 100 μM SOPC vesicles containing the indicated mole % of oleic acid. Data are duplicate determinations of single experiments that were repeated three times with similar results.

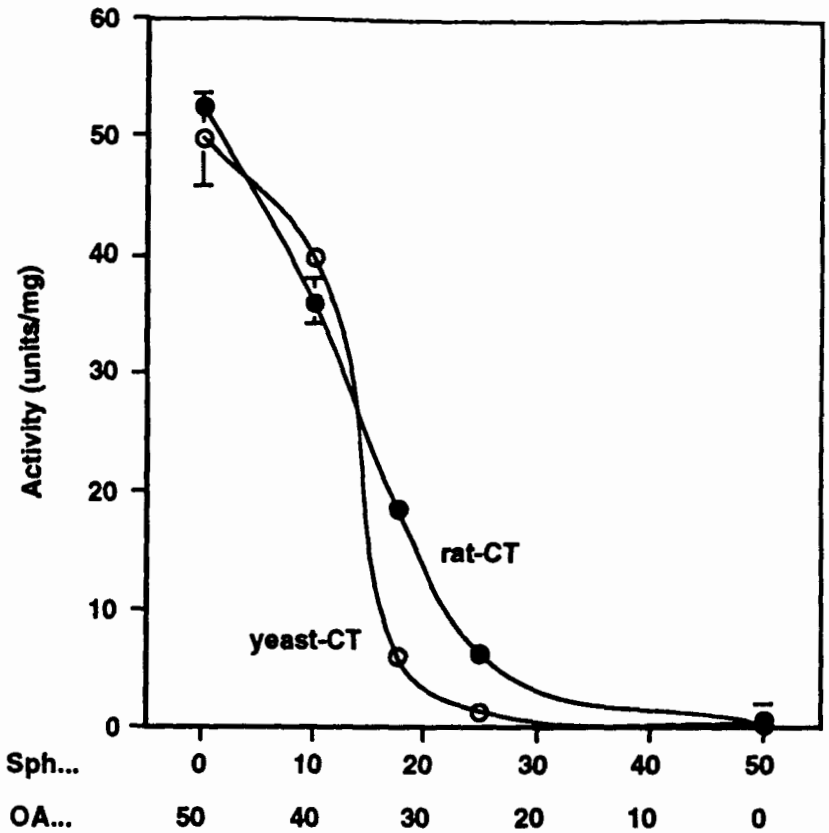

Figure 2.4: Antagonism between oleic acid and sphingosine.

Cytosolic extracts from COS cells expressing rat-CT (●) or yeast-CT (○) were assayed in the presence of 100 μM vesicles containing 50 mol% SOPC and the indicated mole % of oleic acid (OA) and sphingosine (Sph). Data are duplicate determinations of single experiments that were repeated twice with similar results.

2.3.3 Effects of anionic phospholipids

Vesicles composed of cardiolipin, PG, or PI were tested for activation of the CTs as a function of vesicle concentration (Fig. 2.5) or mole % anionic phospholipid in vesicles composed of variable ratios of anionic phospholipid and SOPC (Fig. 2.6). Rat-CT activity plateaued at 10 μM cardiolipin, ~50 μM PG and ~100 μM PI (Fig. 2.5A). On the other hand, the dependence of yeast-CT activity on anionic phospholipid concentration was biphasic, where the activation curve reached a plateau at 2-5 μM and declined at higher concentrations (Fig. 2.5B). The biphasic behavior was most pronounced for cardiolipin, and the least pronounced for PI. When assayed at the vesicle concentration optimum, determined from the data of figure 2.5 (100 μM for rat-CT), the activity dependence of rat-CT on the mole % of anionic phospholipids was saturable at ~50 mol% for cardiolipin, PG, and PI (Fig. 2.6A). Cardiolipin produced the strongest stimulation. For yeast-CT, assayed at the optimal lipid concentration (5 μM), the mol % curve saturated at 25% cardiolipin and 50% PG or PI (Fig. 2.6B). At higher than optimal lipid concentrations, (e.g. 25 and 100 μM) the mole % of anionic lipid required for maximal stimulation of yeast-CT shifted to lower values and the stimulation declined at high mole % of PI, cardiolipin or PG (results not shown). The loss of stimulatory effects of anionic phospholipids at high concentration is not due to metabolism of the added lipid to an inhibitory species. Extraction and TLC analysis of the lipids (Section 2.2.3) after incubation of cardiolipin, PI, PG or PC/oleic acid vesicles with COS-cell cytosol under conditions identical to the enzyme assay revealed no new species (results not shown).

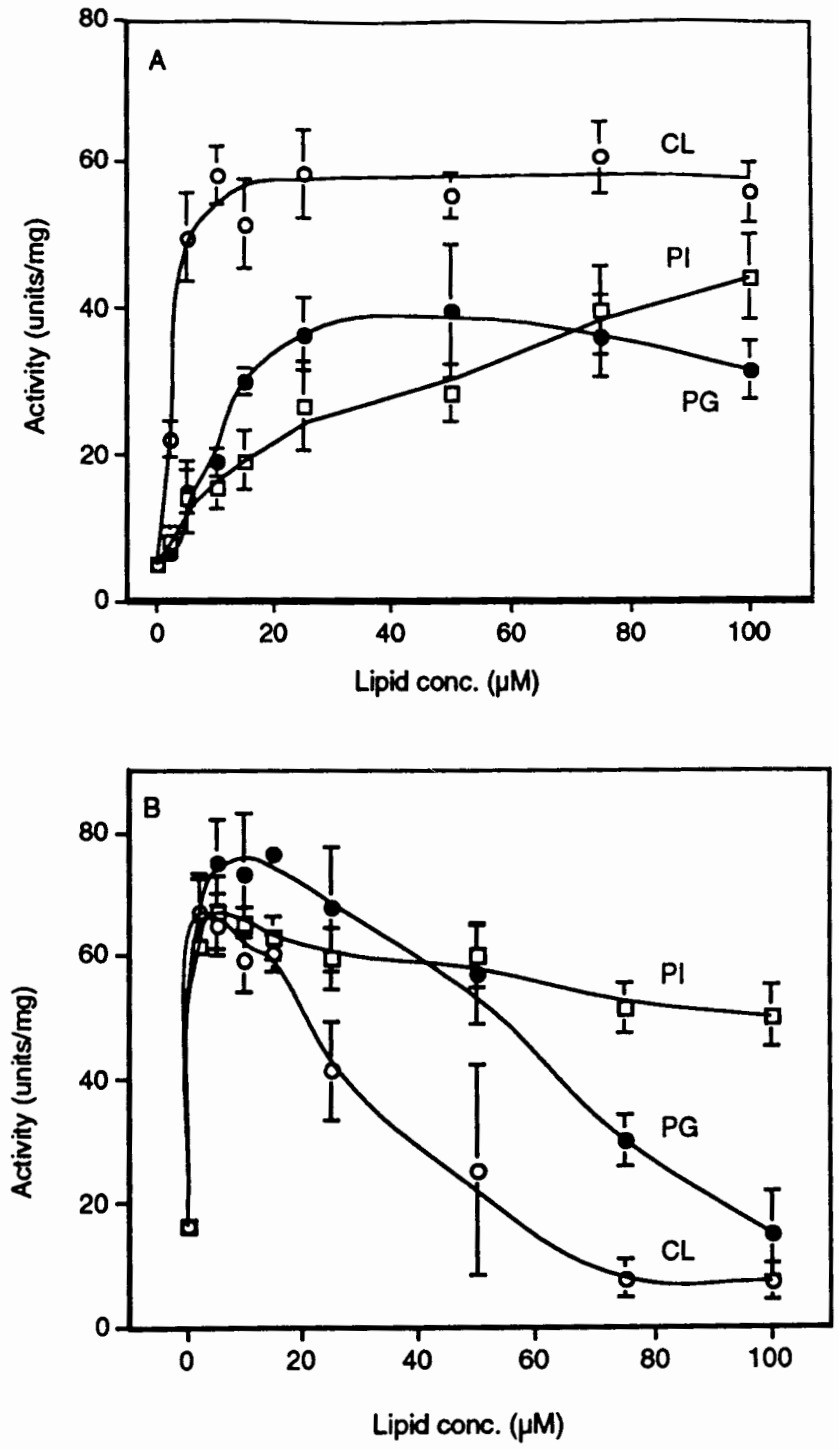

Figure 2.5: Dependence of rat-CT (A) or yeast-CT (B) activity on the concentration of anionic phospholipids.

Cytosolic extracts from COS cells were assayed in the presence of vesicles containing cardiolipin (CL, ○), PI, (□), or PG (■). Data are averages of two to four separate experiments.

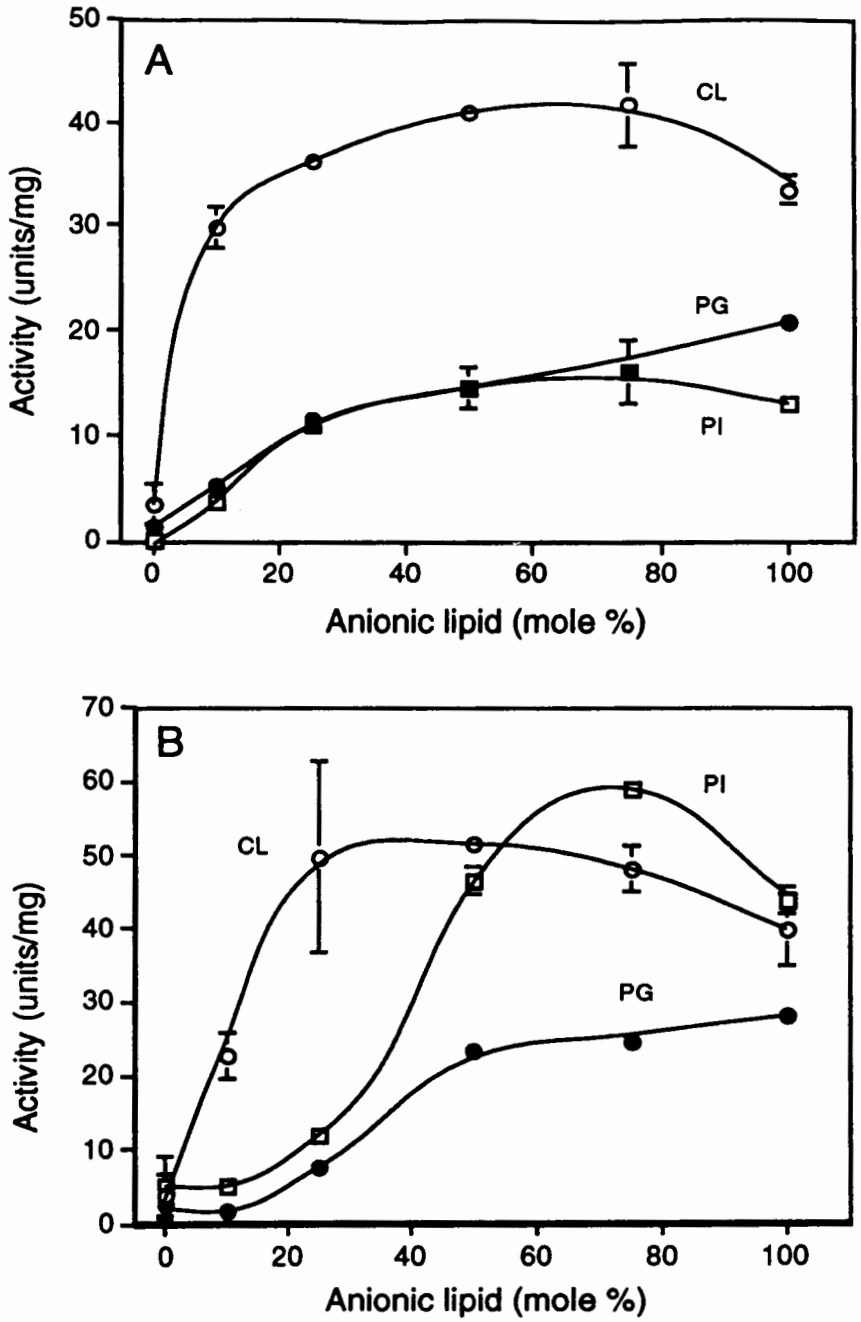

Figure 2.6: Dependence of rat-CT (A) or yeast-CT (B) activity on the mole % of anionic phospholipids.

Cytosolic extracts from COS cells were assayed in the presence of 100 μM SOPC vesicles containing the indicated mole % of anionic lipid : cardiolipin (CL, ○), PI (□), or PG (■). The total lipid concentration was 100μM in (A) and 5 μM in (B). Data are duplicate determinations of single experiments that were repeated twice with similar results.

2.3.4 Effects of neutral lipid activators

It has been shown that CT from mammalian sources binds and is activated by cellular or liposomal membranes enriched with diacylglycerol or other neutral lipids with small uncharged polar head groups (Sections 1.3.1.4 and 1.3.2.2). Anionic phospholipids are not needed in conjunction with the neutral lipid activator. Fig 2.7 compares the effects of three neutral lipids on the activities of yeast-CT and rat-CT: diacylglycerol (derived from egg PC), mono-oleoylglycerol and oleyl alcohol. The mol % of the neutral lipids was varied in SOPC vesicles up to 25%. All three lipids were activators of rat-CT activity (~10-fold stimulation). Diacylglycerol and oleyl alcohol did not stimulate rat-CT above 25 mol%. Diacylglycerol is known to induce non-bilayer phases above 25 mol% (De Boek & Zidovetzki, 1989), which could be related to the lack of stimulation. Yeast-CT activity was not affected by any of these lipids. Mole % curves were examined at three different total lipid concentrations (5, 25 and 100 μM), and no effect on yeast-CT activity was observed. Diacylglycerol, monoacylglycerol and oleyl alcohol were not metabolized to other lipid species, as evidenced by extraction and TLC analysis of the lipids (Section 2.2.3) after incubation with COS-cell cytosols under conditions identical with the enzyme assay (results not shown).

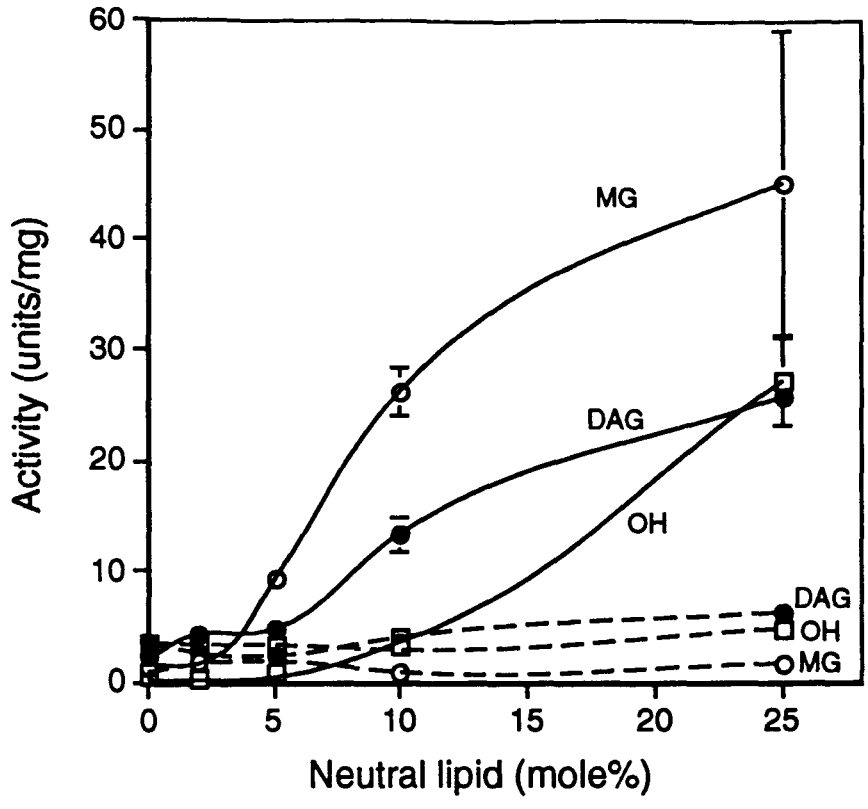

Figure 2.7: Dependence of CT activity on the mole % of neutral lipid in SOPC vesicles.

Cytosolic extracts from COS cells expressing rat-CT (*continuous lines*) or yeast-CT (broken lines) were assayed in the presence of 100 μM SOPC vesicles containing the indicated mole % of egg diacylglycerol (DAG, ●), mono-oleoylglycerol (MG, ○), or oleyl alcohol (OH, □). Data are duplicate determinations of single experiments that were repeated three times with similar results.

2.3.5 Translocation to microsomes

The preceding studies showed that yeast-CT and rat-CT activities have different sensitivities to lipid vesicles, yeast-CT being activated only by class I (anionic) lipids. We investigated whether yeast-CT and rat-CT can be distinguished by differences in enzyme binding to cell membranes enriched with lipids of class I or class II (neutral lipids). Microsomal membranes were used for this analysis, owing to the ease of separation of microsomal-bound CT from unbound CT. Microsomes were enriched with oleic acid, SOPC, diacylglycerol or sphingosine by incubation of the membrane suspensions with sonicated dispersions of oleic acid or sonicated vesicles of SOPC, SOPC/diacylglycerol (2:1) or SOPC/sphingosine (1:1). The extent of incorporation of oleic acid and sphingosine from the vesicles to the microsomes was virtually complete, as assessed by TLC of lipids extracted from the sedimented microsomes or supernatants (Fig. 2.8). In some experiments, a small fraction of the diacylglycerol was not incorporated into the microsomes. Yeast-CT or rat-CT binding to the enriched microsomes was assessed by sedimentation and assay of activity in the supernatant and pellet fraction at an optimum concentration of PC/oleic acid vesicles. In preliminary experiments, rat liver and COS-cell microsomes showed equally effective capacity to bind CT after oleic acid enrichment. Rat liver microsomes were used, due to a more abundant supply.

The results of the binding experiments are shown in Table 2.2. The CT activity endogenous to rat liver microsomes was subtracted from the total pellet-associated CT activity. The percentage distributions show that oleic acid promoted both rat-CT and yeast-CT binding. Diacylglycerol enrichment resulted

in a moderate increase in rat-CT binding, but had negligible affect on yeast-CT binding. Assuming complete incorporation of the added PC/diacylglycerol into microsomes, the diacylglycerol content was ~25 mol% of the total phospholipid. This experiment cannot give a good quantitation of the relative potency of oleic acid and diacylglycerol, as the exact amounts of each lipid incorporated into the membranes is not known. However, it is clear that there is a difference in the binding response of yeast CT and rat CT to diacylglycerol-containing membranes. Controls in which PC/oleic acid vesicles were incubated with cytosolic rat-CT or yeast-CT in the absence of microsomes demonstrated that the sedimenting CT activity represents microsome-bound CT and not dense CT aggregates promoted by contact with lipids. Minimal CT activity (<10%) appeared in the pellet after the standard centrifugation (results not shown).

Figure 2.8: TLC of lipid extracted from enriched microsomes.

Rat liver microsomes (0.4 mg protein, 130 nmol phospholipid) were incubated with 0.4 μMol of PC/sphingosine (1:1; **Sph**), PC/diacylglycerol (2:1; **DAG**), or oleic acid (**OA**) as described in Section 2.2.7, then centrifuged at 100 000*g* for 1 h. Lipids were extracted from the supernatant (**S**) and pellet (**P**) fractions and analyzed by TLC as described (Section 2.2.3). Solvent: (a) $CHCl_3$/MeOH/NH_3 (65:35:5 volume ratio), (b) hexane/diethyl ether/ acetic acid (60:40:1 volume ratio).

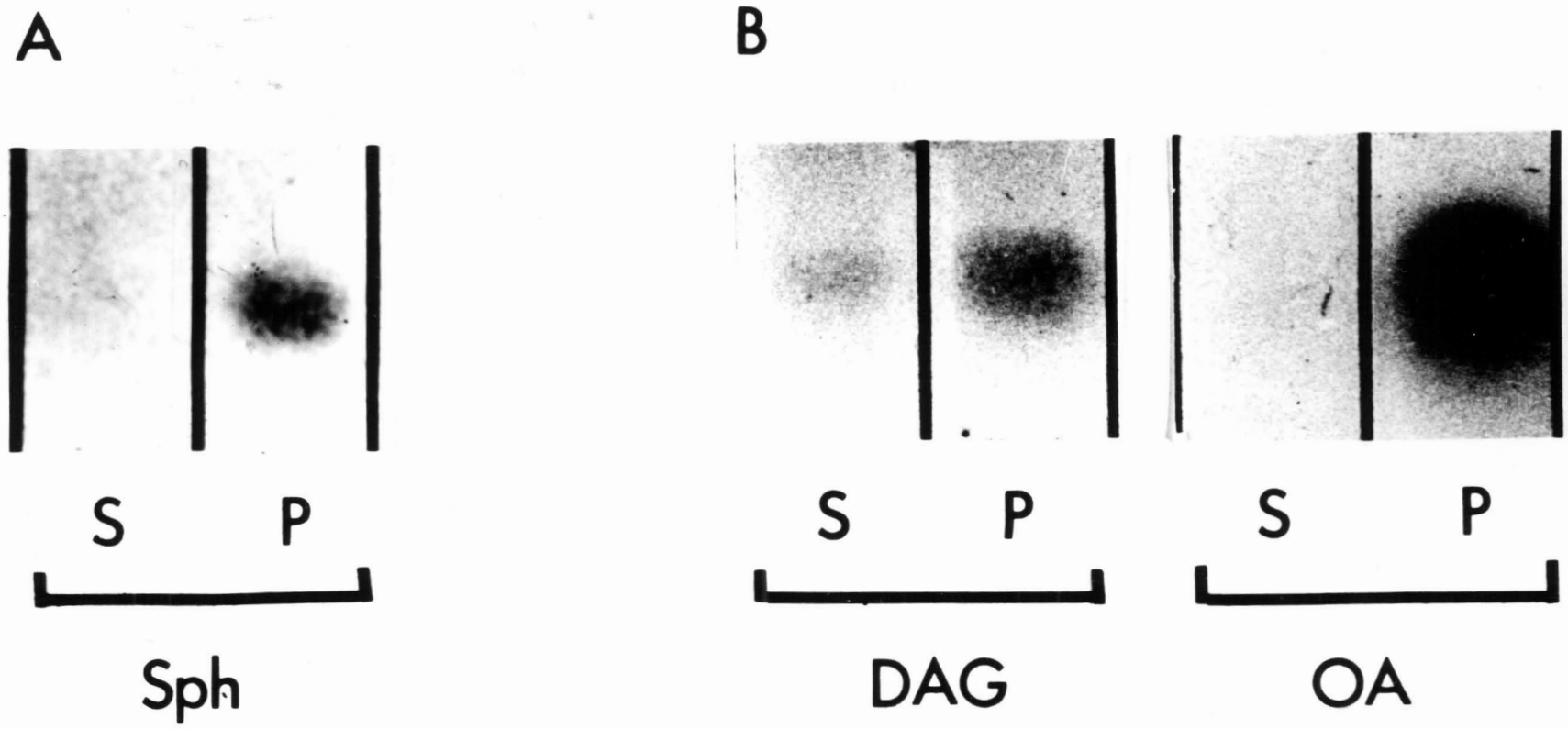
A
S
P
Sph
B
S
P
DAG
S
P
OA

Table 2.2: Yeast-CT and rat-CT translocation to lipid-enriched rat microsomes.

	RAT-CT		YEAST-CT	
Enriched Lipid	Sup.	Pellet	Sup	Pellet
None (N=3)	8.3 ± 0.3	1.7 ± 0.3	8.3 ± 0.7	1.7 ± 0.7
PC (N=4)	9.1 ± 0.2	0.9 ± 0.2	8.7 ± 0.9	1.3 ± 0.9
Oleic acid (N=2)	1.2 ± 0.1	8.8 ± 0.1	2.1 ± 1.0	7.9 ± 1.0
PC/sphingosine (N=2)	8.5 ± 0.4	1.5 ± 0.4	9.5 ± 0.1	0.5 ± 0.1
PC/diacylglycerol (N=3)	6.7 ± 0.5	3.3 ± 0.4	9.0 ± 0.3	1.0 ± 0.3

Rat-CT or Yeast-CT (10 units; 0.15 - 0.25 mg) from COS-cell cytosolic extracts were incubated with 0.25 mg of untreated rat microsomes or microsomes enriched in the indicated lipid, as described in Section 2.2.7. The samples were centrifuged at 100 000*g* for 1 h, and CT activity was determined in the supernatant and pellet fractions under optimal conditions for enzyme activity. For comparison, the numbers presented (units of CT activity) have been normalized to 10 units total. Recovery of added CT activity ranged from 60 - 90 %, except for yeast-CT treated with oleic acid, in which the recovery was 40 - 50 %. The lower recovery is due to the inhibitory effect of high concentrations of oleic acid in the membrane, see, *e.g.* Fig.2.2.

2.4 Discussion

2.4.1 Recombinant CT is activated by membrane in a manner similar to the native protein

This report presents a study of the lipid activation of recombinant rat-CT, overexpressed ~60-fold in a COS-cell system. A bimodal distribution of rat-CT was observed in this system, with the majority (80%) in the soluble fraction and a small fraction in the membrane, as has been previously noted (Section 1.3.1.2). The protein was not activated by membranes composed of PC alone, but was activated by membranes containing class I and class II lipid activators. The anionic lipids oleic acid, PI, PG, and cardiolipin stimulated rat-CT activity, as did the neutral lipids diacylglycerol, monoacylglycerol and oleyl alcohol. This is characteristic of CT activity in cell extracts, or purified from rat-liver (Section 1.3.2.2). The observed antagonism between oleic acid and sphingosine has been previously documented for purified rat liver CT (Sohal & Cornell, 1990). An *in vitro* translocation assay demonstrated rat-CT binding selectively to membranes containing class I or class II activators, which has been previously documented *in vitro* for CT from HeLa cells (Pelech *et al.*, 1984b; Cornell & Vance, 1987a & b) or rat lung (Weinhold *et al.*, 1984). Thus, recombinant rat-CT appears to interact with membranes with characteristics similar to native CT.

Subsequent studies have shown that the recombinant rat-CT used in this study (Kalmar *et al.*, 1990) contains two amino acid changes from natural CT, due to errors incorporated during PCR amplification of the clone (MacDonald & Kent, 1993). The mutant CT used in this study has membrane-interacting

characteristics similar to naturally occurring CT, which suggests that the changed residues are not involved in the binding or activation of CT by lipids. The changes occur at positions 91 (Gly to Ser) and 114 (Ser to Cys) of CT, which both fall in the proposed catalytic domain (Section 1.3.3.1). Consequences of these mutations have been investigated (Veitch & Cornell, 1994). The mutation at position 91, but not 114, resulted in a 20 - 50 fold increase in the K_m for the CTP, suggesting defective substrate binding.

2.4.2 Recombinant yeast-CT is responsive to the lipid environment

The activity of yeast-CT, overexpressed ~60 fold in the COS-cell system, was modulated by the presence of anionic lipids. The protein was located predominantly in the soluble fraction of the COS cells. Activity modulation was biphasic in that low amounts of anionic lipids caused enzyme activation, which diminished at higher lipid concentration. Cationic sphingosine antagonized this activation, suggesting that an electrostatic interaction was involved. Yeast-CT activity was unresponsive to non-anionic vesicles. An *in vitro* translocation assay demonstrated yeast-CT binding to membranes enriched in oleic acid, suggesting that physical binding may accompany activation. There are no other studies of the lipid activation of yeast-CT to aid in interpretation of the mechanism, nor is there any evidence that yeast-CT is regulated by membrane-binding *in vivo*. Thus, the results presented here are the first to demonstrate a potential regulatory mechanism for yeast CT by membrane composition.

CT in yeast was located primarily in the membrane fraction of homogenized cells (Tsukagoshi *et al.*, 1991). However, when overexpressed in *E.coli*, the enzyme was recovered in the soluble fraction, similar to our results,

suggesting that yeast possess a mechanism that promotes the membrane association of CT (Tsukagoshi *et al.*, 1991). Recent evidence points to the involvement of a lipid-binding, regulatory protein that targets CT (Skinner *et al.*, 1995). Sec14p, which functions *in vitro* as a PI / PC transfer protein, is a peripheral membrane protein that is necessary for secretion from the Golgi system, a requirement which can be bypassed by mutation of enzymes in the CDP-choline pathway (Cleaves *et al.*, 1991). The amount of functional Sec14p protein appeared to control the PC content of the Golgi membrane *in vivo*: mutations led to an accumulation, and overexpression led to a decrease of PC synthesized via the CDP-choline pathway (McGee *et al.*, 1994). Sec14p inhibited CT activity, *in vivo* and *in vitro*, under conditions where Sec14p was PC-bound (Skinner *et al.*, 1995). Thus, PC levels in yeast Golgi may be regulated by a lipid-binding protein, which inhibits yeast-CT activity when PC levels are high. Whether the mechanism of this regulation involves the interaction of yeast-CT itself with lipids has not been established.

2.4.3 Yeast-CT and rat-CT respond to lipids via different mechanisms

Two striking differences between the lipid response of yeast-CT and rat-CT were discovered. 1) Yeast-CT appeared to be modulated only in response to anionic lipids (class I), whereas rat-CT activity is modulated by both anionic and neutral lipids such as diacylglycerol (class II). 2) the activation of yeast-CT by anionic lipids occurred over only a small concentration range, and the maximum stimulation occurred at a 5-10-fold lower concentration than rat-CT. The difference in response of the two enzymes was observed both in activation and membrane binding. There are no other studies on the mechanism of yeast-CT-

membrane interactions to guide our explanations of the observed differences in lipid activation. The difference in the activation curves for the two enzymes suggests that yeast-CT does not interact with membranes via a mechanism similar to rat-CT, consistent with its lack of a potential amphipathic helix domain. However, lipid activation of yeast-CT suggests the protein may contain a distinct lipid-association domain. The finding that yeast-CT is modulated only by charged lipids suggests a role for electrostatic interactions in the protein-membrane interaction. The biphasic activation of yeast-CT by anionic lipids suggests that the protein may contain two lipid-interacting sites: a high-affinity stimulatory site and a low-affinity inhibitory site.

In conclusion, while the results presented here demonstrate, for the first time, an activation of yeast-CT by lipids, we are unable to make any strong conclusions regarding a role for the putative amphipathic α-helix region for membrane interactions in rat-CT.

CHAPTER THREE: ANALYSIS OF THE SECONDARY STRUCTURE AND LIPID-BINDING ABILITIES OF SYNTHETIC PEPTIDES CORRESPONDING IN SEQUENCE TO THE PUTATIVE AMPHIPATHIC HELICAL REGION OF CT

3.1 Introduction

Few studies had examined the details of membrane binding of CT at the molecular level. The protocol for purification (Weinhold *et al.*, 1986) produced CT that was very dilute and bound to detergent micelles (Triton X-100) which interfered with analysis. This motivated us to design a model system involving the use of synthetic peptides to study the membrane-binding characteristics of CT. If the putative amphipathic helix operates as a discrete domain within the enzyme to mediate membrane-binding, it is possible that a peptide corresponding to this region would behave in a similar manner. Synthetic peptides have previously been used to study the membrane interactions of the proposed N-terminal binding region of influenza hemagglutinin (Lear & Degrado, 1987; Claque *et al.*, 1991), the putative anionic lipid-binding region of the erythrocyte Ca^{+2} pump (Filoteo *et al.*, 1992), N-terminal signal sequences (Killian *et al.*, 1990; McKnight *et al.*, 1991), peptides derived from ion-channel proteins (Agawa *et al.*, 1991; Chung *et al.*, 1992), and other peptides which model the amphipathic helical structure (Kanellis *et al.*, 1980; Anantharamaiah *et al.*, 1985; Epand *et al.*, 1987).

Synthetic peptides based on the sequence of the proposed amphipathic α-helical, membrane-binding domain of CT allow us to address such questions as:

- Does this domain form an α-helical structure?

- Does this domain interact with membranes?
- What are the effects of CT lipid activators on the secondary structure of this domain?
- Does induction of a specific secondary structure coincide with membrane binding?
- How far into the membrane bilayer core does the domain penetrate?
- What components of this domain determine lipid specificity for binding?
- Do the lipids that stabilize a specific secondary structure correspond to those that are known to activate CT?

In order to investigate the structural and membrane-binding characteristics of the proposed amphipathic α-helix found in CT we have analyzed four synthetic peptides that correspond in sequence to (i) a 33 residue portion of the helix containing the three 11-mer repeats (ii) a peptide with the same sequence as in (i), with 3 serine residues changed to alanine to increase the hydrophobicity of the non-polar face (iii) a peptide corresponding to the N-terminal 33 residues of the amphipathic helical region of CT and (iv) a 62 residue peptide corresponding to the entire region (Fig. 3.1). The binding of the four peptides to vesicles was compared. Circular dichroism was used to analyze the influence of membranes on the secondary structure of the peptide. The membrane interactions of the peptide were studied by monitoring the fluorescence of a tryptophan residue on the hydrophobic face of the helix. The results support a model involving this amphipathic helical region in the membrane interactions of CT, and provide answers to the questions posed above regarding the mechanism.

Figure 3.1: Amino acid sequence of the synthetic peptides.
All peptides are acetylated on the N-terminus and aminated on the C-terminus. Underlines corresponds to residues changed from the original sequence.

PEPTIDE SEQUENCE:

		MW	NET CHARGE
PEP33	^{256}VEEKSKEFVQKVEEKSIDLIQKWEEKSREFIGS^{288}	4038	-2
PEPALA	^{256}VEEKAKEFVQKVEEKAIDLIQKWEEKAREFIGS^{288}	3990	-2
PEPNH1	^{236}NEKKYHLQERVDKVKKKVKDVEEKSKEWVQKVE^{268}	4167	+3
PEP 62:		7485	+1

^{238}KKYHLQERVDKVKKKVKDVEEKSKEFVQKVEEKSIDLIQKWEEKSREFIGSFLEMFGPEGAL^{299}

3.2 Experimental Procedures

3.2.1 Materials

Egg PC, dioleoyl-PG, 1-palmitoyl,2-oleoyl-PE, 1-palmitoyl,2-oleyl-phosphatidic acid (PA), beef heart cardiolipin (CL), 1-palmitoyl,2-stearoyl-6,7-dibromo-PC, 1-palmitoyl,2-stearoyl-9,10-dibromo-PC, 1-palmitoyl,2-stearoyl-11,12-dibromo-PC were purchased from Avanti Polar Lipids (Alabaster, AL). Sphingosine, oleic acid, oleyl alcohol, and *o*-phthaldialdehyde were from Sigma. *sn*-1,2-Diacylglycerol was generated as described (Section 2.2.1.1). Microcon-100 filtration units were purchased from Amicon (Beverly, MA). Lipids were stored in $CHCl_3$ stocks at -20 °C under nitrogen. The concentration and purity of these stocks was checked periodically as described (Section 2.2.3).

3.2.2 Peptide synthesis

Peptides corresponding in sequence to different portions of the amphipathic helix region of CT (Kalmar *et al.*, 1990) were synthesized and HPLC purified by Dr. Ian Clark-Lewis and Philip Owen (Univ. of British Columbia) as described (Clark-Lewis *et al.*, 1991). The sequences and calculated molecular weights corresponding to each peptide are shown in Figure 3.1. The peptides were acetylated on the N-terminus and aminated on the C-terminus to eliminate the charged groups. The peptides were stored as solids at -80 °C. For experiments, stock solution of the peptides (0.2 or 0.6 mM) were made in TE buffer (10 mM Tris-HCl, pH 7.4, 1 mM EDTA), or HEPES buffer (10 mM HEPES,

pH 7.4). Pep33 required 3 or 4 equivalents of NaOH added from a 1 M stock for solubility. The peptide stocks were made by weighing 1.00 to 2.50 mg of solid peptide to an accuracy of ± 0.01 mg. The peptide was dissolved in the appropriate volume of buffer (0.4 to 1.0 ml) with an accuracy of ± 0.005 ml to give a final concentration of 0.6 mM, which was confirmed by measuring the absorbance at 280 nm. The solutions were stored at -20 °C in aliquots which were thawed only once.

3.2.3 Gel filtration analysis of peptide aggregation state

A Sephadex G50 column (1cm x 30 cm) was equilibrated and eluted with TE buffer (10mM Tris, pH 7.4, 1mM EDTA) at a flow rate of 0.4 ml/min. Peptide samples (100 μg, 25 nmol) were in 200 μl TE buffer with 10 % glycerol. Protein elution was monitored by UV absorbance at 280 nm. An molecular weight (Mr) scale for the column was calibrated with cytochrome C (12400), aprotinin (6500), insulin (5700), and insulin treated with 50 mM DTT at 37 °C 2h to dissociate into β (3500) and α-(2200) subunits. V_o and V_t for the column were determined by using BSA (67000) and bromphenol blue (700), respectively.

3.2.4 Peptide-Vesicle Binding Assay

Peptide stocks and lipid vesicles (Section 2.2.4) used in this assay were made in 10 mM HEPES buffer, pH 7.4. Peptide (12 nmol) and varying amounts of lipid vesicles between 0 and 3600 nmol were incubated at room temperature for 10 min in a total volume of 200 μl 10 mM HEPES buffer, pH 7.4. Samples were then transferred to a Microcon-100 filtration unit (molecular weight cutoff of

100,000 Da) and centrifuged at 3000*g* for 4 to 7 min, until all but 5 to 10 μl had gone through the filter. The filter was rinsed with 100 μl HEPES buffer and centrifuged again for 2 to 3 min. Lipid vesicles and bound peptide were recovered from the filter by rinsing with 100 μl HEPES buffer which was then transferred to another vial. Unbound peptide was in the flow-through fraction under the filter. Unbound peptide was quantified with the *o*-phthaldialdehyde assay (Section 3.2.5). Lipids interfered with quantification of peptide in the retentate. The amount of lipid-bound peptide was calculated as (nmol peptide added - nmol peptide in flow-through). Volume partition coefficients (Table 3.6) were calculated using the equation: (nmol bound peptide/volume lipid) / (nmol free peptide/volume solution). Solution volume was 200 μl. Accessible lipid volume was estimated using a density of 1g/ml, taking into account that only ~½ lipid would be on the outer monolayer of the vesicles, accessible to peptide. Control proteins cytochrome C, lysozyme and apolipoprotein A-I were quantified by the method of Bradford (Section 2.2.2).

3.2.5 *o*-Phthaldialdehyde assay for peptide quantitation

For the membrane-binding assay described, peptide was quantified with a fluorescence assay involving a reaction with o-phthaldialdehyde as described by Roth (1971). *o*-Phthaldialdehyde reacts with the amine groups of peptides to produce a fluorescent product. Peptide samples were in HEPES buffer, as Tris contains free amines and would interfere with the peptide assay. Standard curves composed of 0 to 6 nmol of the peptide to be assayed were analyzed with each experiment. To a 100 μl sample of peptide was added 0.5 ml 0.05 M Borate buffer, pH 10, and 0.5 ml 0.5% (v/v) β-mercaptoethanol in ethanol,

vortexing well after each addition. *o*-Phthaldialdehyde (10 mg/ml in methanol) was diluted 10-fold in 0.05 M borate, pH 10, and 0.5 ml of this solution was added to the peptide assay solution with vortexing. The samples were incubated at room temperature for exactly 20 min before measurement, as the fluorescence intensity decayed slightly over time. The fluorescence intensity (excitation at 340 nm, emission at 440 nm) was proportional to the peptide concentration over the range used (0 to 6 nmol peptide). Fluorescence measurements were on a Perkin-Elmer MPF-44B fluorescence spectrophotometer. The presence of high amounts of lipids in the sample (>500 nmol) interfered with the fluorescence analysis.

3.2.6 Circular Dichroism

Sonicated lipid vesicles were prepared in TE buffer (10 mM Tris, pH 7.4, 1 mM EDTA)as described (Section 2.2.4) except that the sonication times were extended to a minimum of 20 min to reduce absorption and light scattering by the lipids in the samples. All vesicles were used the same day as preparation. The samples for spectroscopy were in TE buffer with a peptide concentration of 30 μM and lipid concentration of 4 mM, unless otherwise indicated. Background samples were composed of lipid vesicle suspensions lacking peptide. Samples were incubated for >10 min at room temperature before analysis.

All measurements were taken on a Jasco 700 spectropolarimeter using a 1 mm quartz cell at 25 °C. Each spectrum was measured twice at a 50 nm/min scan rate in steps of 0.5 nm, and the two were averaged and smoothed. Background spectra of the lipid vesicles in buffer were subtracted from the peptide spectra. Values are expressed as mean residue molar ellipticity [θ]. The

percent helix was estimated using the equation $\theta_{222} = (f_h - i\kappa/N)[\theta_{h\,222\,\infty}]$ where θ_{222} is the mean residue molar ellipticity at 222 nm; f_h is the fraction in α-helical form; i is the number of helices, (assumed to be one); κ is a wavelength-specific constant, with a value of 2.6 at 222 nm; N is the number of residues in the peptide; and $\theta_{h\,222\,\infty}$ is the molar ellipticity for a helix of infinite length at 222 nm, and has a value of -39,500 deg·cm^2/dmol (Chen *et al.*, 1974; Chang *et al.*, 1978; Sonnichsen *et al.*, 1992).

3.2.7 Fluorescence Studies

The samples in TE buffer contained 3.25 μM peptide and 0.5 mM lipid vesicles, unless otherwise indicated. At this concentration of well sonicated lipid vesicles (as described in Section 3.2.6), there was no interference from sample turbidity. For iodide quenching experiments, samples in TE buffer contained peptide, lipid, 10 mM $Na_2S_2O_3$, and the indicated concentration of NaI added from a 4 M stock. NaCl, which does not quench fluorescence, was added to maintain a constant ionic strength of 0.2 M. When cesium was used as the quencher, CsCl was added from a 4 M stock, and NaCl was used to maintain constant ionic strength. In the case of quenching by brominated lipid, the specified dibromo PC was incorporated at the indicated mole % into lipid vesicles from a $CHCl_3$ stock as described in vesicle preparation (Section 2.2.4). Lipid and peptide were preincubated at room temperature for >10 min prior to recording spectra.

Spectra were recorded on a PTI-LS100 fluorescence spectrophotometer or a Perkin-Elmer MPF-44B fluorescence spectrophotometer, with emission and excitation slit widths of 3 nm and 8 nm, respectively. Samples were at room

temperature in a 1 cm quartz fluorescence cuvette. The excitation wavelength was 280 nm and the emission spectra were recorded from 300 to 440 nm. Spectra of background samples were recorded and the fluorescence in the absence of peptide was subtracted from the fluorescence obtained in the presence of peptide.

3.3 Results

3.3.1 Properties of the peptides

The sequence of the synthetic peptides are shown in Fig. 3.1. When plotted on an helical wheel projection (Fig. 3.2), each peptide is observed to be highly amphipathic, with a highly-charged polar face and a non-polar face. Each sequence contains a tryptophan residue, found on the non-polar face of the proposed helix. The fluorescence of this tryptophan could be monitored to assess changes in the environment of the peptide. Four peptides corresponding to the putative amphipathic α-helix region of CT were studied:

- *Pep33* corresponds to residues 256 to 288 in rat-liver CT. This peptide was the first chosen for study as it consists of three 11 residue repeats, which implied a functional role in the protein. The peptide, with a net charge of -2, contains nine negatively charged and seven positively charged residues. There are three serine residues in register which interrupt the otherwise hydrophobic face of the helix.
- *PepAla* corresponds to the same sequence as Pep33, except the three serine residues on the hydrophobic face are changed to alanine. This peptide was designed to analyze the role of these serine residues. Alanine lacks the hydroxyl side-chain, thus would increase the hydrophobicity of the non-polar face of the helix.
- *PepNH1* corresponds to the N-terminal 33 residues of the amphipathic α-helix of CT (residues 236 to 268). This peptide, with a net charge of +3, has 8 negatively charged and 11 positively charged residues, as well as a

histidine residue. As this region contained no tryptophan residue, a Trp residue was substituted for Phe at residue 263. Similar substitutions have been implemented in studies of other peptides, with no change in properties (Killian, *et al.*, 1990; McKnight *et al.*, 1991).

- *Pep62* corresponds to the entire amphipathic α-helix region of CT (residues 238 to 299), which constitutes a discrete exon in the mouse CT gene (Rutherford *et al.*, 1993). This peptide, with a net charge of +1, contains 14 negatively charged and 15 positively charged residues, as well as one histidine residue.

In dilute buffer, the majority of each 33-residue peptide, Pep33, PepNH1, PepAla, eluted from a Sephadex G-50 gel filtration column with apparent molecular weights of approximately 8000 when compared to insulin α and β chains, aprotinin and cytochrome C standards (Fig. 3.3), demonstrating that the peptides are not associated in a large aggregate. The molecular weight of the peptide monomer is ~4000. Thus, the peptides elute with an apparent molecular weight of a dimer. Approximately 5 - 10% of the PepAla eluted as a large aggregate (MW > 66,000) in the void volume of the column. Pep62 was not analyzed by gel filtration.

Figure 3.2: Helical wheel projections of the peptides.

Hydrophobic residues are shaded, demonstrating the amphipathic nature of the helix.Dotted lines indicate the approximate polar and non-polar interfaces.

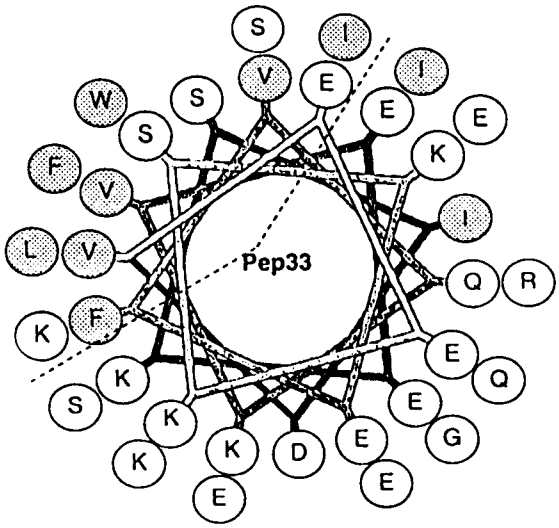
S
I
V
E
I
W
S
E
E
S
K
F
V
I
L
V
Pep33
Q
R
K
F
E
K
Q
S
E
K
G
K
K
D
E
E
E

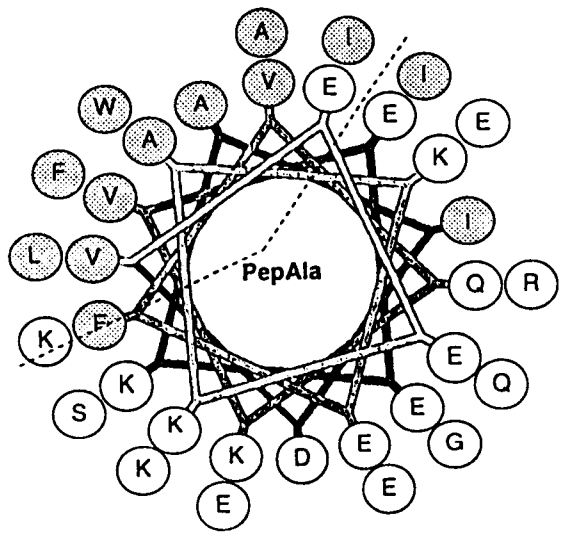
A
I
V
E
I
W
A
E
E
A
K
F
V
I
L
V
PepAla
Q
R
K
F
E
K
Q
S
E
K
G
K
K
D
E
E
E

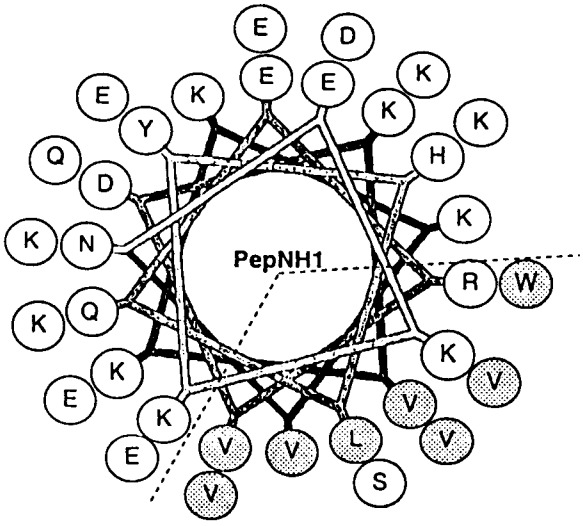
PepNH1

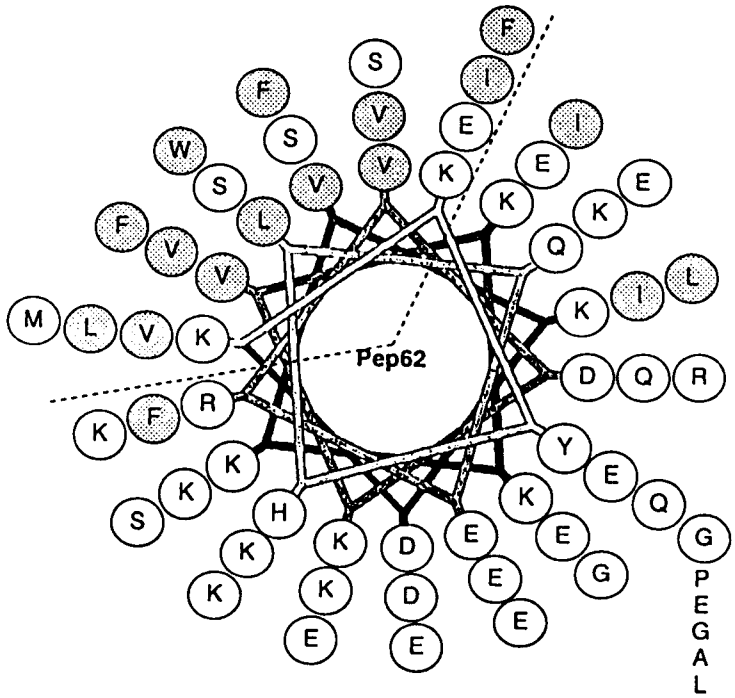
Pep62
PEGAL

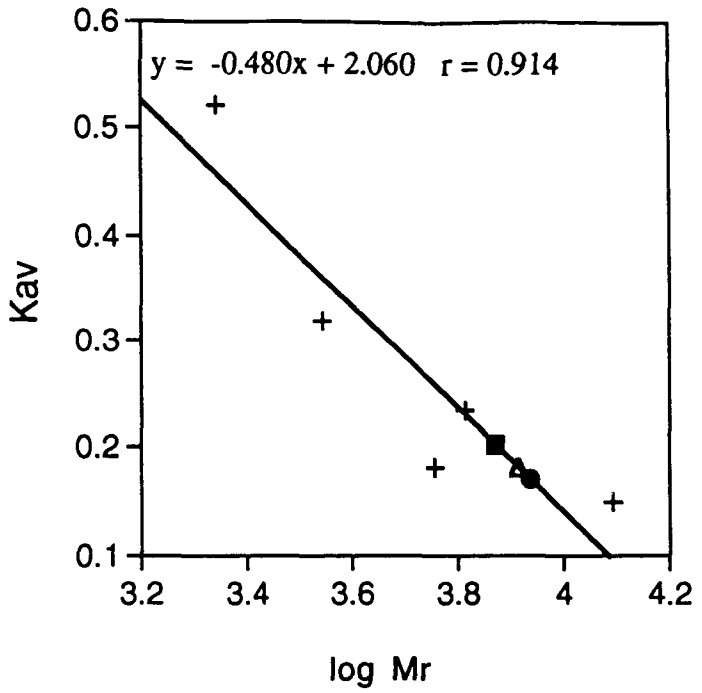

		K_{av}	$logM_r$	M_r
Pep33	■	0.202	3.871	7500
PepAla	Δ	0.181	3.914	8100
PepNH1	●	0.170	3.937	8600

Figure* 3.3: *Determination of the aggregation state of the peptides by gel filtration. Pep 33 (■), PepAla (Δ), PepNH1(●),and the standard proteins cytochrome C, aprotinin, insulin and insulin a and b subunits (+) were chromotographed on a Sephadex G-50 column as described in Section 3.2.3. An equation was determined to describe the linear plot of K_{av} versus log M_r for the standard proteins, and was used to calculate the apparent M_r for the peptides.

3.3.2 Circular Dichroism Indicates a Propensity of the Peptides for a Helical Conformation

The CD spectra were measured to determine the preferred secondary structure of the peptides, especially the propensity to form the predicted α-helix. All peptides in the simple TE buffer alone gave a CD spectrum that is indicative of a predominantly random structure with only a small amount of helix, 12-14% (Fig. 3.4, Table 3.1). Trifluoroethanol (TFE) is a solvent which promotes any favoured secondary structure in peptides and proteins by promoting intramolecular hydrogen bonding (Sonnichsen *et al.*, 1992). The presence of 50% TFE in TE buffer changed the spectrum of each peptide to one indicative of an α-helical structure, with the characteristic minima at 208 nm and 222 nm (Fig. 3.4). The helical content of the peptides in TFE was estimated to be approximately 50% (Table 3.1).

Figure 3.4: Circular dichroism spectra of the peptides.

CD spectra of peptide (30 μM) in buffer (solid line), in a 50% trifluoroethanol solution (– – –), in the presence of PC vesicles (4 mM; ····) or PG vesicles (4 mM;– . – . –). **A**, Pep33; **B**, PepNH1; **C**, PepAla; **D**, Pep62.

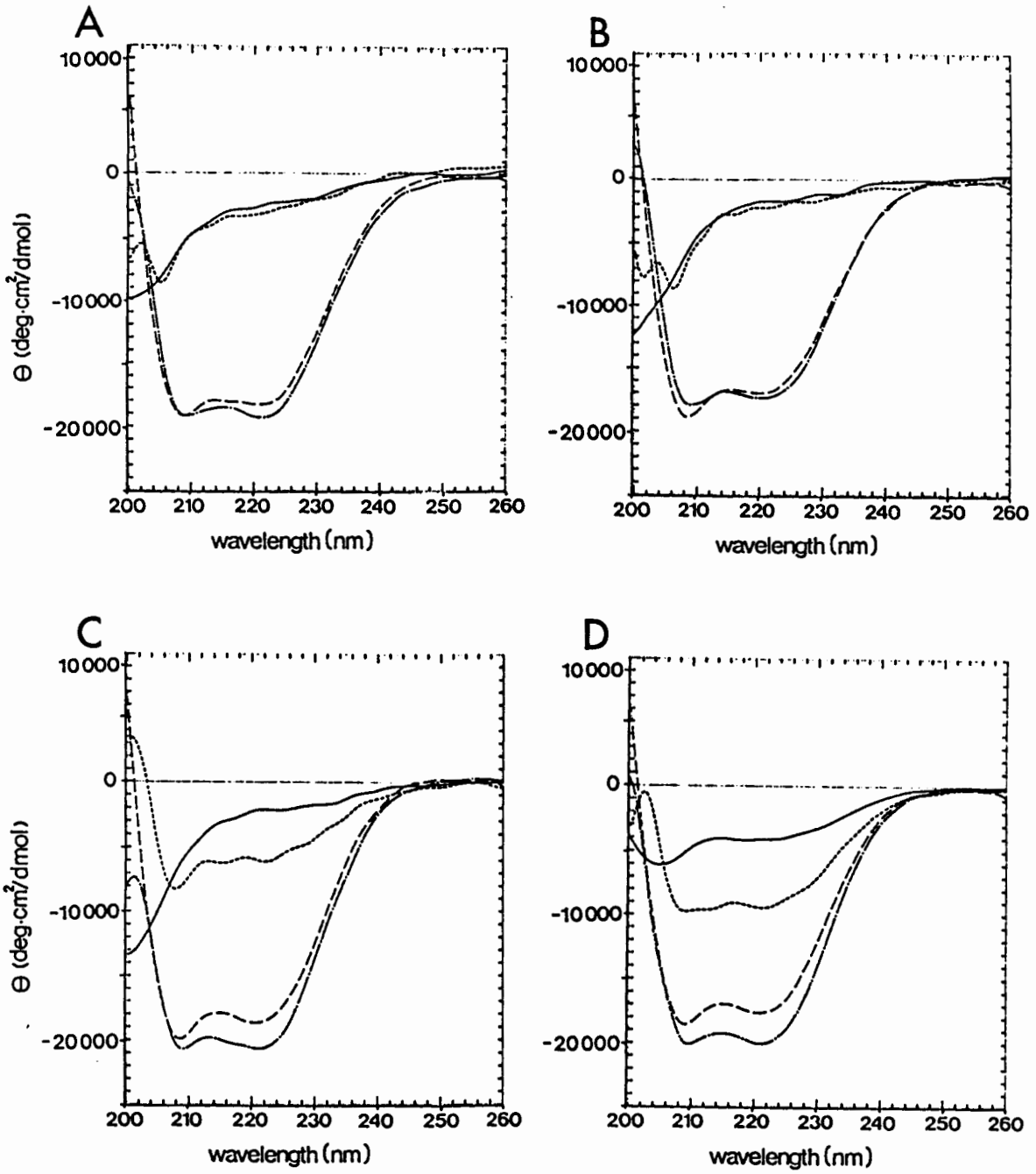
A
B
C
D
10000
0
-10000
-20000
Θ (deg·cm²/dmol)
200 210 220 230 240 250 260
wavelength (nm)

TABLE : 3.1

Circular Dichroism Analysis of Peptides with Various Lipid Vesicles

LIPID	- $[\Theta]_{222}$ deg cm^2/dmol (Estimated % Helix)			
	Pep33	PepAla	PepNH1	Pep62
none	2500 ± 300 (14 %)	1900 ± 250 (13 %)	1760 ± 20 (12 %)	3800 ± 300 (14 %)
PC	3100 ± 700 (16 %)	6100 (23 %)	2200 (14 %)	8700 ±800 (26 %)
PC/ diacylglycerol (3:1)	2300 ± 300 (13 %)	7600 ± 300 (27 %)	2300 ± 500 (14 %)	6800 ± 800 (21 %)
PC/ sphingosine (1:1)	3500 ± 30 (17 %)	11500 (37 %)	1500 (12 %)	9500 (28 %)
PG	19000 ±1500 (57 %)	17000 ± 3000 (52 %)	16500 ± 800 (50 %)	19000 ± 1200 (52 %)
PC/oleic acid (1:1)	18000 ± 2000 (55 %)	20000 (58 %)	16000 (48 %)	18000 ± 1000 (51 %)
in 50% TFE	18200 ± 700 (54 %)	17500 ± 1000 (52 %)	17700 ± 900 (54 %)	15000 ± 2500 (43 %)

Samples contained 30 μM peptide and 4 mM lipid, unless otherwise indicated. Spectra were measured, and % helix estimated from $[\Theta]_{222}$ as described in Section 3.2.6. Pep33 data are from Table 3.2. Data for other peptides are average ± range of 2 separate experiments, except for values without indicated error, which were performed only once

3.3.3 Anionic Lipid Vesicles Promote an α-Helical Structure

The preceding CD experiments show that the peptides do have the propensity to form an α-helical structure. Next, we sought to examine the effect of membranes, in the form of small unilamellar vesicles, on the secondary structure of the peptides in buffer. Fig. 3.4 shows the CD spectra of the peptides in the presence of lipid vesicles composed of PG, an anionic phospholipid. The presence of PG vesicles caused a change in each spectrum from that seen in buffer alone, to one characteristic of an α-helical structure. The percent helicity was similar to that obtained in the presence of 50% TFE. Addition of PC/oleic acid vesicles caused a similar change in the CD spectrum for all peptides (Table 3.1). The CD spectrum of Pep33 was 50 to 60 % helical in the presence other anionic vesicles such as PA, PI, PS and PC/CL (Table 3.2). All of these lipids activate rat-liver CT (Section 1.3.2.2). Addition of PC vesicles to the peptide caused no change in the CD spectrum of Pep33 or PepNH1, and only a small change in the spectrum of PepAla or Pep62 from that in buffer alone (Fig. 3.4; Table 3.1). Other non-anionic lipid vesicles such as PC/PE, (3:1), PC/oleyl alcohol (1:1), as well as the cationic vesicles PC/sphingosine (1:1) did not cause a change in the CD spectrum of Pep33, indicating that the peptide remained in a predominantly random form (Table 3.2). Addition of PC/diacylglycerol or PC/sphingosine did not change the spectra of Pep33 or PepNH1, but did cause a small increase in the helical content of PepAla and Pep62. These results, summarized in Tables 3.I and 3.2, show that there is a lipid induced change in the conformation of each peptide from a primarily random structure to an α-helix, and that this conformational change is selective for anionic lipid vesicles. Selectivity for anionic lipids is more pronounced for Pep33 and PepNH1.

TABLE 3.2:

Circular Dichroism Analysis of Pep33 with Various Lipid Vesicles

LIPID	N	$-[\Theta]_{222}$ (deg cm^2/dmol)	ESTIMATED % HELIX
none	12	2500 ± 300	14
PC	4	3100 ± 700	16
PC/PE (1:1)	2	3800 ± 400	18
PC/diacylglycerol (3:1)	2	2300 ± 300	13
PC/oleyl alcohol (1:1)	2	3000 ± 1000	15
PC/sphingosine (1:1)	2	3500 ± 30	17
PG	5	19000 ± 1500	57
PC/oleic acid (1:1)	4	18000 ± 2000	55
PA	3	21700 ± 900	63
PI	2	25000 ± 3000	72
PS	2	24000 ± 2000	69
PC/CL (1:1)	3	22000 ± 2000	63
in 50% TFE	7	18200 ± 700	54

Samples contained 30 μM peptide and 4 mM lipid, unless otherwise indicated. Spectra were measured as described Section 3.2.6. $[\Theta]_{222}$ is the mean residue molar ellipticity value calculated at 222 nm. % Helix was estimated from $[\Theta]_{222}$ as described in Section 3.2.5.

The structural change of Pep33 induced by anionic lipids was examined in more detail. The effect of anionic lipids on Pep33 conformation was concentration dependent, saturating at a lipid to protein ratio of 33:1 - 66:1 (1 to 2 mM PG), which corresponds to 60 - 120 peptide molecules for each vesicle, assuming 4000 PG molecules per vesicle (Fig. 3.5a). Pep33 conformation showed a dependence on the mole % of anionic lipid in the vesicles (Fig. 3.6a). The presence of PG (charge -1) at 30 mole% in PC vesicles caused little change in the peptide structure from that in the presence of PC, whereas, 40 mole% PG induced the maximal degree of helicity. PA (charge of -2) promoted a conformational change between 20 and 30 mole%. This suggests that there is a minimum charge required on the membrane surface for the peptide to assume an α-helical conformation. A similar sigmoidal charge dependence has been observed for the activation of the native CT enzyme (Cornell, 1991a).

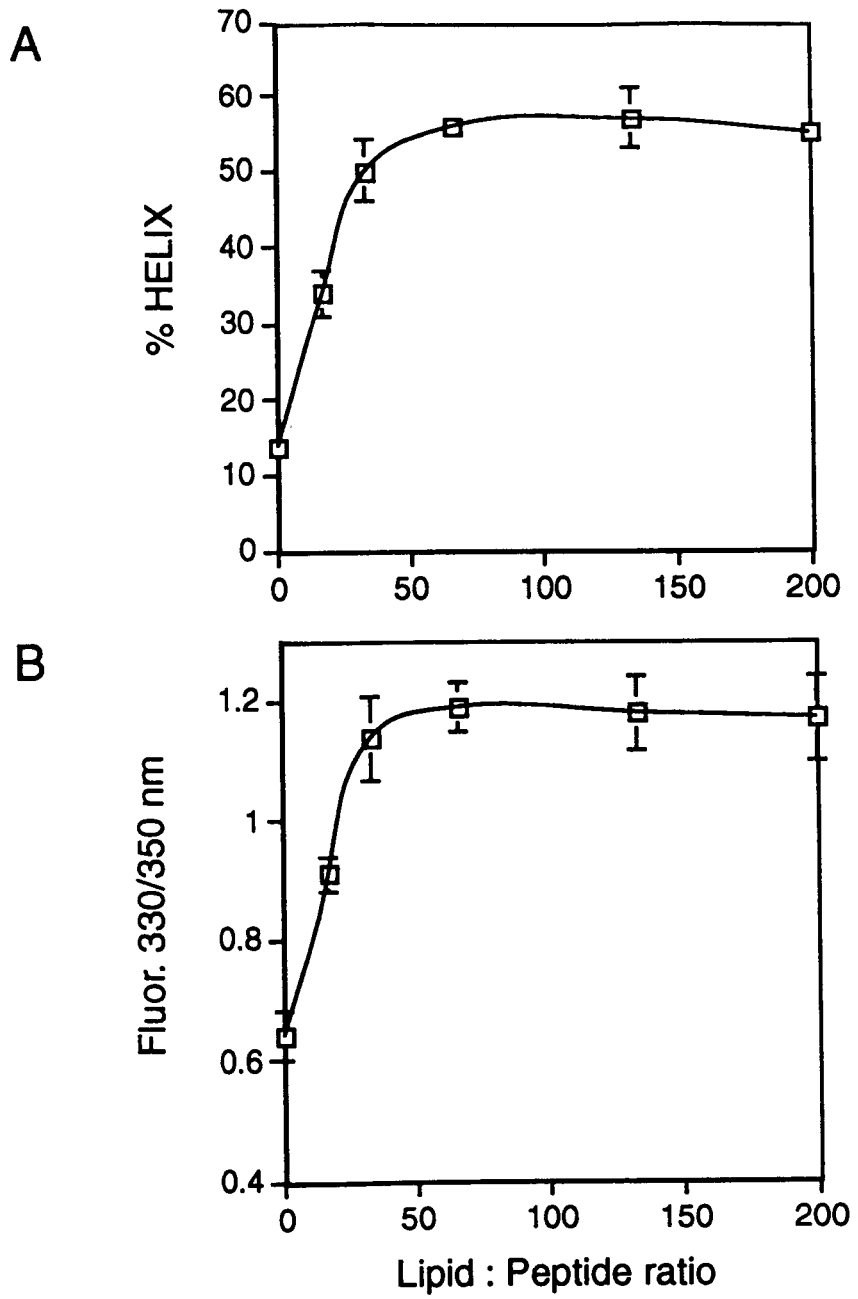

Figure 3.5: Dependence of peptide properties on anionic lipid : peptide molar ratio.
(**A**) Calculated helicity of Pep33 (30 μM) with various amounts of PG vesicles. Spectra were measured and percent helix calculated as described in Section 3.2.5. (**B**) Ratio of fluorescence intensity at 330 nm : 350 nm of Pep33 (3.25 μM) with various amounts of PG vesicles. Data are the average of 2 determinations.

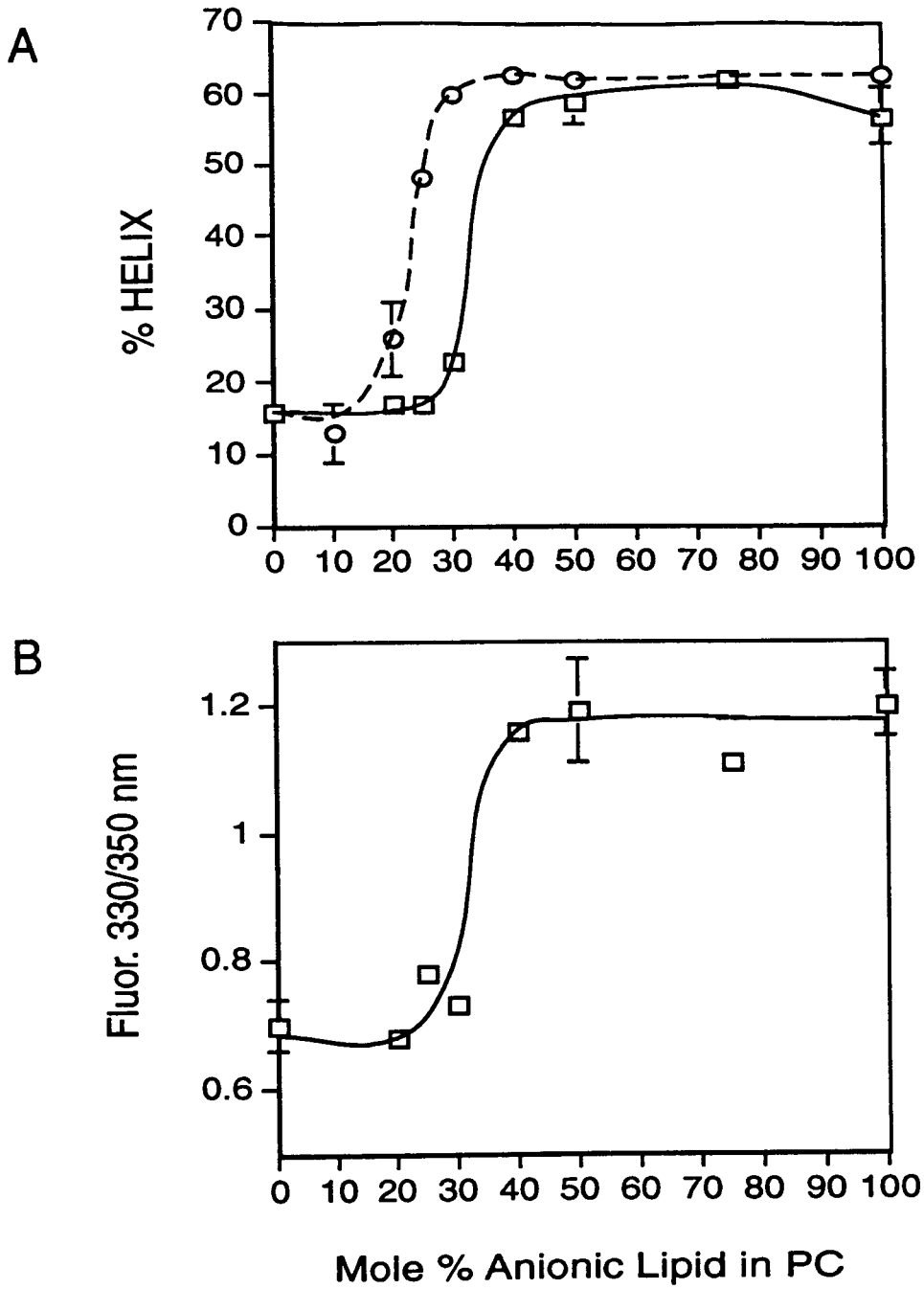

Figure 3.6: Dependence of peptide properties on mole % anionic lipids in PC membranes. (**A**) Calculated helicity of Pep33 (30 μM) in the presence of egg PC vesicles with various mole % PG (□) or PA (o) (4 mM total lipid). Spectra were measured and percent helix calculated as described in Section 3.2.5. (**B**) Ratio of fluorescence intensity at 330 nm:350 nm of Pep33 (3.25 μM) with various mole % PG (□) (0.5 mM total lipid). Data are the average of 2 determinations.

3.3.4 Anionic Lipid Vesicles Promote a Blue Shift in the Fluorescence Emission

The results of the CD experiments demonstrate that the peptides assume an α-helical conformation in the of presence vesicles, with selectivity for anionic lipid . Figure 3.2 shows that the helix formed by each peptide would be highly amphipathic, with a very highly charged polar face and a non-polar face. This leads to a model of peptide-vesicle interaction involving the hydrophobic face of the helical peptide interacting with the hydrophobic membrane. To investigate this possibility, we monitored the fluorescence of a tryptophan residue which resides in the non-polar face of the peptide helix. The tryptophan emission spectrum undergoes a characteristic shift in the emission maximum to a shorter wavelength and an increase in quantum yield when the residue shifts from an aqueous to a hydrophobic environment (Lakowicz, 1983). This "blue shift" in the tryptophan fluorescence would be evident if the aqueous peptide were to bind to lipid vesicles with its hydrophobic face intercalating into the membrane.

Figure 3.7 shows the fluorescence spectrum of Pep33 in buffer, excited at 280 nm. The spectrum of the peptide is indistinguishable from that of free tryptophan in an aqueous environment, with a characteristic emission maximum of 350 nm. Upon addition of PG vesicles (Fig. 3.7) the emission maximum shifted -20 nm to 330 nm, and the intensity of the fluorescence increased, indicative of a shift of the tryptophan to a more hydrophobic environment. This shift resulted in an increase in the intensity ratio of 330 nm : 350 nm (Table 3.3). Other anionic vesicles, such as PC/oleic acid caused a similar shift in the emission maximum of the fluorescence spectra (Table 3.3). However, addition of PC vesicles to the Pep33 caused no change in the fluorescence spectrum (Fig.

3.7; Table 3.3). Similarly, other non-anionic lipid vesicles such as PC/sphingosine, PC/diacylglycerol caused no change in the spectrum of Pep33 (Table 3.3).

The tryptophan fluorescence of PepALA and PepNH1 was monitored in the absence or presence of various lipid vesicles. The spectra for these peptides in the absence of lipids were identical to that of Pep33 (Fig. 3.7, data not shown). For each peptide, addition of anionic vesicles composed of PG or PC/oleic acid increased the fluorescence intensity and shifted the emission maximum from 350 nm to 330 nm, as demonstrated by the increased ratio of intensity at 330 nm : 350 nm (Table 3.3). Non-anionic lipids, such as PC/diacylglycerol or PC/ sphingosine caused no change in the fluorescence peak or intensity of PepNH1 (Table 3.3). These non-anionic lipids did, however, slightly increased the fluorescence intensity of PepAla and caused the appearance of second maxima at 330 nm of equal or less intensity than the peak at 350 nm (Table 3.3). Thus, PepAla appeared to respond to these lipids, but to a lesser extent than to anionic lipids.

For Pep33, the appearance of the peak at 330 nm was dependent on the concentration of anionic vesicles added (Fig. 3.5B). At a lipid to protein ratio of 17:1 (62.5 μM PG) the 330 nm peak consisted of a shoulder on the 350 nm peak. At a lipid to protein ratio of 33:1 (125 μM PG) the spectrum showed a peak at 330 nm, and further increases in the lipid concentration had no effect (Fig 3.5B). An all-or-nothing change in the spectrum was observed in these fluorescence experiments as in the CD experiments between 30 and 40 mole% PG in PC vesicles (Fig. 3.6B). Thus, the induction of the helical conformation in the peptide, as observed in the CD experiments, correlated very well with a shift of the tryptophan to a more hydrophobic environment, as observed in the fluorescence experiments (Fig. 3.5 and 3.6).

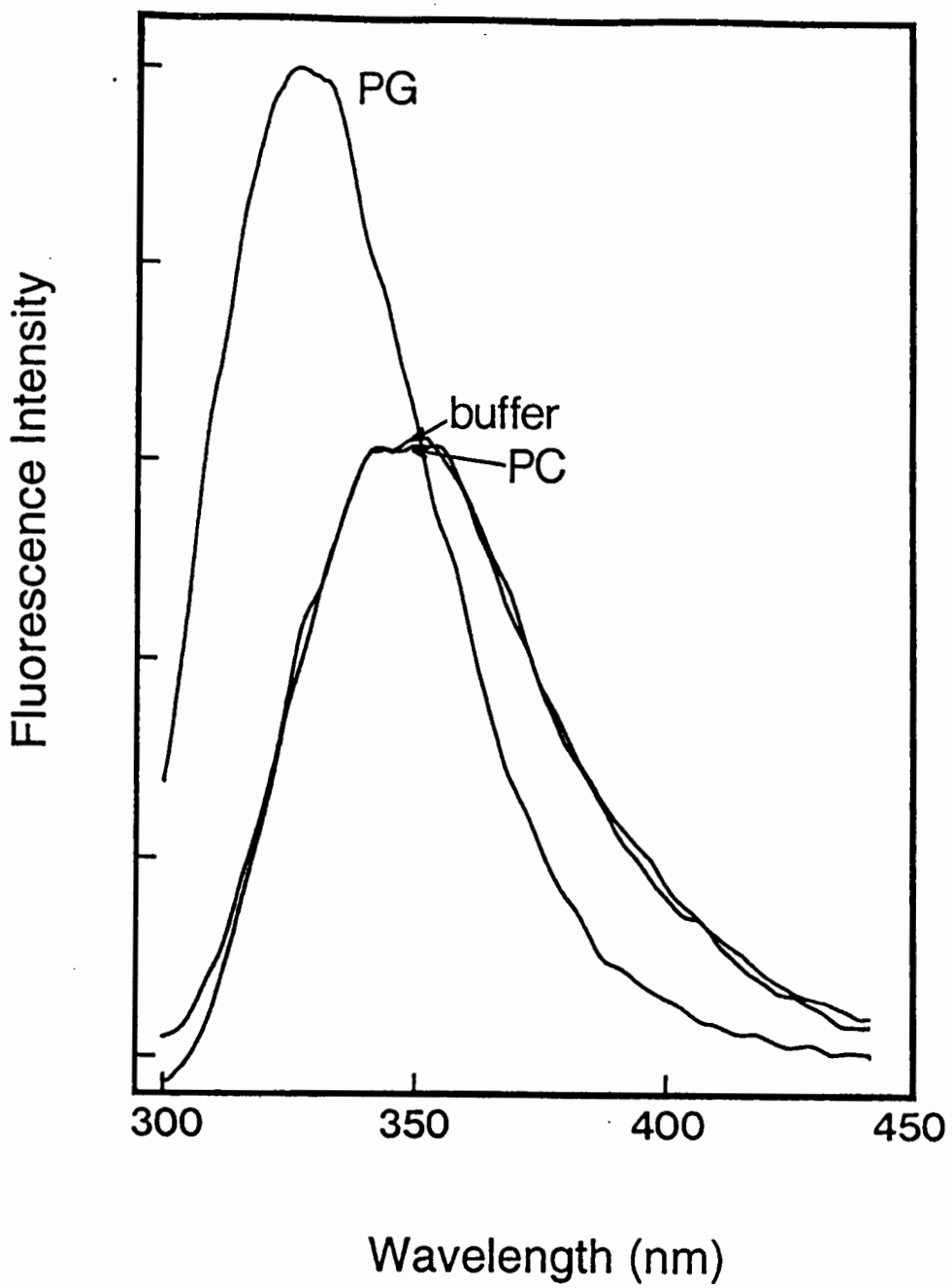

Figure 3.7: Tryptophan fluorescence of Pep33.
Fluorescence emission spectra of Pep33 (3.25 μM) in buffer, and in the presence of 0.5 mM DOPG or egg PC vesicles. The excitation wavelength was 280 nm.

TABLE 3.3: Ratio of fluorescence intensity at 330 nm : 350 nm

LIPID	330 nm / 350 nm		
	Pep33	PepAla	PepNH1
none	0.62 ± 0.05	0.59 ± 0.01	0.55 ± 0.03
PG	1.14 ± 0.07	1.15 ± 0.03	1.04 ± 0.02
PC/oleic acid (1:1)	1.07 ± 0.01	1.21 ± 0.02	1.01 ± 0.03
PC	0.68 ± 0.03	0.68	0.58
PC/diacylglycerol (3:1)	0.69 ± 0.03	0.9 ± 0.2	0.60 ± 0.03
PC/sphingosine (1:1)	0.64 ± 0.01	1.07 ± 0.09	0.62 ± 0.03

Lipid vesicles were present at 0.5 mM . Peptide concentration was 3.25 μM. Fluorescence spectra were measured as described in Section 3.2.7. Data are the average ± standard deviation of 3-4 separate experiments, except for PepAla and PepNH1 in the presence of PC, which was measured only once.

3.3.5 Anionic Lipid Vesicles Shield the Peptide from Aqueous Iodide Quenching

The tryptophan environment was also monitored by its accessibility to quenchers. An aqueous phase quencher, such as iodide, can quench the fluorescence of tryptophan upon collision with the molecule (Lakowicz, 1983; Eftink, 1991). If the tryptophan is not accessible to the aqueous environment, as is the case if the residue is buried in a membrane or in the interior of a protein, the aqueous quenchers will be less able to affect the fluorescence.

Figure 3.8a shows the spectrum of the Pep33 in TE buffer + 0.2 M NaCl, which is identical to the spectra of peptide in TE. NaCl does not quench fluorescence, and was present to maintain a constant ionic strength among all samples. When NaCl was replaced by 0.2 M NaI, there was a 46% reduction in the intensity of the fluorescence at 350 nm. Figure 3.8b shows the spectrum of the peptide in similar buffer containing PG vesicles, with its characteristic peak at 330 nm. Addition of iodide resulted in only a 15 % quenching of the fluorescence peak in this case, suggesting that the presence of the vesicles shields the tryptophan from the aqueous iodide. Similar results were observed for PepNH1 and PepAla (Table 3.4). A decrease in the iodide quenching was also observed in the presence of PC/oleic acid vesicles, which were most effective shields for PepAla. For Pep33 and PepNH1, the quenching in the presence of non-anionic vesicles was similar to that obtained in the absence of lipid (Table 3.4). The presence of PC/diacylglycerol vesicles slightly decreased the iodide quenching of PepAla, suggesting that the tryptophan is shielded to a greater extent than Pep33 in the presence of these vesicles. The presence of sphingosine did not

affect the quenching by iodide. To ensure that anionic iodide was not interacting with the charged membrane surface, similar experiments were performed using the cation cesium as the aqueous quencher. Anionic vesicles protected all three peptides from quenching by Cs^+. Non-anionic vesicles had no affect on Pep33 or PepNH1 while PC/diacylglycerol and PC/sphingosine protected PepAla from quenching by Cs^+ (data not shown).

A quantitative expression for this type of quenching is the Stern-Volmer plot, which relates the fluorescence quenching to the concentration of quencher by the following equation: $F_0 / F = \mathbf{K_{SV}}$ [*quencher*] + 1, where F_0 is the peak fluorescence intensity in the absence of quencher, F is the peak fluorescence intensity in the presence of quencher, and K_{SV} is the Stern-Volmer quenching constant, which can be obtained as the slope of a plot of F_0/F vs. concentration of quencher (Lakowicz, 1983; Eftink, 1991). If a fluorophore becomes less accessible to the quencher, the lower quenching probability will be reflected in a lower K_{SV} value. Figure 3.9 shows the Stern-Volmer plot of iodide quenching for Pep33 in buffer and in the presence of PC, PG, or PC/oleic acid. The similar slopes for peptide in buffer and in the presence of PC suggest that the peptide tryptophan remains in a similar aqueous environment upon addition of PC vesicles. However, the slope is much lower for the peptide in the presence of either PG or PC/oleic acid vesicles, suggesting that the tryptophan is much less accessible to the aqueous environment in the presence of these anionic lipid vesicles.

Figure 3.8: Quenching of tryptophan fluorescence of Pep33 by aqueous iodide.

Fluorescence emission spectra of Pep33 (3.25 μM). The excitation wavelength was 280 nm. Unquenched peptide was in 0.2 M NaCl. Quenched peptide was in 0.2 M NaI. (**A**) Pep33 in buffer. (**B**) Pep33 in the presence of 0.5 mM DOPG vesicles.

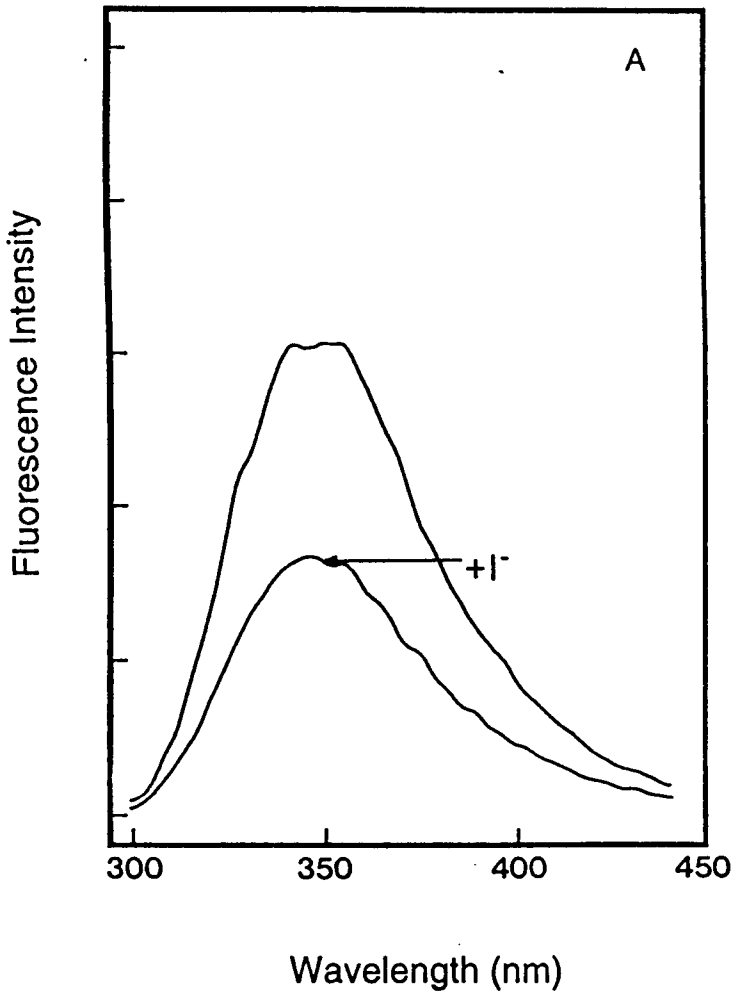
A
Fluorescence Intensity
+I⁻
300
350
400
450
Wavelength (nm)

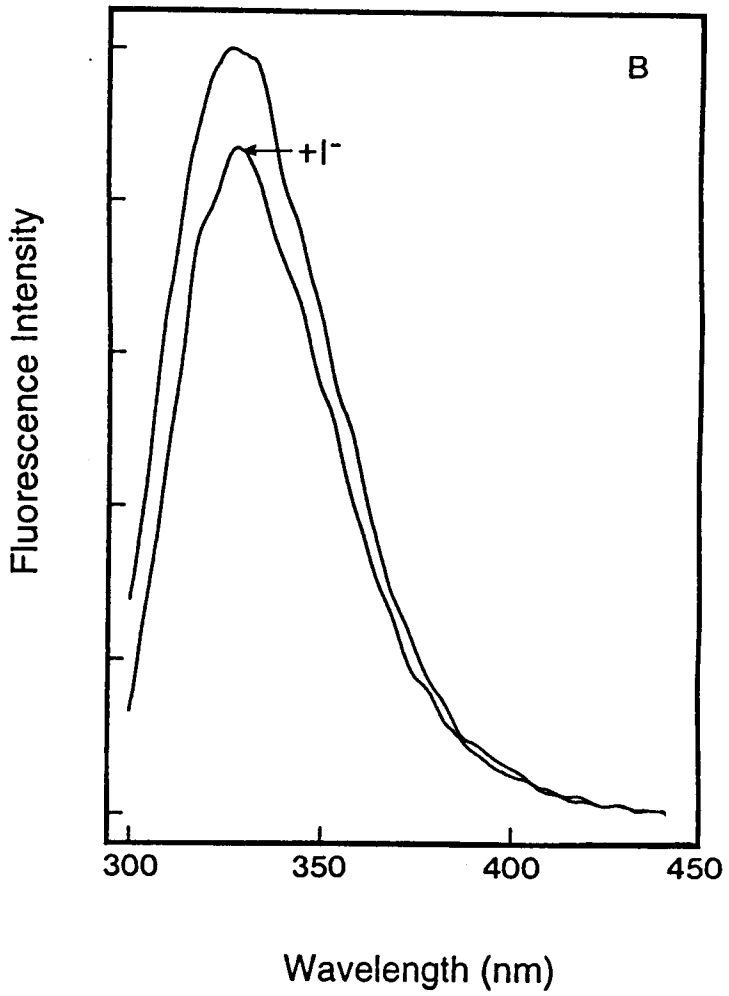
B
Fluorescence Intensity
+I⁻
300
350
400
450
Wavelength (nm)

TABLE 3.4:

Quenching of Peptide Fluorescence by 0.2 M Aqueous Iodide

LIPID	% QUENCH		
	Pep33	PepAla	PepNH1
none	48 ± 4	55 ± 2	58 ± 1
PG	15 ± 2	11 ± 1	12 ± 4
PC/oleic acid (1:1)	24 ± 3	9 ± 5	27 ± 1
PC	45 ± 1	N/D	N/D
PC/diacylglycerol (3:1)	47 ± 6	38 ± 3	60 ± 3
PC/sphingosine (1:1)	51 ± 3	52 ± 0	62 ± 1

Lipid vesicles were present at 0.5 mM or 1 mM (for PC/oleic acid). Peptide concentration was 3.25 μM. Spectra were measured as described in Section 3.2.7. Data are the average ± standard deviation of 2-4 separate experiments. % Quench = $100(1 - F/F_0)$, where F is the fluorescence intensity of the quenched sample obtained in the presence of 0.2 M iodide, and F_0 is the fluorescence intensity of the unquenched sample with 0.2M chloride in place of iodide.

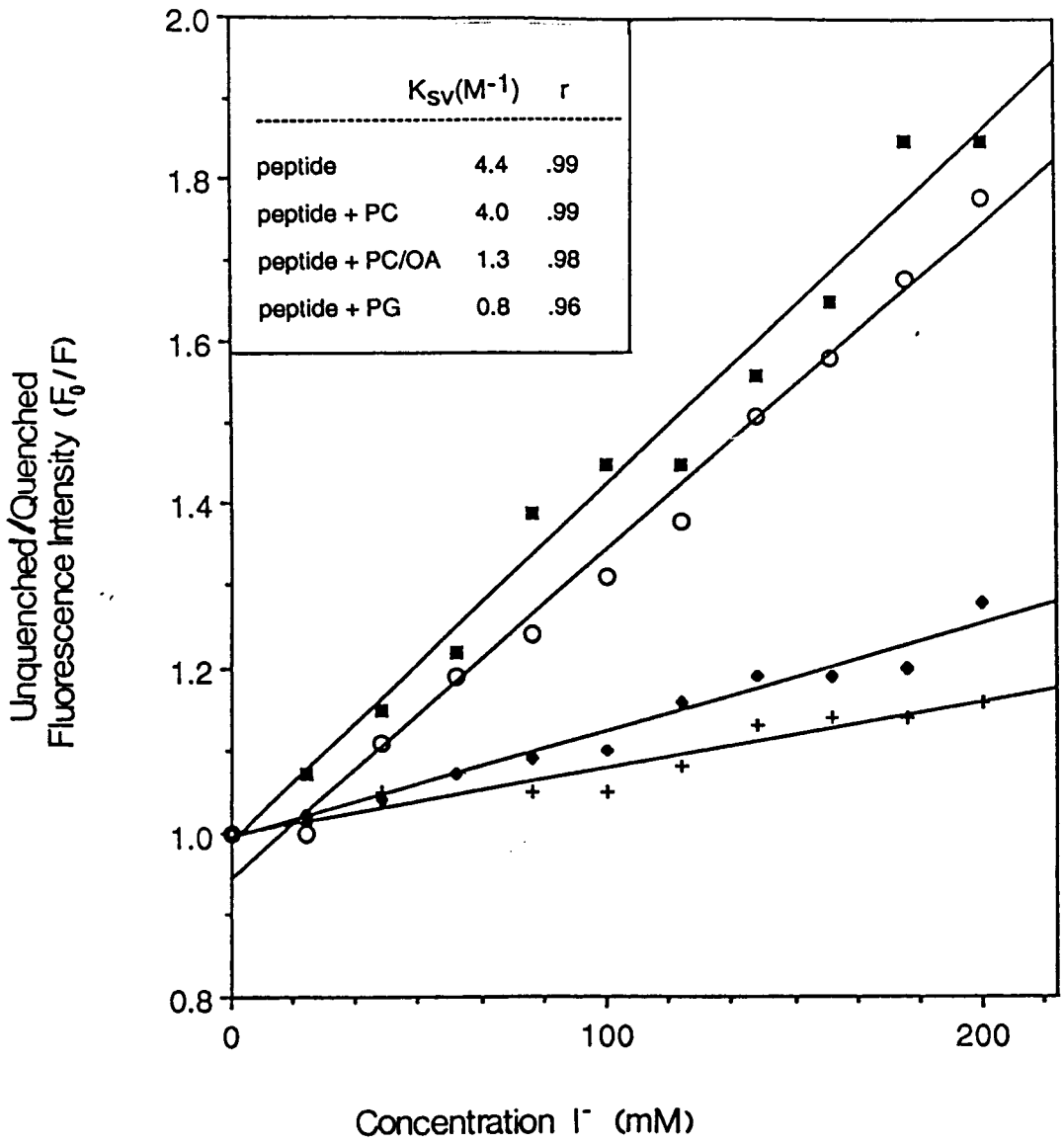

Figure 3.9: Stern-Volmer plot for iodide quenching of Pep33 tryptophan fluorescence. Samples contained 3.25 μM Pep33 in buffer (■), or in the presence of 1 mM vesicles composed of egg PC (o), egg PC/oleic acid (1:1, ◆), or DOPG (+). Iodide concentration was as indicated. The ionic strength was kept constant at 0.2 M by the addition of NaCl.

3.3.6 Fluorescence Quenching by Bromine-labelled PC demonstrates peptide intercalation

There are two possible explanations for the lipid specific changes in the tryptophan environment: 1) The peptide binds to the lipid vesicles and the tryptophan residue, along with the non-polar face of the helix, intercalates into the hydrophobic interior of the membrane bilayer. 2) The tryptophan becomes shielded from the aqueous environment by other residues in the peptide upon the transition to a helical conformation. To discriminate between these two possibilities, we used a quencher that is located in the membrane bilayer - 9,10-dibromo PC. Quenching of the tryptophan fluorescence would occur only if the residue were intercalated into the hydrophobic core of the membrane bilayer, where the bromide is located. Figure 3.10 shows the spectra of the Pep33 with PC/PG vesicles containing either 50% egg PC (unquenched) or 50% 9,10-dibromo PC (quenched). The introduction of bromide into the bilayer quenched the fluorescence of the tryptophan, demonstrating the location of the tryptophan in the bilayer. The quenching efficiency of 9,10- dibromoPC in PG vesicles was ~60% for Pep33, PepNH1 and PepAla (Table 3.5). Similar quenching results were seen for Pep33 when 9,10- dibromo PC was incorporated into PC/oleic acid vesicles. Incorporation of 9,10- dibromo PC into non-anionic lipid vesicles caused minimal or no quenching of PepNH1 or Pep33, suggesting no peptide intercalation into these vesicles (Table 3.5). The fluorescence of PepAla, on the other hand, was quenched by 9,10- dibromoPC in PC/diacylglycerol or PC/sphingosine vesicles. Thus, the tryptophan residue on the non-polar face of each of the peptide helices does intercalate into the hydrophobic bilayer of lipid

vesicles.

To examine the extent of intercalation of the tryptophan residue of Pep33 into the bilayer, the amount of quenching by bromide at different positions on the fatty acyl chain of PC was analyzed (Fig. 3.10). PC with bromide at the 6,7- ; 9,10- ; or 11,12- positions of the fatty acyl chain were incorporated into PC/PG vesicles. The 6,7- and 11,12- dibromo PCs quenched the fluorescence of Pep33 tryptophan by 42 ± 5% (N=3) and 38 ± 2% (N=3) respectively, suggesting they are approximately equidistant from the fluorophore, whereas, the 9,10- dibromo PC quenching was more efficient (58%) suggesting it is closer to the fluorophore. Similarly, PepALA was quenched 46, 65, and 45 %; and PepNH1 quenched 37, 56, and 34 % by 6,7-, 9,10- and 11,12-dibromoPC respectively. A simple conclusion would be that the tryptophan intercalates to between the 6,7 and 11,12 positions, near the 9,10 positions of the fatty acyl chain in the outer leaflet of the membrane bilayer.

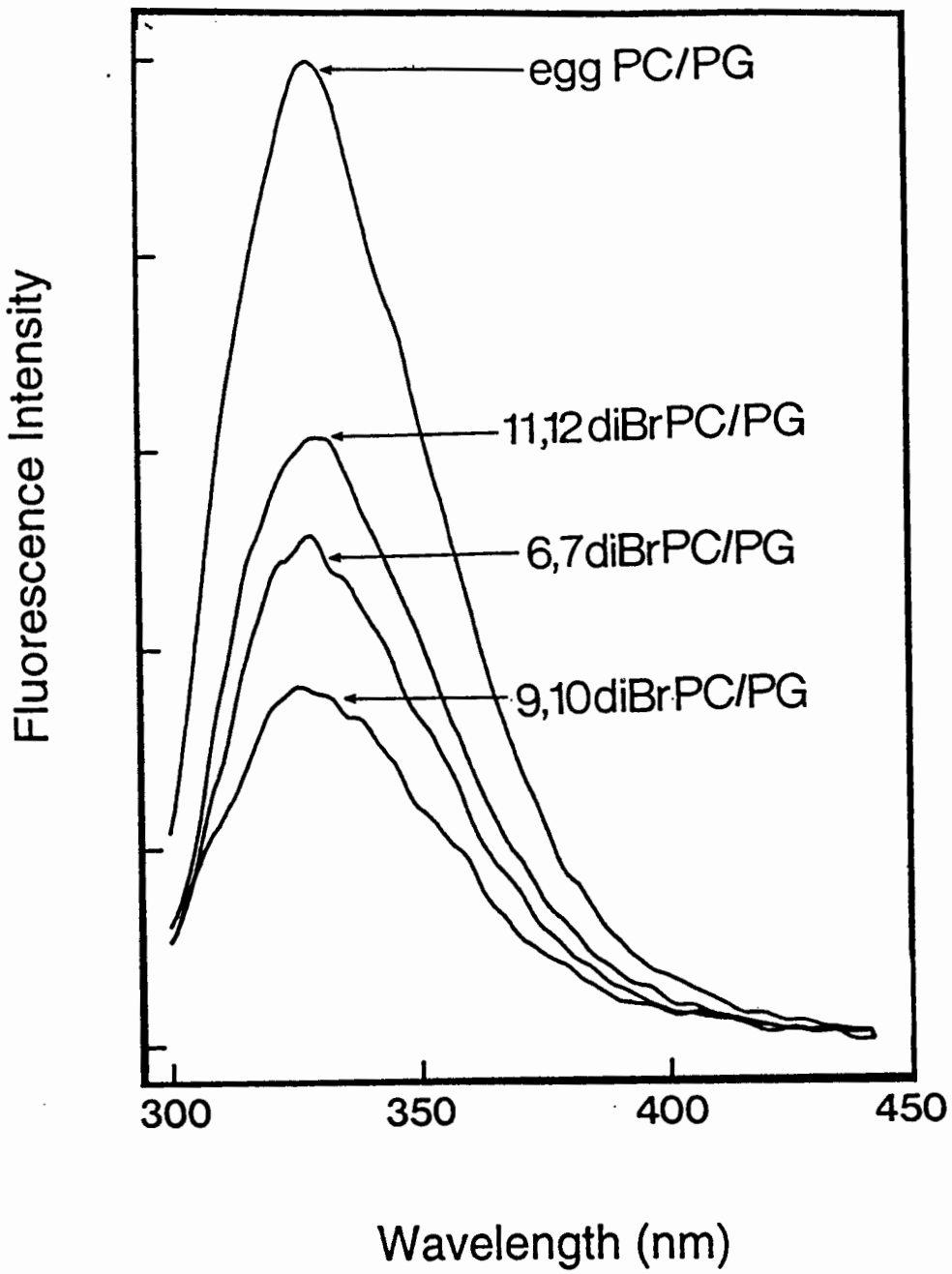

Figure 3.10: Quenching of tryptophan fluorescence of the Pep33 by 9,10-dibromoPC. Fluorescence emission spectra of Pep33 (3.25 μM). The excitation wavelength was 280 nm. Unquenched sample contained 0.5 mM egg PC/DOPG (1:1) vesicles. Quenched samples contained 0.5 mM vesicles composed of either 9,10-dibromo PC/DOPG (1:1), 6,7-dibromo PC/DOPG (1:1) or 11,12-dibromo PC/DOPG (1:1).

TABLE 3.5:

Quenching of Peptide Fluorescence by 50 mol% 9,10-dibromoPC

LIPID	%QUENCH		
	Pep33	PepAla	PepNH1
PC/PG (1:1)	57 ± 2	65 ± 2	56 ± 0
PC/oleic acid (1:1)	67 ± 3	N/D	N/D
PC	1 ± 1	N/D	N/D
PC/diacylglycerol (3:1)	8 ± 2	36 ± 5	10
PC/sphingosine (1:1)	16 ± 2	75 ± 2	0

Lipid vesicles were present at 0.5 mM. Peptide concentration was 3.25 μM. Spectra were measured as described in Section 3.2.7. Data are the average ± standard deviation of 2-4 separate experiments. For unquenched samples, PC indicates egg PC. For quenched samples, 50% of all vesicles was composed of 9,10-dibromoPC, the remainder of the PC being egg PC. % Quench = $100(1 - F/F_0)$, where F is the fluorescence intensity of the quenched sample obtained with vesicles containing 9,10-dibromoPC, and F_0 is the fluorescence intensity of the unquenched sample with egg PC in place of 9,10-dibromoPC.

3.3.7 Physical Binding of the Peptides to Vesicles

To augment the spectroscopic studies, an assay was developed to directly examine the physical binding of the peptides to lipid vesicles. The binding of these peptides to PC/oleic acid (1:1), PC/PG, (anionic) and PC (non-anionic) vesicles was analyzed by an assay in which free peptide was separated from vesicle-bound peptide by filtration in a Microcon-100 filtration unit. With a molecular weight cut off of 100,000, the filter trapped >95% of ^{3}H-labelled lipid ([*methyl*-^{3}H]-DPPC). 85% of cytochrome C or lysozyme, non-membrane proteins, was recovered in the flow-through fraction when PG or PC vesicles were present. Only 15 % of apolipoprotein A-I , which is known to interact with PC vesicles (Wetterau & Jonas, 1982), was recovered in the flow-through fraction when PC vesicles were present. These analyses show that the binding assay is a valid monitor of peptide-lipid binding. Binding curves for the four peptides in PC/oleic acid and PC vesicles are shown in figure 3.11. The amount of each peptide retained with the lipid fraction increased with increasing amounts of PC/oleic acid. Partition coefficient values for the peptides in PC/oleic acid, PC/PG, and PC are given in Table 3.6. The values are obtained at lipid:peptide ratios which fall near the midpoint of the curves.

The lipid selectivity observed in the spectroscopy studies was reflected in the binding properties of the peptides. All peptides bound to the anionic lipid vesicles PC/oleic acid and PC/PG. Over the lipid:peptide range tested there was no significant binding to non-anionic PC vesicles of Pep33 or PepNH1, the two peptides that demonstrated stringent lipid specificity in the spectroscopy studies. PepALA and Pep62 both bound to PC vesicles, but with less affinity than to the

anionic vesicles. Pep62 had the highest affinity of the four peptides for all lipids. PepNH1 bound with high affinity only to anionic membranes. Pep33 had the lowest affinity for membranes, incompletely binding anionic lipids at the highest concentrations tested.

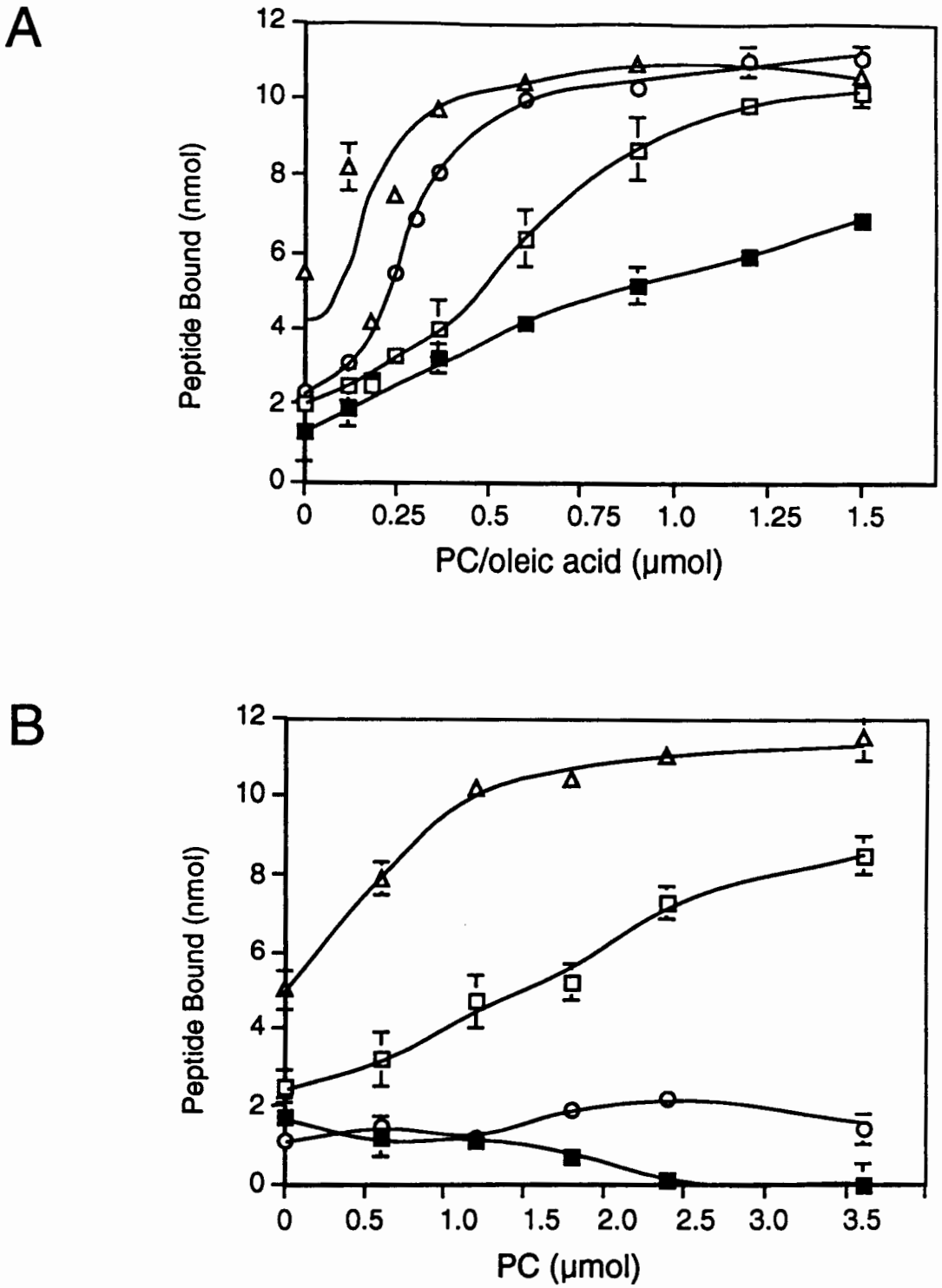

Figure 3.11 Binding of peptides to vesicles as a function of the amount lipid.
Peptide (12 nmol) was incubated with PC/oleic acid (**A**) or PC (**B**) vesicles of the indicated amount. The unbound peptide was separated from the vesicles by filtration and quantified as described in Section 3.2.4. Pep33 (■), PepAla(□), PepNH1(○) and Pep62(Δ).

Table 3.6: Partition coefficients for the peptides

PEPTIDE	PARTITION COEFFICIENTS		
	PC/oleic acid (1:1)	PC/PG (1:1)	PC
PEP 33	700 ± 100	1100 ± 100	30 ± 30**
PEP ALA	1300 ± 300	3000 ± 500	470 ± 100
PEP NH1	5000 ± 1500	8500 ±800	60 ± 20**
PEP 62	8400 ± 400	~150,000*	3100 ± 700

Binding of peptides to vesicles was analysed by a filtration assay, as described in Section 3.2.4. Partition coefficients were determined as described in Section 3.2.4 from the midpoints of the binding curves, where >20% and <90% of the peptide was bound. There are three exceptions to this: * the value obtained for Pep62 binding to PC/PG, which is anomolously high, as less than 10% of the peptide was recovered in the unbound fraction. ** Partition coefficients for PC of Pep33 and PepNH1 are estimates, as < 10% of these peptides bound to lipid. Data are averages of 4 to 8 determinations.

3.4 Discussion

We have used circular dichroism to study the secondary structure, and fluorescence to study the membrane interactions of peptides derived from the proposed amphipathic α-helical membrane binding domain of CT. The results of these spectroscopic experiments have led to three major conclusions about the membrane binding characteristics of these peptides. 1) The peptides interact with membranes in an α-helical conformation. 2) A portion of the peptides intercalate into the hydrophobic core of the membrane. 3) The peptides interact with higher affinity for anionic membranes. These results implicate a membrane-binding role for the corresponding region of CT.

3.4.1 The peptides interact with membranes in an α-helical conformation

The results of the CD studies demonstrate that the peptides, while random in buffer solution, form an α-helical structure in the presence of anionic membranes. In all cases examined, the lipid vesicles that caused a change in the fluorescence properties of the peptides also promoted the helical conformation. For Pep33, there was a close correlation between the lipid to protein ratio required, or mole % anionic lipid required for maximum induction of helix and for complete disappearance of the 350 nm tryptophan emission peak. These observations argue that the peptide binds to and intercalates into these vesicles as a helical structure.

The percentage α-helix in the anionic membrane-bound structures was

estimated to be 55-70%, while in buffer solution the peptides were only ~14% helical. For both forms of the peptides, the remainder of the structure seems to be largely random with <10% β–sheet structure, by comparison to the reference polylysine spectra of Greenfield and Fasman (1969). Similar estimations for percentage helicity were obtained by CD for other membrane binding amphipathic peptides: a peptide derived from the N-terminal region of influenza hemagglutinin was 45% helical (Lear & DeGrado, 1987); model ion-channel peptides were 60-70% helical (Agawa *et al.*, 1991, Chung *et al.*, 1992); and peptides modelled from apolipoproteins were up to ~50% helical (Kanellis *et al.*, 1980; Anantharamaiah *et al.*, 1985; Epand *et al.*, 1987; Yoshimura *et al.*, 1992). The solved NMR structures of SDS-bound PepNH1 and a 22mer peptide, corresponding to the C-terminal two-thirds of Pep33, demonstrate α-helical conformations over >80% of each peptide, confirming these CD results (Dunne, Cornell, Johnson, and Tracey, manuscript in progress). In addition, preliminary NOESY data derived for Pep62 indicate an α-helical structure over the entire length of the peptide.

3.4.2 The peptides intercalate into the hydrophobic core of the membrane

Once the helical structure of the peptides was confirmed, the tryptophan located in the non-polar face proved to be a useful handle in assessing the location of the non-polar helix face with respect to membranes. The maximum fluorescence emission wavelengths and quenching abilities of iodide demonstrated that the tryptophan was less accessible to the aqueous environment in the presence of anionic lipids, while the quenching abilities of the

hydrophobic dibromo PCs in anionic lipid vesicles confirmed the location of the tryptophan in the hydrophobic interior of the membrane.

The use of the three dibromo-PC's, with the bromine quencher at different positions in the membrane, allowed us to localize the depth of intercalation of the tryptophan. The bromines in 9,10-dibromo PC, which was the most efficient quencher of the tryptophan in the peptides, have been localized by x-ray diffraction to 8 Å from the bilayer center, or 7 Å from the headgroup/ hydrocarbon boundary (Wiener & White, 1991). The bromines in 6,7-dibromo PC and 11,12-dibromo PC have been localized to 11 Å and 6.5 Å , respectively, from the center of the bilayer, or 4 Å and 8 Å , respectively, from the headgroup/hydrocarbon boundary (McIntosh & Holloway, 1987). Quenching by these two lipids was approximately the same, but less than that of the 9,10-dibromo PC, suggesting that the tryptophan was located at a position approximately equidistant from the two probes. This would place the tryptophan at the same depth in the bilayer as the 9 position on the fatty acyl chain, 9 Å from the bilayer center or ~6 Å from the headgroup/hydrocarbon boundary. In studies of a model ion-channel peptide that interacts with the membrane via an amphipathic helical structure intercalating on the surface of the bilayer, a tryptophan on the hydrophobic face of the helix was found to intercalate to 7-9 Å from the bilayer center (Chung *et al.*, 1992). These results are similar to ours, which lends support for our model of the peptide helix interacting parallel to the membrane surface, with its hydrophobic face intercalated.

3.4.3 The peptides interact selectively with anionic membranes

We have found, in binding, CD, and fluorescence studies, that these peptides respond preferentially to anionic lipid vesicles. In the case of Pep33 or PepNH1, vesicles composed of zwitterionic lipids or cationic lipids caused no change in the fluorescence characteristics or secondary structure relative to that of the peptide in buffer solution, demonstrating an inability to induce an α-helical structure which predicates membrane intercalation. These peptides were unable to physically bind to non-anionic membranes. In the case of PepAla and Pep62, non-anionic membranes caused a small change in the spectroscopic properties, and indicated an increase in helicity to ~25 %. These peptides bound to PC vesicles, but with lower affinity than to anionic vesicles.

Pep33 interacted with a variety of anionic lipids, showing no preference for any specific head group, which demonstrated that the peptide is indeed responding to the negative charge on the lipids. There was a minimum surface charge required on the membrane for peptide binding, as illustrated by the sigmoidal dependence of the percentage α-helical structure on the mole % PG or PA in the zwitterionic PC membrane. Furthermore, the maximal helicity (60%) was achieved at a lower mole % of PA (charge of -2) than PG (charge of -1). These responses to the negative surface charge were also reflected in the shift of the fluorescence emission spectra, which occurred at the same mole % as the helical conformational change.

While lipid selectivity has been demonstrated for other membrane-binding amphipathic α-helical peptides, these CT peptides appear to have a more stringent requirement for anionic lipids. Apolipoprotein-derived model amphipathic helical peptides (Kanellis *et al.*, 1980; Anantharamaiah *et al.*, 1985;

Epand *et al.*, 1987), the N-terminal peptide from influenza hemagglutinin, (Lear & DeGrado, 1987) and model ion channel peptides (Agawa *et al.*, 1991; Chung *et al.*, 1992) all bind to the non-anionic PC vesicles in an amphipathic α-helical conformation. The PhoE model signal peptide (Killian *et al.*, 1990), mellitin (Dufourq & Faucon, 1977) and a model fusogenic peptide (Yoshimura *et al.*, 1992) are examples of amphipathic helical peptides that preferentially interact with anionic lipid vesicles, but each peptide also interacts with PC vesicles to a lesser extent.

The CT peptides interact preferentially with anionic vesicles. This lipid selectivity is not just due to a "non-specific" electrostatic attraction because Pep33 and PepAla each have a net charge of -2, and thus should be attracted to positively charged vesicles. There must be some specific feature in the structure which confers this lipid selectivity. In the theoretical CT amphipathic α-helical structure (Fig. 3.2), there exists a cluster of cationic lysine residues at one interface of the non-polar and polar face, which could function to attract the peptide to a negatively charged membrane surface. These lysine clusters are a key feature of the apolipoprotein amphipathic α-helix (Segrest *et al.*, 1990). Unlike the apolipoprotein amphipathic α-helices, CT contains an anionic cluster at the other interface. Possibly the negative surface charge requirement on the membrane involves a localized decrease in the pH near the membrane surface, leading to protonation of acidic residues on the peptide. This would increase the positive charge on the peptide, leading to stronger electrostatic binding to the negatively charged membrane. Interestingly, the two peptides with the highest affinity for anionic membranes, PepNH1 and Pep62, both contain a histidine residue which would be located near the membrane surface. This residue could be a candidate for a protonation event. Alternatively, protonation could neutralize

a negatively charged residue, facilitating its intercalation into the hydrophobic bilayer. Membrane insertion promoted by protonation of a peptide was enhanced by the presence of anionic lipids in the membrane (Leenhouts *et al.*, 1995).

3.4.4 Determinants of membrane affinity

The relative affinity of the peptides for lipid vesicles reflected the importance of both hydrophobic and electrostatics interactions. PepNH1, containing the N-terminal portion of the amphipathic helix, has a net positive charge (+3) while the C-terminal derived 33-mer peptides Pep33 and PepAla have a net negative charge (-2). PepAla has a more hydrophobic polar face than PepNH1, and has a much higher affinity for non-anionic membrane, with which PepNH1 did not measurably interact (Fig 3.11A). However, PepNH1 had a higher affinity than PepAla for anionic lipids (Fig 3.11B), suggesting that charges on the peptide may influence the interaction with anionic membranes. The size of the hydrophobic face is also important in determining membrane affinity. Pep33 did not completely bind to the anionic lipids over the lipid:peptide range tested, and did not measurably interact with non-anionic vesicles. Substitution of three serine residues for alanine residues in PepAla, which would effectively increase the hydrophobic face of the helix, increased the affinity of the peptide for all lipids and caused an observable association of the peptide with PC. This finding therefore suggests that the role of the three serine residues that interrupt the hydrophobic face of the amphipathic α-helix is to lower the hydrophobicity and in this way, contribute to the determinants of lipid selectivity for CT binding. Pep62 had the highest affinity of all peptides for both anionic and non-anionic lipids. This may reflect both a larger hydrophobic interaction, due to the larger

hydrophobic face, and a larger number of charged residues involved in electrostatic interactions. A 22-mer peptide, encompassing the latter two-thirds of Pep33, was even less responsive to lipid vesicles as assessed by CD and fluorescence, needing higher concentrations of 100% anionic vesicles to respond (Cornell & Johnson, unpublished observation). All peptides contain a lysine cluster at the non-polar/polar helical interface, which has been proposed to extend the hydrophobic face via the long hydrocarbon chains (Segrest *et al.*, 1990, 1992; Mishra *et al.*, 1994). Thus, these results agree with the suggestion (Segrest *et al.*, 1992) that the hydrophobicity of the helix is a main determinant for membrane affinity, but implicate a role for electrostatics in determining selectivity for anionic membranes.

3.4.5 Relation to the Native Cytidylyltransferase

This study presents evidence for a CT domain that may be responsible for the binding and activation of the enzyme by anionic lipid vesicles. Presumably, the mechanism whereby anionic phospholipid vesicles activate CT involves stabilization of the α-helical conformation of residues 236-299. Stabilization of an α-helix transforms this region into a highly amphipathic structure, the non-polar face of which can readily intercalate into the hydrophobic core of a membrane.

The membrane interactions of the isolated domain of CT mimic in several respects the interactions of the native enzyme. The interactions of both seem to involve electrostatic and hydrophobic components. (Sections 1.3.2.3 and 3.4.4). Like the peptide, CT responds poorly to PC vesicles, while anionic lipid vesicles promote enzyme binding and are potent activators. For both the peptide and the

enzyme, the negative surface charge on the membrane rather than the chemical structure of the head groups is a determining factor in the binding (Cornell, 1991a; Section 1.3.2.2). The CT-membrane interaction also involves a hydrophobic component, and previous observations have suggested an intercalation of a portion of the enzyme into the bilayer (Section 1.3.2.3), an event that is observed for the peptide. Thus, it is reasonable to propose that the region of CT that is represented by these peptides is involved in membrane binding.

One major difference in the membrane-binding characteristics of CT and the peptides is that the enzyme is activated by a second class of lipids, those with small polar head groups, such as diacylglycerol and oleyl alcohol, when present in a PC membrane (Section 1.3.2.2). These lipids had minimal effect on the peptides, either in the CD structural analysis or in the fluorescence characteristics above that seen for PC alone. Thus, this region may not contain all of the elements necessary to impart the lipid specificity of the native CT. Possibly, a separate domain exists in the enzyme which is responsible for interactions with this class of activators. Removal of the amphipathic α-helical region by chymotrypsin degradation produces fragments unable to bind to either class of activating lipid (Craig *et al*, 1994), suggesting that this is the main domain which mediates lipid binding. Thus, although the amphipathic α-helix is required for CT-membrane interactions, it is not sufficient. There may be another distinct region of the protein which is involved in imparting the actual specificity for these neutral, polar, lipids.

CHAPTER FOUR: IDENTIFICATION OF THE MEMBRANE BINDING DOMAIN OF NATIVE CT BY HYDROPHOBIC PHOTOLABELLING

4.1 Introduction

Chapter Three demonstrated that synthetic peptides corresponding to the amphipathic helix domain of CT bind to lipid vesicles in a helical conformation. However, it has not been shown directly using the whole enzyme that the amphipathic α-helix contacts and intercalates into the membrane. To obtain sufficient pure enzyme for this study, we have expressed recombinant rat-liver CT in insect-derived cells using a recombinant baculovirus system. These cells were grown in suspension, and produced large amounts of CT.

Using purified, recombinant CT, we have applied the technique of hydrophobic photolabelling (reviewed by Brunner, 1993) to directly determine the regions of the CT protein that intercalate into the hydrophobic core of the membrane. The hydrophobic probes 3-(trifluoromethyl)-3-(*m*-[^{125}I]iodo-phenyl)diazirine ([^{125}I]TID) and 11-[4-[3-(trifluoromethyl)diazirinyl]phenyl]-[2^{3}H]-undecanoic acid ([^{3}H]TUA) partition specifically into the hydrophobic membrane core (Brunner *et al.*, 1980; Brunner & Semenza, 1981, Brunner, 1989). Photoactivation of the diazirine functional group produces a highly reactive carbene species which has the potential to react non-selectively with any molecule in the vicinity. Thus, any regions of the protein which are embedded in the hydrophobic core of the membrane should become labelled by the probe. This technique has been used to identify membrane interacting

regions of integral membrane proteins, such as bacteriorhodopsin (Brunner *et al.*, 1985), a light-harvesting protein B870 (Meister *et al.*, 1985), the nicotinic acetylcholine receptor (Blanton & Cohen, 1992.); as well as amphitropic intercalating proteins such as synapsin I (Benfenati *et al.*, 1989), Sec A (Ulbrandt *et al.*, 1992) and a soluble fragment of hemagglutinin (Harter *et al.*, 1988; 1989). In a few cases the pattern of labelling was dissected (Brunner *et al.*, 1985; Meister *et al.*, 1985; Blanton & Cohen, 1992; Harter *et al.*, 1989). The labelling of the membrane fragment showed a periodicity of ~3.6, highly suggestive of an α-helical conformation for the lipid-embedded peptide.

Using a combination of photolabelling and proteolysis, we have determined that a region of CT does indeed penetrate into the hydrophobic core of the membrane and this region corresponds to the amphipathic helical region of the protein. One objective was to identify the amino acids with covalently bound label, to generate proof that the domain was bound as a helix. However, this latter objective was not acheived due to low incorporation of radioactivity.

4.2 Experimental Procedures

4.2.1 Materials

A 62 residue peptide corresponding to the putative amphipathic helix region of CT (residues 238 to 299) was as described (Section 3.2.2). [^{125}I]-TID, [^{3}H]DPPC and [^{14}C]oleic acid were from Amersham, and [^{3}H]-Triton X-100 was from Dupont/NEN. Egg PC was from Avanti. *sn*-1,2,-diacylglycerol was generated by digestion of egg PC using phospholipase C as described (Section 2.2.1.2). Oleic acid, α-Chymotrypsin (Type II: from bovine pancreas), Ovalbumin, Sephacryl-S400-HR, and the goat-anti-rabbit horseradish peroxidase antibody were from Sigma. PVDF was from Biorad. BSA (fraction V, fatty acid free) was from Calbiochem. CT recombinant baculovirus, *T. ni* cells and antiserum raised against a C-terminal peptide of CT were kindly provided by Dr. Claudia Kent (U. Michigan). [^{3}H]TUA was provided by Dr. J. Brunner (Zurich, Switzerland). Apolipoprotein A-1 was kindly provided by Dr. R.J. Cushley (Simon Fraser U.) Rabbit antiserum against the N-terminus of CT was as described (Cornell *et al.*, 1995). Rabbit antiserum raised against a 33 residue peptide corresponding to a portion of the amphipathic helix domain of CT (residues 255 to 288) was generated by Dr. Adrienne Drobnies as described (Johnson *et al.*, submitted). Electrophoresis reagents were Molecular Biology Grade purchased from BRL or Sigma.

4.2.2 Preparation of Recombinant CT from insect cells using a baculovirus expression vector

The expression and purification of recombinant rat-liver CT from insect cells using the baculovirus system is based on the protocol described by MacDonald and Kent (1993). This group based their purification scheme on that described for purification from rat liver by Weinhold *et al.* (1986).

4.2.2.1 Maintaining *T.ni* cells

Insect cells of the *T. ni* cell line were maintained as monolayers in Complete Graces Media (Graces media supplemented with yeastolate, lactalbumin hydrolysate,10 % (v/v) fetal calf serum) at 28 °C. When confluent, cells were loosened from flasks, centrifuged 2 min at 200*g*, resuspended and diluted in fresh media, and transferred to new flasks. To establish *T. ni* cells in suspension, 1 x 10^7 cells from monolayer culture were collected and centrifuged 2 min at 200*g*, and resuspended in 100 ml fresh media (cell density of 1 x 10^5 cells/ml) in a 100 ml spinner flask. Cells were grown in spinning suspension at 28 °C until cell density reached 1.5 x10^6 cells/ml, at which time portions of the cell suspension were centrifuged and diluted into fresh media.

4.2.2.2 Maintaining virus stocks

Stocks of recombinant baculovirus encoding rat-liver CT were stored at 4 °C in the dark. Virus amplification and determination of virus titer by plaque

assay were performed as outlined by Summers (1987). The titer of the virus stock used was ~10^8 pfu (plaque-forming units per ml).

4.2.2.3 Infection of Insect cells with CT recombinant baculovirus

For infection, *T. ni* cells in suspension were grown to a density of 1.5 to 2 x 10^6 cells/ml in complete Graces medium. The day before infection, the cells were diluted two-fold in order to be in optimum growth phase for infection. On the day of infection, 3 x 10^8 cells of >90% viability were pelleted and resuspended in the virus stock solution (60 ml) with a multiplicity of infection of 20 virus particles per cell. This solution was diluted to 300 ml with Serum-free media (SF900) to a final cell density of ~10^6 cells/ml and transferred to 3-100ml spinner flasks. Cells were incubated at 28 °C until harvested.

4.2.2.4 Harvesting cells and preparation of cell cytosol

Cells expressing recombinant CT were harvested 65 to 70 hr after infection. The cell suspension was centrifuged 5 min at 1000*g*, cell pellets were washed with PBS and recentrifuged for 3 min at 200*g*. After this stage, all steps were performed at 0 to 4 °C, and the following protease inhibitors were added to all buffers immediately before use: 2.5 μg/ml leupeptin, 2 μg/ml chymostatin, 1 μg/ml antipain, 2 μg/ml pepstatin, 10μg/ml ρ-aminobenzadine, 10 μg/ml benzamidine, 2 mM PMSF. The cell pellet was resuspended in 12 ml homogenization buffer (10 mM Tris, pH 7.5, 0.2 mM EDTA, 30 mM NaCl, 2 mM DTT, protease inhibitors) and homogenized with 30 strokes of a glass homogenizer. The NaCl concentration in the cell homogenate was brought to

0.15 M by stepwise addition of a concentrated (1.2 M) NaCl solution. The cell homogenate was centrifuged for 1 hr at 100,000*g* to separate the cytosolic fraction (supernatant) from the microsomal fraction (pellet).

4.2.2.5 Purification of Recombinant CT from Insect Cell Cytosol

To the insect cell cytosol was added PC/oleic acid (1:2) vesicles at a ratio of 450 nmole PC per mg cytosolic protein. Typically 120 to 180 mg of protein was present, and 10 to 15 ml of a sonicated PC/oleic acid suspension (5mM PC, 10mM oleic acid, 50 mM Tris, pH 7.5, 1 mM EDTA, 0.15 M NaCl, 2 mM DTT, protease inhibitors) was added to the cytosol. The mixture was stirred 1 hr, after which the pH was adjusted to 5.0 with dropwise addition of 1 M acetic acid. After stirring on ice a further 10 min, the PC/oleic acid vesicles, along with the CT, were precipitated from the acidic solution by centrifugation for 20 min at 20 000*g*. The resulting pellet was washed with buffer A (50 mM Tris, pH 7.5, 1 mM EDTA, 0.15 M NaCl, 2 mM DTT, protease inhibitors) and recentrifuged. The pellet was then suspended in 0.3 ml octylglucoside extraction buffer (buffer A / 50 mM octylglucoside) per mg cytosolic protein. The solution was stirred 30 min and the insoluble material was removed by centrifugation for 20 min at 20 000*g*. To this octylglucoside extract was added 1/10 th of a volume of PC/oleic acid vesicles (5mM PC/ 10 mM oleic acid in the buffer described above). The solution was applied to a 36 ml (1.6 x 18 cm) DEAE-sepharose column (pre-equilibrated with Buffer A) at a 0.5 ml/min flow rate. The column was washed at 1 ml/min with two volumes of buffer A, two volumes buffer A / 0.3 M NaCl (total NaCl concentration) and eluted into 40 fractions of 2 ml with buffer A / 0.4 M NaCl / 50 mM octylglucoside. CT enzymatic activity was assayed (Section 2.2.5) in each

fraction, and the active fractions pooled, diluted 2.5 fold in buffer A, and loaded onto a 36 ml (1.6 x 18 cm) hydroxylapatite column at a flow rate of 0.5 ml/min. The column was washed at 1 ml/min with two volumes buffer A, two volumes buffer P (buffer A with 0.2 M Na_2HPO_4, pH 7.4), two volumes buffer P/ 50 mM octylglucoside and eluted into 70 fractions of 1.5 ml with buffer P/ 0.05 % (v/v; 73 mM) Triton X-100. Enzymatic activity of CT was measured in each fraction. The active fractions were pooled, aliquoted and stored at -80 °C. Typical yields were ~35 ml of ~0.5 mg/ml protein with a specific activity of ~2000 activity units/mg protein.

4.2.3 Gel filtration analysis of CT binding to PC/oleic acid vesicles

The association of CT with PC/oleic acid vesicles was analyzed by the method described by Cornell (1991a). CT was incubated with PC/oleic acid vesicles (1:350 protein to lipid molar ratio, 4 mM total lipid) or with Triton-X100 micelles (10 mM) for 10 min at room temperature. [^{3}H]DPPC, or [^{14}C]oleic acid and [^{3}H]Triton X-100 were included in trace amounts. [^{3}H]Triton X-100 was vortexed into the sample, and [^{3}H]DPPC or [^{14}C]oleic acid was added to the solvent-mixed lipids prior to evaporation and sonication. The sample was loaded on a Sephacryl-S400 column (44.5 cm x 1 cm) that had been pre-equilibrated with column buffer (10 mM Tris, pH 7.5, 1 mM EDTA, 0.5 mM Triton X-100, 2 mM DTT), and run at 0.3 ml/min. Fractions (~0.9 ml) were collected and samples analyzed: 1) for ^{3}H/^{14}C-labelled lipid by scintillation counting; and 2) for CT by gel electrophoresis and subsequent densitometry of the Coomassie-stained gels. The void volume and total volume of the column were identified using Blue-Dextran and [^{3}H]glycerol, respectively.

4.2.4 Partial digestion of CT with chymotrypsin

CT was partially digested with chymotrypsin as previously described (Craig *et al.*, 1994). CT (~20 μg) was mixed with PC/oleic acid (1:1) vesicles at a protein to lipid molar ratio of 1:300, and incubated with chymotrypsin at the indicated chymotrypsin:CT mass ratio for 10 to 15 min at 37°C, at which time the reaction was terminated by addition of PMSF to a final concentration of 2 mM. Samples were prepared for electrophoresis by extensive dialysis against 10 mM Tris, pH 7.5, 0.5 mM EDTA, 0.005 % (w/v) SDS, 2 mM DTT, 0.5 mM PMSF. Samples were concentrated in a Savant Speed-Vac evaporator prior to addition of sample buffer, and were electrophoresed on a 12 % polyacrylamide gel as described (Section 4.2.5).

4.2.5 Gel Electrophoresis

Three SDS-PAGE systems were employed in these studies:

1) A 12% polyacrylamide gel by the method of Laemmli (1970) was employed to analyze CT, and was used to characterize the high molecular weight chymotrypsin fragments of CT. In this system a ~6 cm separating gel was composed of 0.375 M Tris, pH 8.7, 0.1% (w/v) SDS, 12% (w/v) acrylamide, 0.32% (w/v) Bis-acrylamide. Acrylamide polymerization was achieved by addition of a 10% APS solution (0.07% (w/v) final concentration) and TEMED (0.2% (v/v) final concentration). This gel was overlaid with a ~1 cm stacking gel composed of 0.125 M Tris, pH 6.8, 0.1% (w/v) SDS, 4% (w/v) acrylamide, 0.1% Bis-acrylamide, APS (0.05% (v/v)) and TEMED (0.1% (v/v)). Protein samples were

loaded on the gel after boiling 5 min in sample buffer I (65 mM Tris, pH 6.8, 4% (w/v) SDS, 1% (v/v) β-mercaptoethanol, 10% (w/v) glycerol, ~0.001% (w/v) bromphenol blue), and electrophoresed in running buffer (25 mM Tris, pH ~8.3, 192 mM glycine, 0.1% (w/v) SDS) at 200 V, for 1.5 to 2 h at room temperature.

2) A 16 T/ 3 C[1] Tricine gel of Schagger and von Jagow (1987) was employed to analyze the low molecular weight chymotryptic fragments of CT. In this system a ~5cm separating gel was composed of 1M Tris, pH 8.25, 0.1% (w/v) SDS, 16% (w/v) acrylamide, 0.5 % (w/v) Bis-acrylamide, 13.3%(w/v) glycerol. Acrylamide polymerization was achieved by addition of a 10% APS solution (0.05% w/v final concentration) and TEMED (0.1% v/v final concentration). This gel was overlaid with a ~1.5 cm stacking gel of 0.74M Tris, pH 8.25, 0.07% (w/v) SDS, 3.8 % (w/v) acrylamide, 0.12 % (w/v) Bis-acrylamide, APS (0.048% (w/v)) and TEMED (0.096% (v/v)). Proteins were loaded on the gel after boiling in sample buffer II (50 mM Tris, pH 6.8, 4% (w/v) SDS, 2 % (v/v) β-mercaptoethanol, 12 % (w/v) glycerol, ~0.001% bromphenol blue). The gel was electrophoresed with an anode buffer of 0.2 M Tris, pH 8.9, and a cathode buffer of 0.1M Tris, 0.1M Tricine, 0.1% (w/v) SDS, pH ~ 8.25, at 50 V through the stacking gel, 100-150 v through the separating gel, for 3-5 h at room temperature.

3) A 16 T/ 6 C + spacer Tricine gel of Schagger and von Jagow (1987) was employed to analyze synthetic peptides derived from CT. In this system a ~5cm

---

[1] T refers to the total percent (w/v) concentration of both acrylamide monomers. C refers to the percent of total acrylamide that is the crosslinker bisacrylamide.

separating gel was composed of 1M Tris, pH 8.25, 0.1% (w/v) SDS, 15.5% (w/v) acrylamide, 1% (w/v) Bis-acrylamide, 13.3%(w/v) glycerol. Acrylamide polymerization was achieved by addition of a 10% APS solution (0.05% w/v end) and TEMED (0.1% v/v end). This gel was overlaid with a ~1 cm spacer gel of 1 M Tris, pH 8.25, 0.1% (w/v) SDS, 10 % (w/v) acrylamide, 0.3 % (w/v) Bis-acrylamide, APS (0.05% (w/v)) and TEMED (0.1% (v/v)). This gel was overlaid with a stacking gel of 0.74M Tris, pH 8.25, 0.07% (w/v) SDS, 3.8 % (w/v) acrylamide, 0.12 % (w/v) Bis-acrylamide, APS (0.048% (w/v)) and TEMED (0.096% (v/v)). Proteins were loaded on the gel after boiling in sample buffer II, described above. The gel was electrophoresed with the anode and cathode buffers described above at 70 to 80 V at 4 °C for ~15 hr.

4.2.6 Immunoblotting

After separation by electrophoresis as described above, proteins were transferred to PVDF membrane using a Pharmacia LKB Novablot system at 2 mA/cm^2 for 1 to 1.5 hr with a minimum amount of transfer buffer (39 mM Glycine, 48 mM Tris, 0.0375% (w/v) SDS). The membrane was incubated in "blotting buffer" (TBS: 20 mM Tris, pH 7.4, 0.15 M NaCl), 0.05 % (w/v) Tween-20, 5% (w/v) skim milk powder) for 2 hr at room temperature with agitation. The membrane was then incubated overnight at 4 °C with the primary antibody, diluted as indicated with blotting buffer. The membrane was washed with blotting buffer at room temperature, and subsequently incubated for 1.5 hr with a 1/2000 dilution of the goat peroxidase-conjugated secondary antibody. The membrane was washed with each of: blotting buffer; TBS/0.05% Tween-20; and TBS; then developed with 1.6 mM diaminobenzadine in 50 mM Tris, pH 7.6, 0.03 % (w/v) NiCl, 0.03 % (v/v) H_2O_2. The reaction was stopped with excess water.

4.2.7 Sequence analysis

For N-terminal sequence analysis, chymotryptic fragments of CT were electrophoresed in the 16T/ 3%C Tricine gel system (Section 4.2.5) and transferred to PVDF membrane (Section 4.2.6). Protein was stained with 0.1% (w/v) Amido Black dye in methanol/acetic acid/H_2O (45:10:45 volume ratio). Sequencing was performed by Dr. R. Aebersold at University of Washington (Seattle, WA).

4.2.8 Protein and Radioactivity quantitation

To visualize protein, gels were stained with 0.01% (w/v) Coomassie-blue in methanol/acetic acid/H_2O (45:10:45 volume ratio). The protein associated with the bands was estimated using a Microtek Scanmaker densitometer with NIH image software. ^{125}I-labelling of protein was visualized by autoradiography and quantified by gamma-counting of the excised bands. ^{3}H-labelling of protein was visualized by fluorography, and quantitated by liquid scintillation counting of the excised bands, after dissolution in 0.5 ml H_2O_2 overnight at 70 °C. For fluorography and autoradiography, the Coomassie-stained gels were dried and exposed to preflashed Reflections film with an intensifying screen (Dupont) at -80°C for the indicated time. For fluorography, the ^{3}H- labelled gel was soaked in 1 M salicylate for 30 min prior to drying.

4.2.9 Photolabelling experiments

4.2.9.1 [^{3}H]TUA Photolabelling of CT

[3H]TUA (1 mol%) from a toluene/ethanol stock was added a PC/oleic acid mixture in $CHCl_3$. Sonicated vesicles were prepared from this solution as described (Section 2.2.4) in a dimly-lit room. CT (10 μg) was added to PC/oleic acid/[3H]TUA vesicles (300 nmol) in 10 mM Tris, pH 7.4, 1mM EDTA, 1mM DTT, and the solution was incubated 10 min at room temperature. Samples were transferred to a 1 ml quartz cuvette and irradiated for 10 min at room temperature using a 100 W Hg lamp with a filter to exclude light <300 nm. Samples were prepared for electrophoresis by extensive dialysis against 10 mM Tris, pH 7.5, 0.5 mM EDTA, 0.005 % SDS (w/v), 2 mM DTT, and concentrated in a Savant Speed-Vac evaporator prior to addition of sample buffer. Samples were electrophoresed on a 12 % polyacrylamide gel (Section 4.2.5).

4.2.9.2 [^{125}I]TID Photolabelling of CT

[^{125}I]TID (0.2 to 2 mol% of total lipid) was preincubated 10 min at room temperature with sonicated PC/oleic acid (1:1) vesicles in 10 mM Tris, pH 7.4, 1 mM EDTA, 1 mM DTT. CT (~20 μg per lane on gel) was added so that the final Triton-X100 concentration was <20 mol% of the total lipid, and the CT:lipid molar ratio was 1:300. After a 10 min incubation at room temperature, the protein/lipid mixture was transferred to a 1 ml quartz cuvette. Samples were irradiated for 10 min at room temperature using a 100 W Hg lamp with a filter to exclude light <300 nm. At this stage, some photolabelled samples were digested with chymotrypsin (Section 4.2.4).

Samples containing whole or digested CT were prepared for electrophoresis by extensive dialysis against 10 mM Tris, pH 7.5, 0.5 mM EDTA, 0.005 % SDS (w/v), 2 mM DTT, 0.05% BSA (fatty acid free). For chymotrypsin-digested samples, 0.5 mM PMSF was included in the dialysis buffer. Samples were concentrated in a Savant Speed-Vac evaporator prior to addition of sample buffer. CT and large fragments were separated on a 12 % polyacrylamide gel (Section 4.2.5). Small CT fragments were separated on a 16.5%T / 3%C Tricine gel system (Section 4.2.5). In both cases, the portion of the gel containing the bromphenol blue dye-front was excised, as it contained labelled lipid present in the sample.

4.2.9.3 [^{125}I]TID Photolabelling of Peptide 62

Peptide 62 (see figure 3.1, Section 3.3.1), was added to preincubated [^{125}I]TID and PC/oleic acid in 10 mM Tris, 1 mM EDTA (1:200 peptide to lipid molar ratio). The sample was incubated 10 min, transferred to a 1 ml quartz cuvette and photoreacted as described (Section 4.2.9.2).

Samples containing peptide were delipidated prior to electrophoresis by precipitation with cold acetone at -80°C for 3 to 8 hours, followed by a wash with cold diethyl ether. The resulting precipitate was resuspended in sample buffer and electrophoresed overnight at 4°C on a 16.5%T, 6% C polyacrylamide gel with a spacer gel (Section 4.2.5).

4.3 Results

4.3.1 Gel filtration analysis of CT binding to PC/oleic acid vesicles

Our objective was to photoreact CT with [^{125}I]TID under conditions where all of the CT was in the membrane-bound form. The purified CT was obtained bound to Triton-X100 micelles, to which we added egg PC/oleic acid vesicles containing traces of [^{125}I]TID resulting in a PC/oleic acid/Triton-X100 ratio of 2/2/1. This mixture forms vesicles that fully activate CT (Cornell, 1991a). Sephacryl S400 gel filtration chromatography was used to analyze the degree of binding of CT to the vesicles under photolysis conditions (Fig. 4.1). In the presence of Triton-X100 micelles alone, CT eluted slightly ahead of the peak of Triton-X100 radioactivity (Fig. 4.1A). Since Triton-X100 was in large excess (10 mM), the bulk of the detergent was in the form of a protein-free micelle (90 000 daltons). CT associates with Triton-X100 as a 84 kDa dimer (Cornell, 1989b), thus the few micelles containing protein would be significantly bigger and elute earlier. The size of Triton-X100 micelles containing a CT molecule was previously estimated at ~2 x 10^5 daltons, by Sephacryl S-400 chromatography (Cornell, 1991a).

In the presence of PC/oleic acid/Triton-X100 (2/2/1), the conditions used for the photolabelling reaction, CT eluted earlier than in the presence of Triton-X100 alone (Fig. 4.1A and B). [^{14}C]oleic acid was incorporated into the vesicles as a tracer. In some experiments, [^{3}H]DPPC was instead incorporated into the vesicles and eluted at the same volume as did the oleic acid, demonstrating that the two lipids remain complexed. [^{14}C]oleic acid or

[^{3}H]DPPC, along with a small amount of the Triton-X100, eluted early in the column presumably as large vesicles in the absence (data not shown) or presence of CT (Fig. 4.1B). In the presence of PC/oleic acid, CT eluted from the column as a single peak corresponding exactly to the peak of radiolabelled [^{14}C]oleic acid, and much earlier than the peak of [^{3}H]Triton-X100 present in the sample. No CT protein eluted in fractions between 26 to 29 ml where CT was found when mixed with Triton-X100 only (Fig. 4.1A). We conclude that 100% of the CT in the sample was bound to PC/oleic acid vesicles under these conditions which were the same as those used in the photolabelling experiment.

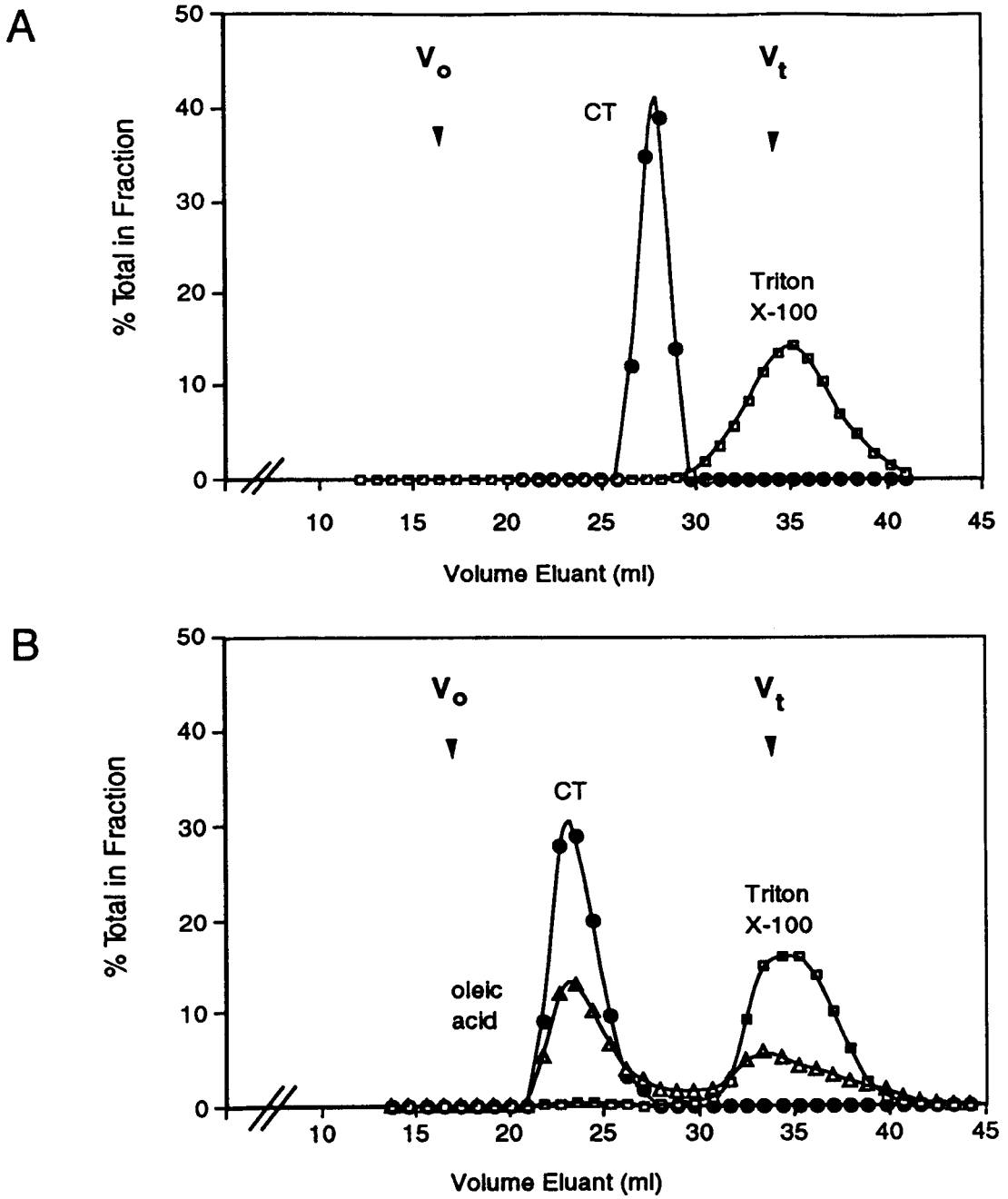

Figure 4.1: Gel filtration analysis of the binding of CT to PC/ oleic acid vesicles. The samples applied to the Sephacryl-S400 column were prepared and chromatographed, and fractions were analysed for radioactivity and CT as described in Section 4.2.3. [^{14}C]oleic acid was incorporated into the vesicles and [^{3}H]Triton-X100 was added to the samples in trace amounts. **A)** Chromatography of CT plus 10 mM Triton X-100. **B)** Chromatography of CT plus 4 mM PC/oleic acid (1:1) vesicles. The lipid to protein molar ratio in this sample was 350:1; the Triton X-100 content was 20 mol% of the total amphiphile. CT protein (●), [^{3}H]Triton-X100 (□), [^{14}C]oleic acid (Δ).

4.3.2 [^{125}I]TID labelling of CT in the presence of PC/oleic acid vesicles

Purified CT was photoreacted with [^{125}I]TID incorporated into PC/oleic acid vesicles (1:1). Irradiation of the enzyme under the conditions described did not affect the CT activity (data not shown). Electrophoresis was utilized to separate the protein from lipid, which migrated at the dye front and contained >99% of the label. As seen in figure 4.2, CT was significantly labelled by [^{125}I]TID. CT contained 0.03 to 0.05% of the total label added. When 0.2 mol% [^{125}I]TID was used, approximately 1 in 5000 CT molecules became labelled, while at 1 mol% [^{125}I]TID, an estimate of 1 in 650 CT monomers had label associated. The lack of stoichiometric labelling of CT does not imply that 100 % of the molecules present are not bound and intercalated in the membrane. TID photolabelling is a trace labelling technique. When TID is activated by irradiation, the carbene formed reacts quickly and with low specificity with any molecule in the vicinity. It can react with methylene groups of the acyl chains of lipid and, as the lipid is in large excess, the bulk of the label becomes lipid associated. To demonstrate the selectivity for membrane interacting proteins, a soluble protein, ovalbumin, was subjected to photolabelling under the same conditions as CT. Ovalbumin was not significantly labelled by the probe (Fig. 4.2B, lane 2). Apolipoprotein AI, which associates with PC, is also thought to interact with membranes via an amphipathic helix (Segrest *et al.*, 1994). When reacted with [^{125}I]TID in the presence of PC vesicles under the same conditions as CT, this protein was labelled to approximately the same extent as CT (Fig. 4.2B, lane 3). These results confirm that the membrane-bound form of CT is embedded in the

hydrophobic core of activating membranes, as opposed to interacting only with the membrane surface.

Figure 4.2: [^{125}I]TID labelling of CT and control proteins.

Proteins were labelled with [^{125}I]TID (0.2 mole %, 3 μCi) in vesicles as described in Section 4.2.9.2. Samples were electrophoresed on a 12% acrylamide gel. (**A**) Gel stained with Coomassie blue. (**B**) Autoradiograph of dried gel, exposed for 20 hr. *Lane 1*: CT (20 μg) labelled in the presence of 0.75 mM PC/oleic acid (1:1). *Lane 2*: Ovalbumin (12 μg) labelled in the presence of 0.75 mM PC/oleic acid (1:1). *Lane 3*: Apolipoprotein A-1 (11 μg) labelled in the presence of 0.5 mM PC. The positions of molecular weight standards are shown. Under these gel conditions, Apolipoprotein A-1 (28 kDa) appears to run fast relative to the molecular weight standards.

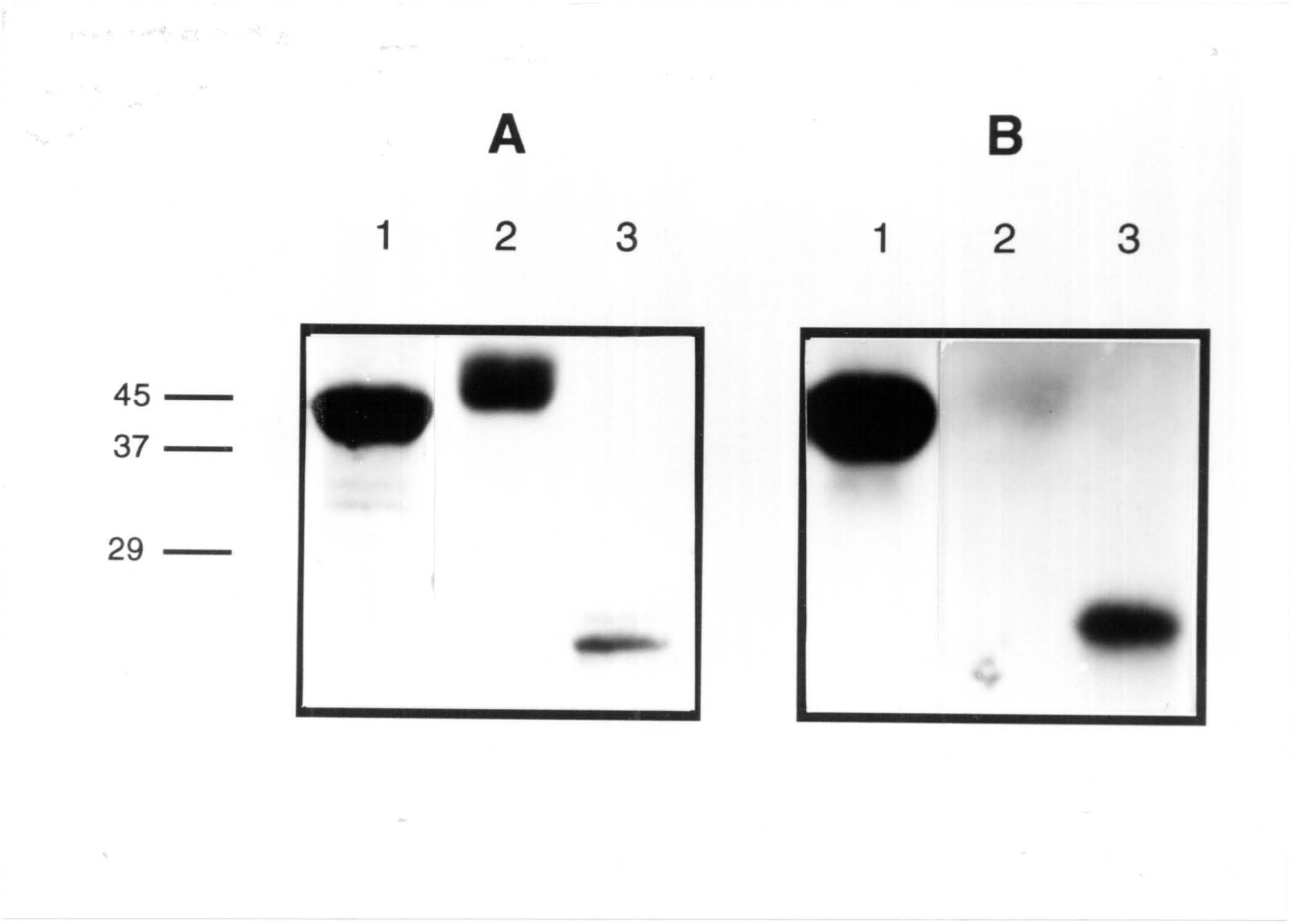
A
B
1
2
3
1
2
3
45
37
29

4.3.3 [^{3}H]TUA labelling of CT in the presence of PC/oleic acid vesicles

Purified CT was photoreacted with [^{3}H]TUA incorporated into PC/oleic acid vesicles (1:1) under conditions similar to the [^{125}I]TID experiment. Electrophoresis was utilized to separate the protein from lipid, which migrated at the dye front and contained >99% of the label. CT was significantly labelled by [^{3}H]TUA (Fig. 4.3, lane 3). CT contained 0.04 % of the total label added. When 1 mol% [^{3}H]TUA was used, approximately 1 in 500 CT molecules became labelled. TUA photolabelling, like TID, is a trace labelling technique. To demonstrate the selectivity for membrane interacting proteins, ovalbumin and apolipoprotein AI were subjected to photolabelling under the same conditions as CT. The Coomassie-stained gel revealed protein bands at ~28 kDa, 45 kDa and 42 kDa in lanes 1, 2, and 3 respectively. Ovalbumin was not significantly labelled by the probe in the presence of PC/oleic acid (Fig. 4.3, lane 2), while apolipoprotein AI became covalently labelled in the presence of PC vesicles under the same conditions as CT (Fig. 4.3, lane 1). The results with this second probe confirm that the membrane-bound form of CT is embedded in the hydrophobic core of activating membranes, as opposed to interacting only with the membrane surface.

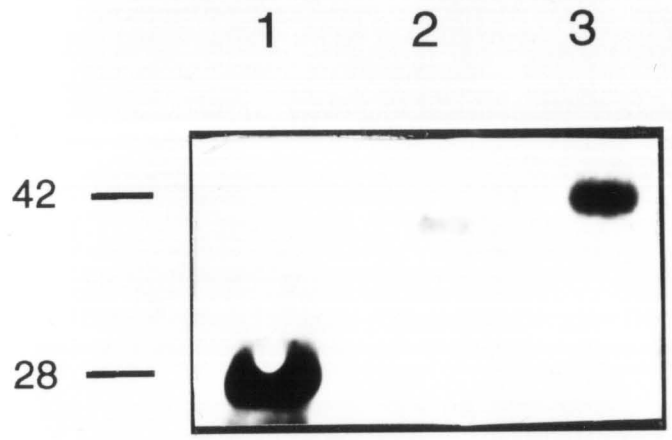

Figure 4.3: [^{3}H]TUA labelling of CT and control proteins.
Proteins were labelled with [^{3}H]TUA (0.5 mol%) in PC/oleic acid vesicles as described in Section 4.2.9.1. Samples were electrophoresed on a 12% acrylamide gel. The fluorograph of the dried, salicylate-soaked gel, exposed for 9 days, is shown. *Lane 1*: Apolipoprotein A-1 (10 μg) labelled in the presence of 0.5 mM PC. *Lane 2*: Ovalbumin (10 μg) labelled in the presence of 0.75 mM PC/oleic acid (1:1). *Lane 3*: CT (10 μg) labelled in the presence of 0.75 mM PC/oleic acid (1:1).

4.3.4 Chymotrypsin Fragmentation Pattern of CT

The products of partial proteolysis of CT by chymotrypsin have been previously characterized (Craig *et al.*, 1994). Under those conditions, CT was digested from the C-terminus to produce discrete fragments of ~39, 35, 30, 28, and 26 kDa which contained the N-terminal domain but were missing different lengths of the C-terminal region, as mapped using antibodies directed against these regions. The C-terminal residue of each fragment was estimated (Fig. 4.4) based on the apparent molecular weight, CT amino acid sequence and chymotrypsin selectivity for large, hydrophobic amino acids. The two largest fragments contained the amphipathic helix region of CT, while the ~30, 28 and 26 kDa fragment were missing most or all of this region. Under the current digestion and electrophoresis conditions, fragments of 39, 35 and one in the 30 to 26 kDa region were produced (Fig. 4.6A)[2] , along with a faint band migrating immediately behind the dye front (Fig. 4.6A, lane 3). To further investigate this band, we used a Tricine gel system, which effectively separates low molecular weight proteins/peptides. Separation revealed four previously uncharacterized low molecular weight CT fragments with apparent molecular weights of ~19, 17, 15 and 11 kDa. (Fig. 4.5A). The largest of the fragments reacted with an antibody directed against the C-terminal 13

---

[2] The purified CT contains an endogenous protease which partially digests the protein during the incubation at 37 °C (Fig. 4.6A, lane 2). A number of different proteases have been shown to produce similar fragmentation patterns for CT, suggesting that there are a few very sensitive sites in the native protein (Craig and Cornell, unpublished observation).

residues of CT (Fig. 4.5B) and all fragments reacted with an antibody directed against a 33 residue peptide of the amphipathic helix domain (Fig. 4.5C). Sequence analysis revealed that all four fragments have the same N-terminal sequence, beginning at Thr226. This position lies 10 residues N-terminal to the amphipathic helix domain. As the largest fragment (M_{ap} = 19 kDa) reacted with the C-terminal antibody, it is assumed to comprise the entire C-terminal region, giving it a calculated molecular weight of 16,200. The apparent discrepancy in electrophoretic mobility may be attributed to its highly phosphorylated state (Cornell *et al.*, 1995; MacDonald & Kent, 1994). The three smaller fragments appear to be produced by progressive digestion of the C-terminus from the 16.2 kDa fragment. The molecular weights of these fragments have been estimated at ~14, 12 and 9 kDa based on potential cleavage sites. The lowest molecular weight fragment would approximately comprise the amphipathic helix region with a 10 amino acid extension at the N-terminus. The exact C-terminal residue is not known. Thus, in addition to the susceptible C-terminal cleavage sites which yield the 39 and 35 kDa fragments upon digestion, a main site for cleavage of CT by chymotrypsin is at Tyr225, producing an N-terminal 26 kDa fragment and a series of low molecular weight fragments derived from the C-terminal portion containing the amphipathic helix domain.

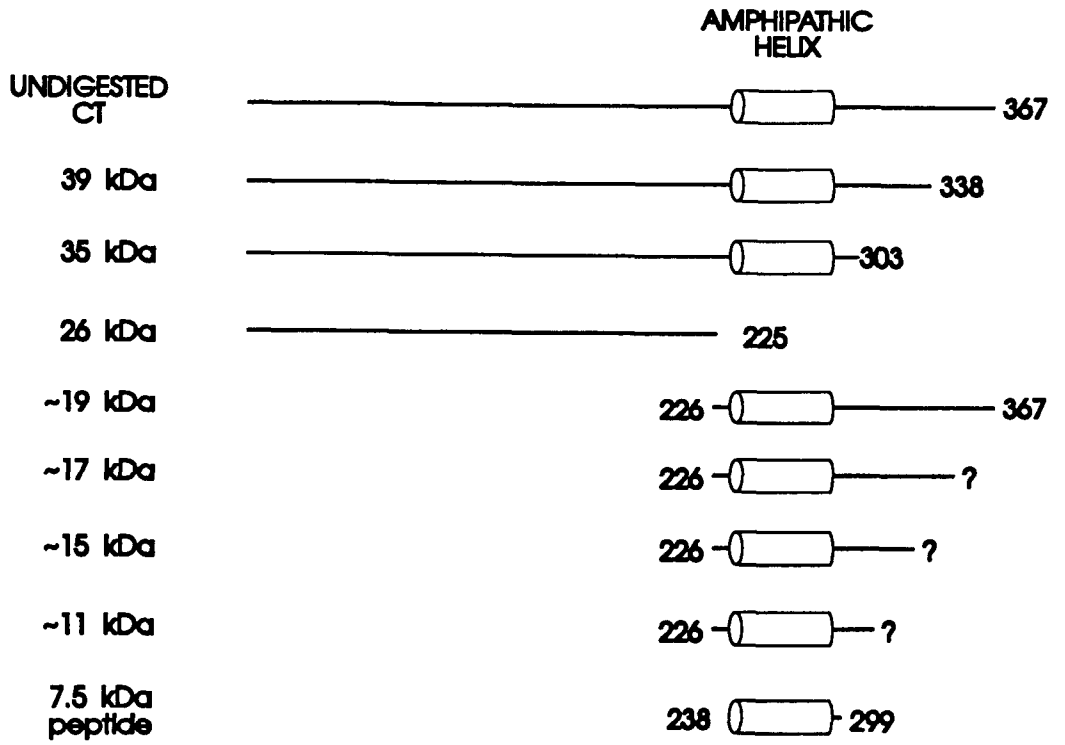

Figure 4.4: Proposed CT fragments generated by chymotryptic digestion.

The large 39, 35 and 26 kDa fragments were mapped by Craig *et al.* (1994). The N-terminal residues of the low molecular weight fragments of M_{ap}= 19, 17, 15 and 11 kDa were determined by N-terminal sequencing. The 19 kDa fragment contains the C-terminal residues (determined by antibody mapping, Fig. 4.5), and has a calculated molecular weight of 16,200. The exact molecular weights of the smaller fragments remain undetermined. All low molecular weight fragments contain the amphipathic helix region as determined by antibody mapping.

Figure 4.5: Antibody mapping of the low molecular weight chymotryptic fragments of CT. Undigested CT (4 μg, *lane 1*), CT (12 μg) digested by chymotrypsin at 1:10 (chymotrypsin:CT) mass ratio (*lane 2*) or 1:8 ratio (*lane 3*), were electrophoresed on 16.5% T / 3% C Tricine gel system as described in Section 4.2.5. The gel was Coomassie-stained (**A**), or transferred to PVDF membrane and immunoreacted with a 1/200 dilution of antibody directed against the amphipathic helix region (**B**), or a 1/1250 dilution of antibody directed against the C-terminal region (**C**).

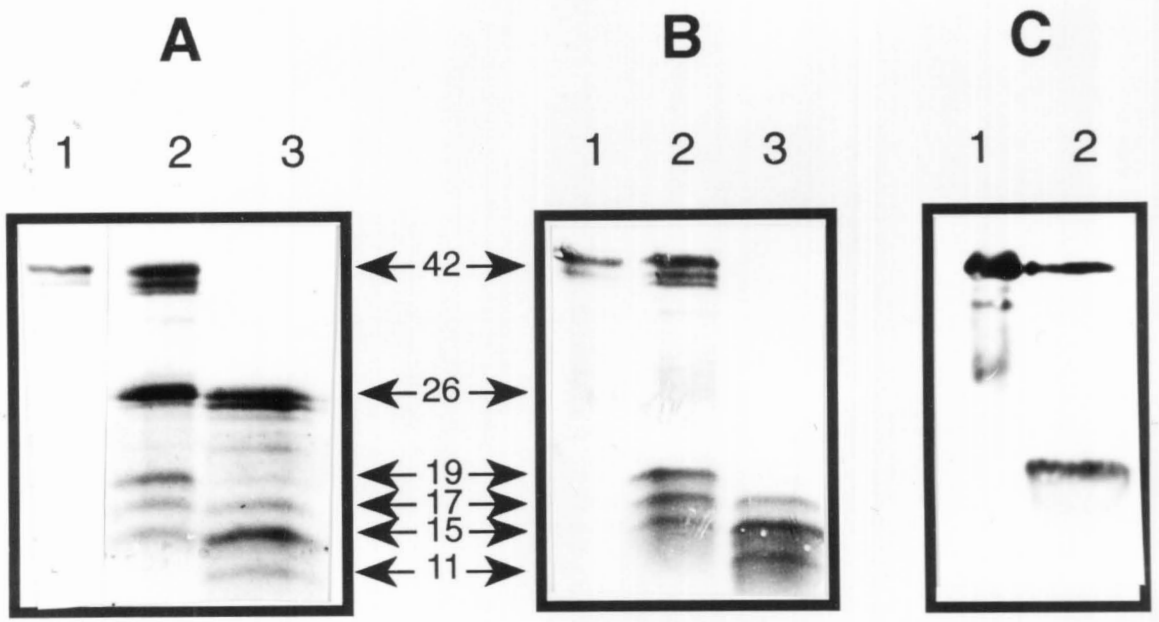
A
B
C
1
2
3
1
2
3
1
2
42
26
19
17
15
11

4.3.5 Localization of [^{125}I]TID Labelling on the CT Protein

To establish which region of CT becomes membrane embedded, the protein was labelled with [^{125}I]TID in the presence of PC/oleic acid vesicles followed by digestion with chymotrypsin to produce the series of characterized fragments. The fragments were separated by 12 % Laemmli SDS-PAGE and the label analyzed by autoradiography (Fig. 4.6). Low protease concentration produced the 39 and 35 kDa fragments containing the proposed amphipathic helical domain (Fig. 4.6, lane 2). These fragments were both associated with [^{125}I]TID. At high chymotrypsin:CT ratios, the 26 kDa fragment was the dominant protein formed (Fig. 4.6A, lane 3). This fragment, which lacks the entire amphipathic helix region had only a small amount of label associated (Fig. 4.6B, lane 3). Also evident in this lane is a protein band at the dye front corresponding to the low molecular weight fragments of CT. As seen in the autoradiograph this band was highly labelled by [^{125}I]TID.

In a separate experiment, CT was photolabelled by [^{125}I]TID in presence of PC/oleic acid vesicles, digested with chymotrypsin, and the fragments separated by the Tricine gel system to analyze the low molecular weight fragments. Autoradiography revealed that the fragments at 19, 17, 15 and 11 kDa all contained [^{125}I]TID label in high levels (Figure 4.7). These fragments encompass the amphipathic helix region of CT. Whole CT, as well as the 39, 35, 26 kDa fragments, was also evident on this gel. In a separate experiment, the label associated with each fragment was quantitated (Table 4.I). The 39 and 35 kDa fragments contained as much or more label as the whole CT (110-170 cpm/μg), while the 26 kDa fragment which is the dominant

protein on the Coomassie-stained gel contained less label (70 cpm/μg). The low molecular weight fragments were more enriched in label than the whole CT molecule (500 -1200 cpm/ug). This pattern is consistent with the amphipathic helix region, contained in the low molecular weight fragments but lacking in the 26 kDa fragment, playing the key role in membrane intercalation.

Figure 4.6: Analysis of the high molecular weight fragments derived from [^{125}I]TID labelled CT. CT (20 μg per lane) was photolabelled with [^{125}I]TID (~4 μCi) in the presence of 0.75 mM PC/oleic acid. *Lane 1*: undigested sample. *Lane 2:* digestion by an endogenous protease. *Lane 3*: digestion by chymotrypsin at a mass ratio of 1:100 (chymotrypsin:CT). Proteins were separated on a 12% gel as described in Methods section. **A**) Gel stained with Coomassie blue. **B**) Autoradiograph of dried gel, exposed for 20 hr. The position of molecular weight standards is shown.

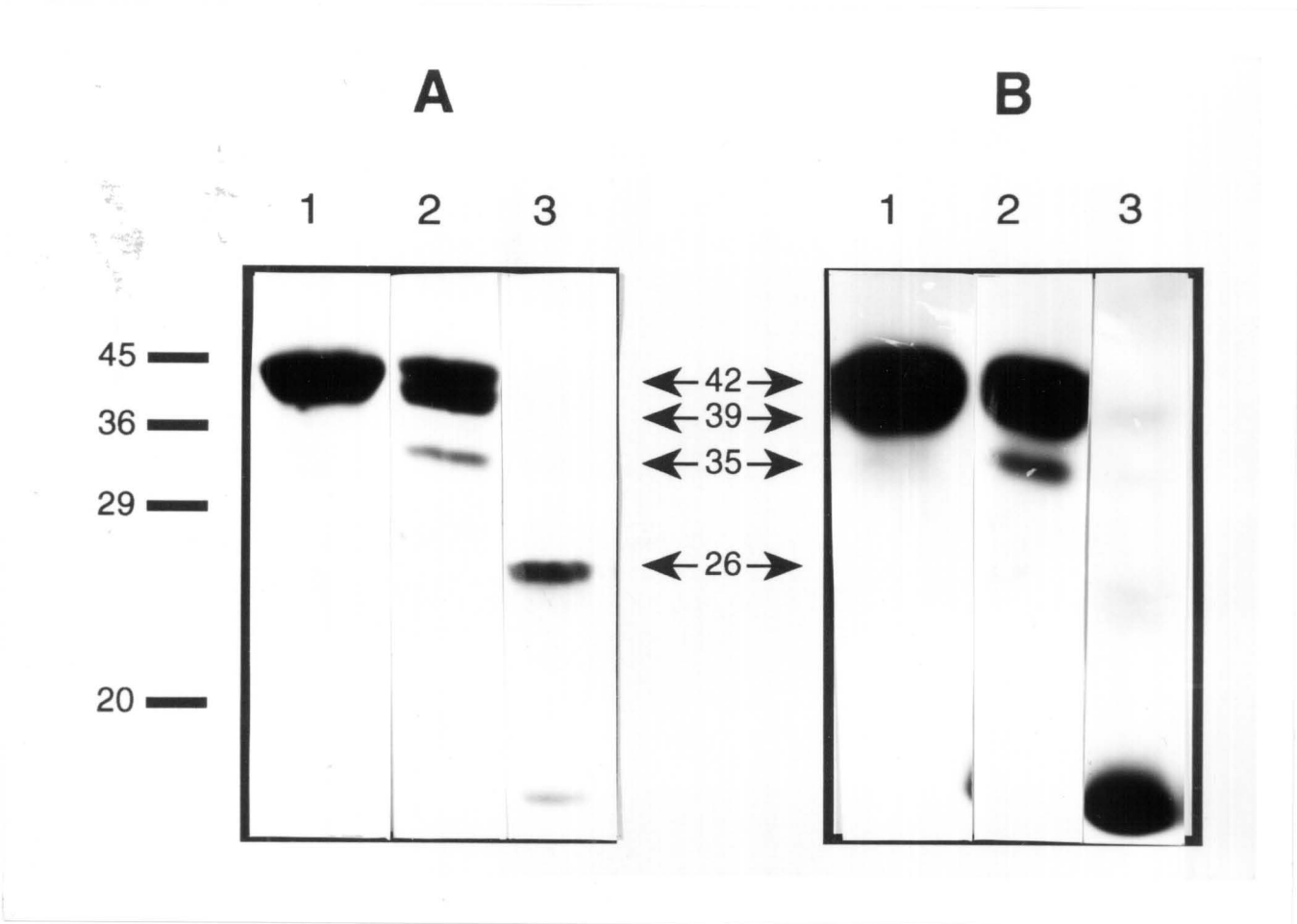
A
B
1
2
3
1
2
3
45
36
29
20
42
39
35
26

Figure 4.7: Analysis of the low molecular weight fragments derived from [^{125}I]TID labelled CT. CT (20 μg per digested lane) was photolabelled with [^{125}I]TID (0.2 mole %, ~3 μCi per digested lane) in the presence of 0.75 mM PC/oleic acid. *Lane 1:* undigested sample (~1.5 μg). *Lane 2:* digestion by chymotrypsin at a mass ratio of 1:100 (chymotrypsin:CT). *Lane 3*: chymotrypsin:CT ratio of 1:30. Proteins were separated on a 16.5%T / 3%C Tricine gel as described in Methods section. **A**) Gel stained with Coomassie blue. **B**) Autoradiograph of dried gel, exposed for 3 days.

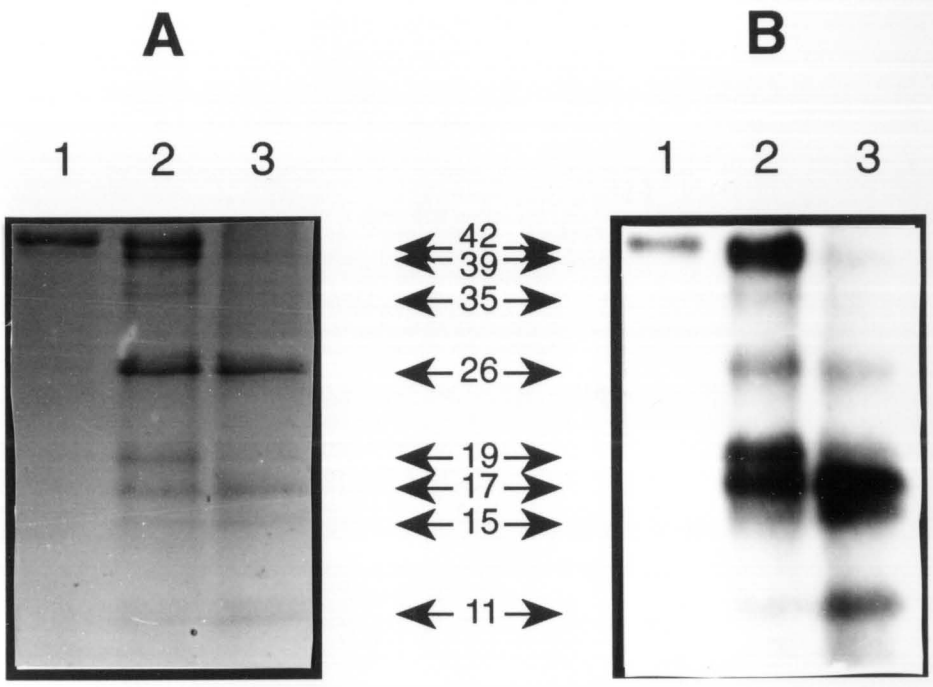
A
B
1
2
3
1
2
3
42
39
35
26
19
17
15
11

TABLE 4.I: Extent of [^{125}I]TID Labelling of the Fragments of CT

FRAGMENT	% DISTRIBUTION OF PROTEIN	CPM / μg protein	TID:PROTEIN MOLAR RATIO
undigested CT	-	110	1:4600
39	21	170	1:3300
35	8	160	1:4100
26	48	70	1:12000
19	2	1200	1:1100
17	10	510	1:3200
15	4	490	1:3700
11	7	790	1:3200
peptide	-	870	1:3100

CT or peptide was photolabelled in the presence of PC/oleic acid with 0.2 mole% [^{125}I]TID. An aliquot of the CT sample was removed (undigested CT), the remainder digested with chymotrypsin, and the fragments separated by electrophoresis as described in Methods section. Protein was quantified by densitometry of the Coomassie stained gel, normalized to a CT standard. The percent distribution of protein mass among the fragments is given. ^{125}I was quantified by gamma-counting of the excised bands. TID:protein molar ratio was calculated. Moles of CT were estimated from the quantified mass of protein using the estimated true molecular weights for each fragment of 16, 14, 12 and 9 kDa. Moles of TID was calculated from CPM and specific activity of the [^{125}I]TID.

4.3.6 Photolabelling of CT in the presence of PC/diacylglycerol vesicles

In addition to anionic lipids, typified by PC/oleic acid vesicles, CT is also activated by membranes containing diacylglycerol. Since the synthetic peptides corresponding to the amphipathic α-helix domain did not bind preferentially to vesicles containing diacylglycerol (Chapter 3), it was possible that domains in CT outside this region might be labelled by [^{125}I]TID when CT was bound to diacylglycerol-containing vesicles. To probe this interaction, [^{125}I]TID labelling of CT was attempted in the presence of egg PC/diacylglycerol vesicles (4:1). CT was subsequently digested with chymotrypsin and the fragments separated on the 16%T/ 3%C Tricine gel system. The fragmentation pattern of CT and [^{125}I]TID labelling patterns obtained in the presence of PC/diacylglycerol (data not shown) were identical to those obtained in the presence of PC/oleic acid (Fig. 4.7). The whole enzyme and the large 39 and 35 kDa fragments contained associated label. The low molecular weight fragments including the amphipathic helix region of the enzyme contained the large majority of the label, while the 26 kDa fragment lacking this region was not highly labelled. Thus, the intercalation of CT into PC/diacylglycerol membranes involves the same amphipathic helix region involved in interaction with anionic membranes.

4.3.7 Photolabelling of a Peptide Corresponding to the Entire Amphipathic Helical Domain

Analysis of digested, photolabelled CT supports our hypothesis for the amphipathic helix region as the membrane-binding domain. To further substantiate this model, we obtained a 62 residue peptide corresponding in sequence to the entire proposed amphipathic helical domain of CT (residues 238 - 299). This peptide has a partition coefficient for PC/oleic acid vesicles of ~8400, and adopts a helical conformation in response to lipid vesicles or detergent micelles, as analyzed by CD (Section 3.3.3) and NMR (Dunne, Cornell, Johnson and Tracey, unpublished). This peptide was photoreacted with [^{125}I]TID in presence of PC/oleic acid and was separated from lipid on a 16.5%T, 6% C Tricine gel system. The peptide was highly labelled by [^{125}I]TID (Table 4.I). The efficiency of [^{125}I]TID incorporation into the peptide was 0.05 to 0.08%, slightly higher than that obtained for the whole enzyme. The radioactivity per μg of peptide was similar to that obtained for the low molecular weight fragments of CT. At 0.2 mol% [^{125}I]TID, 1 in 3100 peptide molecules became associated with [^{125}I]TID. These results confirm that this region of the protein can intercalate into membranes independently of the rest of the protein. We attempted N-terminal sequencing of [^{125}I]TID labelled peptide, as well as the low molecular weight chymotrypsin fragments, to identify the labelled amino acids, but the degree of labelling was insufficient, and all cycles in the Edman degradation contained background levels of radioactivity.

4.4 Discussion

4.4.1 The CT-membrane interaction involves intercalation into the hydrophobic membrane core

We have used the photoreactive probes [^{125}I]TID and [^{3}H]TUA to investigate the mechanism of the CT-membrane interaction. The fact that [^{125}I]TID and [^{3}H]TUA significantly label CT suggests a mechanism of membrane interaction whereby the protein intercalates into the hydrophobic membrane core. It is well accepted that CT interacts with membranes, but the mechanism of membrane interaction is not known. There are several lines of evidence to suggest that the binding is not solely a peripheral charge interaction between protein and lipid head groups, but that penetration into the hydrophobic core is involved (Section 1.3.2.3). While ionic strength effects the enzyme activity (Cornell, 1991a), high salt is insufficient to extract enzyme from the membrane; detergents are needed (Cornell & Vance, 1987b). Intercalation was postulated due to dependence of activity on a fluid membrane phase, enhancement of activity at the phase transition and dependence on bilayer curvature (Cornell, 1991b). Intercalation has been demonstrated for synthetic peptides corresponding in sequence to a proposed membrane-binding region of the protein (Chapter 3; Johnson & Cornell, 1994). Thus, although previous studies had suggested that the protein is embedded in the hydrophobic core of the membrane, this had never been demonstrated directly using the purified native enzyme.

The degree of labelling with [^{125}I]TID is consistent with an interaction

of CT involving membrane intercalation. While the [^{125}I]TID labelling efficiency depends on the mole percent and type of protein in the membrane as well as the reaction efficiency of TID under the irradiation conditions used, a range of 0.5 to 0.01 % of the [^{125}I]TID generally becomes incorporated into membrane-embedded proteins (Brunner, 1993). The [^{125}I]TID labelling efficiency of CT, 0.03 to 0.05%, falls within this range. A bromelain-released soluble fragment of hemagglutinin lacking the trans-membrane anchor (BHA2) was [^{125}I]TID labelled with an efficiency of 0.025% using conditions similar to ours (Harter *et al.*, 1988). The key region of BHA2 labelled by [^{125}I]TID was a small membrane-interacting region proposed to be involved in fusion.

4.4.2 The amphipathic helix of CT is the key region involved in intercalation

The results obtained using proteolysis of CT in combination with photolabelling demonstrate the key role of the amphipathic helix region in the membrane intercalation of the protein. The 39 and 35 kDa N-terminal fragments containing this region were associated with the hydrophobic photolabel, while the 26 kDa fragment lacking this region contained a low level of labelling. We have identified low molecular weight fragments that had not been previously characterized (Craig *et al.*, 1994) due to the gel conditions and antibodies used for detection in that study. These fragments, with molecular weights in the range of ~9 kDa to 16 kDa, comprise the entire amphipathic helix region as well as various lengths of the C-terminal domain. The persistence of these fragments demonstrates the resistance of the amphipathic helix region to digestion, consistent with a membrane-bound

location where it would be inaccessible to the protease. The high [^{125}I]TID labelling of the low molecular weight fragments comprising the amphipathic helix region demonstrates the key role for this region in CT membrane binding. A synthetic peptide corresponding in sequence to the amphipathic helix region became labelled to the same extent as these fragments, substantiating our conclusion that this region functions as the key membrane binding site for CT. The same region of CT is labelled by [^{125}I]TID whether the lipid vesicles contain oleic acid or diacylglycerol, suggesting a common mechanism of binding to the two different classes of activating lipids. It remains to be explained why this region on its own does not interact with PC/diacylglycerol vesicles. This region is required for diacylglycerol binding (Craig *et al.*, 1994), but is not sufficient (Chapter 3).

There is some label found in the 26 kDa fragment, which appears to be more than just background. [^{125}I]TID has a partition coefficient for egg PC or red cell membranes of 4 x 10^4 (Brunner & Semenza, 1981), which in our system (500 µl solution volume, ~ 0.17 mg lipid) would result in 93% of the TID partitioning into hydrophobic core of vesicles, and 7% in the aqueous phase. Lack of significant labelling of ovalbumin suggests that this small amount of free TID does not contribute to the labelling of soluble proteins. CT is not a soluble protein, and the proximity of the N-terminal region to the vesicle may contribute to the small amount of labelling. When labelling the integral F_o subunits of *E.coli* ATP synthase, a peripheral F_1 subunit (β) became associated with a low level of label, suggesting that [^{125}I]TID can potentially react with peripheral membrane proteins (Hoppe *et al.*, 1984). While the N-terminal region of CT does not associate with membranes on its

own (Craig *et al.*, 1994; Cornell *et al*, 1995; Wang & Kent, 1995b), a small portion could penetrate the membrane as this region is held in close proximity to membrane surface by the amphipathic helix. However, a truncation mutant lacking the amphipathic helix and C-terminal phosphorylation region was constitutively active in the absence of membranes (Wang & Kent, 1995b), suggesting that lipid is not directly required for catalysis. Non-membrane proteins have been photolabelled with [^{125}I]TID in the absence of lipid. It is thought that [^{125}I]TID probes for hydrophobic patches or pockets in the soluble proteins. Hydrophobic sites in calmodulin (Krebs *et al.*, 1984), troponin C (Buerkler & Krebs, 1985) and lactalbumin (Van Ceunebroeck *et al.*, 1986) involved in the interaction with target proteins have been labelled by [^{125}I]TID in a Ca^{+2} dependent manner in the absence of lipids. A cytochrome P-450 (Frey *et al.*, 1986) and an H^+-ATPase from yeast (Seto-Young *et al.*, 1992) are both labelled in their membrane-embedded regions and in a soluble region attributed to hydrophobic substrate-binding pockets. While the active site of cytochrome P-450 would be designed to accommodate its hydrophobic substrates, the active site for the H^+-ATPase may more closely resemble the active site of CT which is also involved in nucleotide reactions. While little is known about the environment of the active site of CT, there may exist a hydrophobic pocket involved in substrate binding or interaction with the hydrophobic face of the amphipathic α-helix domain when the protein is in the soluble form.

CHAPTER 5: CONCLUDING DISCUSSION

5.1 The amphipathic α-helix region of CT plays a key role in the membrane interactions

The results in this thesis have established a key role for the proposed amphipathic α-helix region of CT in its membrane interactions. Spectroscopic studies of synthetic peptides demonstrated that the region is indeed capable of forming a helical conformation, and is induced to form this structure by anionic lipids. These same peptides intercalated to the acyl chain core of lipid vesicles with a selectivity for anionic lipids, supporting an intercalation event for the protein. In a different approach, the photoreactive probes [^{125}I]TID and [^{3}H]TUA were utilized to investigate the membrane interaction of native CT. [^{125}I]TID and [^{3}H]TUA significantly labelled CT, establishing a mechanism of membrane interaction whereby the protein intercalates into the hydrophobic membrane core. CT proteolytic fragments and a synthetic peptide containing the amphipathic α-helix were highly labelled, while the fragment lacking this region contained a low level of labelling. Resistance of the amphipathic helix region to proteolysis in the presence of lipids, demonstrated by the persistence of the low molecular weight fragments, implied a membrane-bound location where it would be inaccessible to the protease. Thus, proteolysis in combination with photolabelling has demonstrated the key role of the amphipathic helix region in the membrane intercalation of CT.

Additional evidence to support involvement of the putative amphipathic α-helix region of CT in membrane binding has emerged recently. 1) The amphipathic α-helix region of CT was observed to have sequence homologies with the sequence of oleosin, a protein which is also proposed to interact with membranes via an amphipathic α-helix (Li *et al.*, 1993). 2) Chymotrypsin proteolysis of CT produced discrete fragments that were mapped to the N-terminus and were missing various amounts of the C-terminal region of the protein. Those fragments which lacked all or part of the putative amphipathic helical region were unable to bind to lipid vesicles *in vitro* (Craig *et al.*, 1994). 3) Antibodies directed against a 10 amino acid segment of this region inhibited membrane binding (Wieder *et al.*, 1994). 4) Overexpressed in COS cells (Cornell *et al.*, 1995) or CHO cells (Wang & Kent, 1995b), or purified from a baculovirus overexpression system (Yang *et al.*, 1995), CT deletion mutants lacking this domain had a decreased association with the membrane fraction of cells, and were unable to translocate in response to stimuli. While these results provide indirect evidence for an involvement of the amphipathic helical domain in CT-membrane interactions, an indirect effect of this helical region on the membrane binding was not ruled out until it was shown by hydrophobic photolabelling to be directly associated with the membrane.

5.2 An amphipathic α-helix model is consistent with other known features of CT membrane interactions

In addition to the data presented in this thesis, previous observations are consistent with a mode of interaction involving an amphipathic helix domain lying with its axis parallel to the surface of membrane, with the non-polar face

embedded to the acyl chain region of the membrane, and polar face interacting with lipid head groups, the aqueous solution or a distinct part of the protein. Such a model involves hydrophobic intercalation, as was proposed for CT based on the dependence of the activity on lipid phase and other parameters that disrupt membrane packing (Section 1.3.2.3). The amphipathic helix domain does not form a specific "binding pocket" designed to interact with a specific head group or with lipid monomers, but rather forms a relatively non-specific, low affinity hydrophobic surface, consistent with the lack of monomer activation and lipid head-group specificity of CT (Section 1.3.2.2). This model of interaction with the membrane could be readily reversible as demonstrated by the reversible association of apolipoprotein A-1 with lipoprotein particles. An amphipathic helix has the potential to convert between a structure compatible with a soluble or a membrane-bound form, upon structural reorganization (see below Section 5.3).

5.3 Amphipathic α-helices have been proposed to mediate membrane binding of other proteins

The amphipathic α-helix structure mediates the membrane interactions of several other proteins. A few key examples are discussed below.

Apolipoproteins:

The original model for amphipathic α-helices as membrane-surface interacting motifs was proposed for apolipoproteins (see Section 1.3.3.3). These protein components of serum lipoproteins stabilize the lipoprotein structure. Apolipoproteins of types A (I & II), C (I, II, III, & IV) and E are exchangeable, in that they move from one lipoprotein to another, binding to a PC membrane

surface (reviewed by Segrest *et al.*, 1992, 1994). These types of lipoproteins contain 11- or 22-mer repeats in the amino acid sequence which correspond to amphipathic helix motifs. Studies of proteolytic digestion fragments and synthetic peptides have identified regions of each protein capable of membrane binding, all of which correspond to regions predicted to form an amphipathic α-helix (Segrest *et al.*, 1992). Circular dichroism studies have demonstrated that these regions are stabilized in a helical conformation upon membrane binding (*e.g.* Mao *et al.*, 1977; Sparrow, *et al.*, 1985; Sparrow, *et al.*, 1992). Recently, the NMR structures of two SDS-bound, synthetic peptides corresponding to membrane-binding regions of Apolipoprotein C-1 confirmed the adoption of a helical structure upon binding to a hydrophobic surface (Rozek *et al.*, 1995). The first crystal structure of an apolipoprotein was reported for insect apolipophorin-III, an exchangeable protein involved in lipid transport via a lipoprotein complex (Breiter *et al.*, 1991). The solution form of insect apolipophorin (from *L. migratoria*) is a five amphipathic-helix bundle with the hydrophobic faces in the interior. Reversible membrane binding, for this and other apolipoproteins, has been proposed to involve the helices spreading on the membrane surface to expose the hydrophobic faces to the membrane without disrupting the secondary structure (Segrest *et al.*, 1992; Breiter *et al.*, 1991).

Pyruvate oxidase

Pyruvate oxidase is an amphitropic protein which, upon binding substrates, associates and is activated by membranes. Activation is promoted by many different amphiphiles, including detergents, fatty acids and phospholipid, with very little head group specificity, although there is a slight preference for an anionic surface (Blake *et al*, 1978). The binding is proposed to be hydrophobic in

nature (Blake *et al.*, 1978). The C-terminal portion of the protein contains the membrane-binding region, demonstrated with a deletion mutant (Grabau & Cronan, 1986), and by covalent labelling with [^{14}C]lauric acid (Hamilton *et al.*, 1986). Proteolysis of the substrate-bound enzyme, releasing the 23 C-terminal residues, mimics membrane-binding for enzymatic activation, suggesting that this domain may serve an auto-inhibitory function (Recny *et al.*, 1985). The released peptide associated with PC vesicles (Zhang & Hager, 1987), and contains a putative amphipathic α-helix (Recny *et al.*, 1985). Introduction of a helix-disrupting proline residue in the middle of this proposed helix abolished membrane-binding and activation of the protein, without affecting its activation by proteolysis, suggesting an important role in membrane binding for this helical structure (Grabau *et al.*, 1989). These results have led to a model for the activation of pyruvate oxidase in which substrate binding to the soluble protein induces a conformation change that exposes a lipid binding site, the amphipathic helix. Membrane binding prevents interaction of this region with the catalytic region of the protein and thus activates the enzyme (Recny *et al.*, 1985; Hamilton *et al.*, 1986; Grabau *et al.*, 1989).

Triglyceride Lipase

The crystal structure of lipases bound to a lipid substate analog led to a model whereby an amphipathic helix, together with the catalytic site, forms a hydrophobic face for the interaction of lipase with membranes (Brzozowski *et al.*, 1991; van Tilbeurgh *et al.*, 1992). In the soluble form of these lipases, the hydrophobic active site is covered by the hydrophobic face of a small amphipathic helix. Upon membrane binding, the helix flips open to expose the

hydrophobic surfaces to the membrane surfaces, thus allowing the active site to access the lipophilic substrate.

Prostaglandin H_2 synthase-1

In its crystal structure, a bundle of short amphipathic helices mediates the interaction of a prostaglandin H_2 synthase-1 with a hydrophobic surface (Picot *et al.*, 1994). This protein is permanently bound to the endoplasmic reticulum membrane, and thus does not have an alternate soluble conformation. In the crystal structure, the protein interacted with the hydrophobic detergent surface in a dimer form, via a series of four short (8 - 10 residue) amphipathic α-helices .

5.4 How does membrane binding of the amphipathic helix induce activation of CT

As little is known about the conformation of the soluble form of CT, it is difficult to propose what conformational changes are involved in the interconversion between active, membrane-bound CT and inactive, soluble CT. CT is a dimer in its active membrane-bound form (Cornell, 1989b) as well as its inactive cytosolic form (Weinhold *et al.*, 1989), eliminating a role for oligomerization in the activation of the enzyme. A mechanism involving a structural reorganization of the amphipathic helix, similar to that of prolipase or apolipophorin, could account for the conversion of CT between membrane-bound and soluble forms. How this could cause activation at the catalytic site is unknown.

The amphipathic helix region has been proposed to form an autoinhibitory domain, which is displaced from the catalytic domain upon membrane binding,

thereby activating the enzyme (Wang & Kent, 1995b). This type of model has been proposed for pyruvate oxidase (Section 5.3) and is also evident for another membrane-activated enzyme, protein kinase C (Orr *et al.*, 1992). However, removal of an autoinhibitory domain by proteolysis or mutation is expected to result in a constitutively active enzyme, as observed for pyruvate oxidase. While a constitutive activation of CT was reported for a mutant lacking the entire C-terminal amphipathic helix region (Wang & Kent, 1995b), studies with similar deletion mutants (Cornell *et al*, 1995; Yang *et al.*, 1995b; Veitch & Cornell, unpublished observations) and chymotrypsin proteolysis (Craig *et al.*, 1994) suggest that removal of the lipid binding domain results in an inactive enzyme that is unresponsive to lipids. Alternately, the membrane-binding event may induce a secondary event in the catalytic region of CT which stimulates activity. It has recently been shown that membrane-binding greatly increased the affinity of CT for CTP (Yang *et al.*, 1995b), suggesting that membrane binding induces a change in the active site, thereby activating the enzyme. In summary, at this time there is conflicting data on the mechanism whereby the lipid binding domain of CT regulates the catalytic domain.

In 1990, Kalmar *et al* (Kalmar *et al*, 1990) proposed that a putative amphipathic α-helix between residues 238 and 300 of rat-liver CT might mediate the reversible binding of CT to target membranes. They proposed a model for the membrane-bound form of the enzyme in which the amphipathic α-helix would lay parallel to the membrane surface with its hydrophobic face penetrating into the lipid acyl chains. The work in this thesis has validated this model. Using synthetic peptides I have established that the region between 238 and 300 is α-helical, but only in the presence of membranes containing "activating" lipids.

Furthermore, using lipid fluorescence quenchers and photoreactive probes I have demonstrated that the hydrophobic face intercalates into the outer monolayer of lipid bilayers. Thus, the mechanism whereby anionic lipids stimulate the activation of CT is to stabilize an α-helical conformation in this domain, which creates a hydrophobic binding site leading to membrane intercalation. The structural changes involved in this reversible interaction, and the mechanism whereby these changes activate the enzyme are now key questions in the elucidation of the regulation of PC metabolism by this enzyme.

REFERENCES:

Aeberhard, E. E., Barrett, C. T., Kaplan, S. A., and Scott, M. L. (1986) *Biochim. Biophys. Acta* **876**, 6-11.

Agawa, Y., Sannamu, L., Ono, S., Aoyagi, H., Ohno, M., Taniguchi, T., Anzai, K., and Kirino, Y. (1991) *J. Biol. Chem.* **266**, 20218-20222.

Anantharamaiah, G. M., Jones, J. L., Brouillette, C. G., Schmidt, C. F., Chung, B. H., Hughes, T. A., Bhown, A. S., and Segrest, J. P. (1985) *J. Biol. Chem.* **260**, 10248-10255.

Bartlett, G. R. (1959) *J. Biol. Chem.* **234**, 466-468.

Benfenati, F., Greengard, P., Brunner, J., and Bahler, M. (1989) *J .Cell Biol.* **108**, 1851-1862.

Blake, R., Hager, L.P., and Gennis, R.B. (1978) *J. Biol. Chem.* **253**, 1963-1971.

Blanton, M. P., and Cohen, J. B. (1992) *Biochemistry* **31**, 3738-3750.

Bligh, E. G. , and Dyer, W., J. (1959) *Can J Biochem. Physiol.* **37**, 911-917.

Bradford, M. (1976) *Anal. Biochem.* **72**, 248-253.

Breiter, D. R., Kanost, M. R., Benning, M. M., Wesenberg, G., Law, J. H., Wells, M. A., Rayment, I., and Holden, H. M. (1991) *Biochemistry* **30**, 603-608.

Brown, M. S., and Goldstein, J. L. (1983) *Ann. Rev. Biochem.* **52**, 223-261.

Brunner, J. (1993) *Ann. Rev. Biochem.* **62**, 483-514.

Brunner, J. (1989) *FEBS Letters* **257**, 369-372.

Brunner, J., Franzusoff, A.J ., Luscher, B., Zugliani, C., and Semenza, G. (1985) *Biochemistry* **24**, 5422-5430.

Brunner, J., Senn, H., and Richards, F. M. (1980) *J. Biol. Chem.* **255**, 3313-3318.

Brunner, J., and Semenza, G. (1981) *Biochemistry* **20**, 7174-7182.

Brzozowski, A. M., Derewenda, U., Derewenda, Z. S., Dodson, G. G., Lawson, D. M., Turkenburg, J. P., Bjorkling, F., Huge-Jensen, B., Patkar, S. A., and Thim, L. (1991) *Nature* **351**, 491-494.

Buerkler, J., and Krebs, J. (1985) *FEBS Letters* **182**, 167-170.

Burn, P.; (1988) *Trends Biochem. Sci.* **13,** 79-83.

Carman, G. M., and Henry, S. H. (1989) *Ann. Rev. Biochem.* **58**, 635-669.

Casey, P. J. (1995) *Science* **268**, 221-224.

Chang, C. T., Wu, C-S. C., and Yang, J. T. (1978) *Anal. Biochem.* **91**, 13-31.

Chen, Y-H., Yang, J. T., and Chau, K. H. (1974) *Biochemistry* **13**, 3350-3359.

Chou, P. Y., and Fasman, G. D. (1978) *Ann. Rev. Biochem.* **47**, 251-276.

Choy, P. C., and Vance, D. E. (1976) *Biochem. Biophys. Res. Comm.* **72**, 714-719.

Choy, P. C., Lim, P.H. and Vance, D. E. (1977) *J. Biol. Chem.* **252**, 7673-7677.

Choy, P. C., and Vance, D. E. (1978) *J. Biol. Chem.* **253**, 5163-5167.

Choy, P. C. and Arthur, G. (1989) in *Phosphatidylcholine metabolism* (ed. D. E. Vance) CRC Press, Boca Raton, Florida. pp. 87-101.

Choy, P.C., Farren, S.B., and Vance, D. E. (1979) *Can. J. Biochem.* **57**, 605-612.

Chung, L. A., Lear, J. D., and DeGrado, W. F. (1992) *Biochemistry* **31**, 6608-6616.

Clague, M. J., Knutson, J. R., Blumenthal, R., and Herrmann, A. (1991) *Biochemistry* **30**, 5491-5497.

Clark-Lewis, I., Moser, B., Walz, A., Baggiolini, M., Scott, G. J., and Aebersold, R. (1991) *Biochemistry* **30**, 3128-3135.

Cornell, R., B., and Goldfine, H. (1983) *Biochim. Biophys. Acta*, **750**, 504-520.

Cornell, R., and Vance, D. E. (1987a) *Biochim. Biophys. Acta*, **919**, 26-36.

Cornell, R., and Vance, D. E. (1987b) *Biochim. Biophys. Acta*, **919**, 37-48.

Cornell, R. (1989a) in *Phosphatidylcholine metabolism* (ed. D. E. Vance) CRC Press, Boca Raton, Florida. pp. 47-64.

Cornell, R. (1989b) *J. Biol. Chem.* **264**, 9077-9082.

Cornell, R. B. (1991a) *Biochemistry* **30**, 5873-5880.

Cornell, R. B. (1991b) *Biochemistry* **30**, 5881-5888.

Cornell, R. B., Kalmar, G. B., Kay, R. J., Johnson, M. A., Sanghera, J. S., and Pelech, S. P (1995) *Biochem. J.* **310**, 699-708.

Craig, L., Johnson, J. E., and Cornell, R. B. (1994) *J. Biol. Chem.* **269**, 3311-3317.

De Boek, H., and Zidovetzki, R. (1989) *Biochemistry* **28**, 7439-7446.

Dufourcq, J., and Faucon, J-F. (1977) *Biochim. Biophys. Acta.* **467**, 1-11.

Eftink, M. R. (1991) in *Biophysical and Biochemical Aspects of Fluorescence Spectroscopy* (Dewey, T. G. ed.) Plenum Press, New York, NY.

Epand, R. M., Gawish, A., Iqbal, M., Gupta, K. B., Chen, G. H., Segrest, J. P., and Anantharamaiah, G. M. (1987) *J. Biol. Chem.* **262**, 9389-9396.

Epand, R. M., Shai, Y., Segrest, J. P., and Anantharamaiah, G. M. (1995) *Biopolymers (Peptide Science)* **37**, 319-338.

Esko, J. D., and Raetz, C. R. H. (1980) *Proc. Natl. Acad. Sci.* **77**, 5192-5196.

Esko, J. D., Nishijima, M., and Raetz, C. R. H. (1982) *Proc. Natl. Acad. Sci.* **79**, 1698-1702.

Exton, J. H. (1990) *J. Biol. Chem.* **265**, 1-4.

Exton, J. H. (1994) *Biochim. Biophys. Acta* **1212**, 26-42.

Feldman, D. A., Kovac, C. R., Dranginis, P. L., and Weinhold, P. A. (1978) *J. Biol. Chem.* **253**, 4980-4986.

Feldman, D. A., Brubaker, P. G. and Weinhold, P. A. (1981) *Biochim. Biophys. Acta.* **665**, 53-59.

Feldman, D. A., Rounsifer, M. E., and Weinhold, P. A. (1985) *Biochim. Biophys. Acta*, **833**, 429-437.

Feldman, D. A., and Weinhold, P. A. (1987) *J. Biol. Chem.* **262**, 9075-9081.

Filoteo, A. G., Enyedi, A., and Penniston, J. T. (1992) *J. Biol. Chem.* **267**, 11800-11805.

Fiscus, W. G., and Schneider, W. C. (1966) *J. Biol. Chem.* **241**, 3324-3330.

Frey, A. B., Kreibich, G., Wadhera, A., Clarke, L., and Waxman, D. J. (1986) *Biochemistry* **25**, 4797-4803.

Fulmer, J. D., and Crystal, R. G. (1976) in *The Biochemical Basis of Pulmonary Function* (ed. R. G. Crystal) Marcel Dekker Inc., New York, NY. pp. 435-436.

Garnier, J., Osguthorpe, D. J., and Robson, B. (1978) *J. Mol. Biol.* **120**, 97-120.

Gennis, R.B. (1989) in *Biomembranes: molecular structure and function.* (ed. Gennis, R.B., Cantor, C.R.) Springer-Verlag, New York Inc. p. 21.

Gluzman, Y. (1981) *Cell* **23**, 175-182.

Grabau, C., Chang, Y., and Cronan, J. E. (1989) *J. Biol. Chem.* **264**, 12510-12519.

Grabau, C., and Cronan, J.E. (1986) *Biochemistry* **25**, 3748-

Grabau, C., Chang, Y., and Cronan, J.E. (1989) *J. Biol. Chem.* **264**, 12510-12519.

Greenfield, N., and Fasman, G. D. (1969) *Biochemistry* **8**, 4108-4116.

Hamilton, S.E., Recny, M., and Hager, L.P. (1986) *Biochemistry* **25**, 8178-8183.

Harter, C., Bachi, T., Semenza, G., and Brunner, J. (1988) *Biochemistry* **27**, 1856-1864.

Harter, C., James, P., Bachi, T., Semenza, G., and Brunner, J. (1989) *J. Biol. Chem.* **264**, 6459-6464.

Hatch, G. M., Lam, T-S., Tsukitani, Y., and Vance, D. E. (1990) *Biochim. Biophys. Acta.* **1042**, 374-379.

Hatch, G. M., Tsukitani, Y., and Vance, D. E. (1991) *Biochim. Biophys. Acta.* **1081**, 25-32.

Hatch, G. H., Jamil, H., Utal, A.K., and Vance, D. E. (1992) *J. Biol. Chem.* **267**, 15751-15758.

Hoppe, J., Brunner, J., and Jorgensen, B.B. (1984) *Biochemistry* **23**, 5610-5616.

Houweling, M., Jamil, H., Hatch, G., and Vance, D. E. (1994) *J. Biol. Chem.* **269,** 7544-7551.

Ishdate, K. (1989) in *Phosphatidylcholine metabolism* (ed. D. E. Vance) CRC Press, Boca Raton, Florida. pp. 9-32.

Jackowski, S. (1994) *J. Biol. Chem.* **269**, 3858-3867.

Jacobson, G. R., Schaffer, M. H., Stark, G. R., and Vanaman, T. C. (1973) *J. Biol. Chem.* **248**, 6583-6591.

Jamil, H., Hatch, G. M., and Vance, D. E. (1993) *Biochem. J.* **291**, 419-427.

Jamil, H., Yao, Z., and Vance, D. E. (1990) *J. Biol. Chem.* **265**, 4332-4339.

Jamil, H., Utal, A. K., and Vance, D. E. (1992) *J. Biol. Chem.* **267**, 1752-1760.

Johnson, J. E., Kalmar, G. B., Sohal, P. S., Walkey, C. J., Yamashita, S., and Cornell, R. B. (1992) *Biochem. J.* **285**, 815-820.

Johnson, J.E, and Cornell, R.B. (1994) *Biochemistry* **33**, 4327-4335.

Kaiser, E. T., and Kezdy, F. J. (1984) *Science* **223**, 249-255.

Kalmar, G. B., Kay, R.J., LaChance, A. C., and Cornell, R. B. (1994) *Biochim. Biophys. Acta* **1219**, 328-334.

Kalmar, G. B., Kay, R. ., Lachance, A., Aebersold, R., and Cornell, R. B. (1990) *Proc. Natl. Acad. Sci.* **87**, 6029-6033.

Kanellis, P., Romans, A. Y., Johnson, B. J., Kercret, H., Chiovetti, R. Jr., Allen, T. M., and Segrest, J. P. (1980) *J. Biol. Chem.* **255**, 11464-11472.

Kay, R., and Humphries, R. H. (1991) *Meth. Mol. Cell Biol.* **2**, 254-265.

Kennedy, E. P. (1989) in *Phosphatidylcholine metabolism* (ed. D. E. Vance) CRC Press, Boca Raton, Florida. pp. 1-8.

Kent, C. (1990) *Prog. Lipid Res.* **29**, 87-105.

Kent, C. (1979) *Proc. Natl. Acad. Sci.* **76**, 4474-4478.

Killian, J. A., Keller, R. C. A., Struyve, M., de Kroon, A. I. P. M., Tommassen, J., and de Kruijff B. (1990) *Biochemistry* **29**, 8131-8137.

Kolesnick, R. N., and Hemer, M. R. (1990) *J. Biol. Chem.* **265**, 10900-10904.

Kostner, G. M. (1981) in *High Density Lipoproteins.* (ed. C. E. Day) Dekker Inc., New York, NY. pp. 1-26.

Krebs, J., Buerkler, J., Guerini, D., Brunner, J., and Carafoli, E. (1984) *Biochemistry* **23**, 400-403.

Laemmli, U. K. (1970) *Nature* **227**, 680-685.

Lakowicz, J. R. (1983) *Principles of Fluorescence Spectroscopy* Plenum Press, New York, NY.

Lear, J. D., and DeGrado, W. F. (1987) *J. Biol. Chem.* **262,** 6500-6505.

Leenhouts., J. M., van den Wijngaard, P. W. J., de Kroon, A. I. P. M., and de Kruijff, B. (1995) *FEBS Letters* **370**, 189-192.

Li, M., Keddie, J.S., Smith, L.J., Clark, D.C., and Murphy, D.J. (1993) *J. Biol. Chem.* **268**, 17504-17512.

Lim, P., Cornell, R., and Vance, D. E. (1986) *Biochem. Cell Biol.* **64**, 692-697.

Lim, P. H., Pritchard, P. H., Paddon, H. B., and Vance, D.E. (1983) *Biochim. Biophys. Acta* **753**, 74-82.

Liscovitch, M. (1992) *Trends Biochem. Sci.* **17**, 393-399.

MacDonald, J. I. S., and Kent, C. (1993) *Prot. Express. Purif.* **4**, 1-7.

MacDonald, J. I. S., and Kent, C. (1994) *J. Biol. Chem.* **269**, 10529-10537.

Mao, S.J.T., Sparrow, J.T., Gilliam, E.B., Gotto, A.M., and Jackson, R.L. (1977) *Biochemistry* **16**, 4150-4156.

Mauel, C., Young, M., and Karamata, D. (1991) *J. Gen. Microbiol.* **137**, 929-941.

McIntosh, T. J., and Holloway, P. W. (1987) *Biochemistry* **26**, 1783-1788.

McGee, T. P., Skinner, H. B., Whitters, E. A., Henry, S. A., and Bankaitis, V. A. (1994) *J. Cell Biol.* **124**, 273-287.

McKnight, C. J., Rafalski, M., and Gierasch, L. M. (1991) *Biochemistry* **30**, 6241-6246.

McMaster, C. R., and Bell, R. M. (1994) *J. Biol. Chem.* **269**, 14776-14783.

Meister, H., Bachofen, R., Semanza, G., and Brunner, J. (1985) *J. Biol. Chem.* **260**, 16326-16331.

Menashe, M., Romero, F., Biltonen, R. L., and Lichtenberg, D. (1986) *J. Biol. Chem.* **261**, 5328-5333.

Mishra, V. K., Palgunachari, M. N., Segrest, J.P., and Anantharamaiah, G. M. (1994) *J. Biol. Chem.* **269**, 7185-7191.

Morand, J. N., and Kent, C. (1989) *J. Biol. Chem.* **264**, 13785-13792.

Morash, S., Cook, H., and Spence, M. (1988) *Biochim. Biophys. Acta* **961**, 194-202.

Myher, J., and Kuksis, A. (1979) *Can. J. Biochem.* **57**, 117-124.

Newton, A. C. (1993) *Ann. Rev. Biophys. Biomol. Structure* **22**, 1-25.

Nikawa, J., Yonemura, K., and Yamashita, S. (1983) *Eur. J. Biochem.* **131**, 223-229.

Niles, R. M., and Makarski, J. S. (1979) *J. Biol. Chem.* **254**, 4324-4326.

Orr, J. W., Keranen, L. M., and Newton, A. C. (1992) *J. Biol. Chem.* **267**, 15263-15266.

Paddon, H. B., and Vance, D. E. (1980) *Biochim. Biophys. Acta* **620**, 636-640.

Park, Y. S., Sweitzer, T. D., Dixon, J. E., and Kent, C. (1993) *J. Biol. Chem.* **268**, 16648-16654.

Pelech, S. L., and Vance, D. E. (1989) *Trends Biochem. Sci.* **14**, 28-30.

Pelech, S. L., Pritchard, P. H., and Vance, D. E. (1982) *Biochim. Biophys. Acta*, **713**, 260-269.

Pelech, S. L., and Vance, D. E. (1982) *J. Biol. Chem.* **257**, 14198-14202.

Pelech, S. L., Pritchard, H., Brindley, D. N., and Vance, D. E. (1983) *J. Biol. Chem.* **258**, 6782-6788.

Pelech, S. L., Pritchard, P. H., and Vance, D. E. (1981) *J. Biol. Chem.* **256**, 8283-8386.

Pelech, S. L., Paddon, H. B., and Vance, D. E. (1984a) *Biochim. Biophys. Acta* **795**, 447-451.

Pelech, S. L., Cook, H. W., Paddon, H. B., and Vance, D. E. (1984b) *Biochim. Biophys. Acta*, **795**, 433-440.

Picot, D., Loll, P.J., and Garavito, R.M. (1994) *Nature* **367**, 243-249.

Possmayer, F. (1989) in *Phosphatidylcholine metabolism* (ed. D. E. Vance) CRC Press, Boca Raton, Florida. pp. 205-223.

Post, M., Batenburg, J., Schuurmans, E., and Van Golde, L. M. (1982) *Biochim. Biophys. Acta* **712**, 390-394.

Pritchard, P. H., Chiang, P. K., Cantoni, G. L., and Vance, D. E. (1982) *J. Biol. Chem.* **257**, 6362-6367.

Rao, N. M., and Sundaram, C. S. (1993) *Biochemistry* **32**, 8547-8552.

Rebecchi, M., Peterson, A., and McLaughlin, S. (1992) *Biochemistry* **31**, 12742-12747.

Recny, M., Grabau, C., Cronan, J.E., and Hager, L.P. (1985) *J. Biol. Chem.* **260**, 14287-14291.

Ridgeway, N. D. (1989) in *Phosphatidylcholine metabolism* (ed. D. E. Vance) CRC Press, Boca Raton, Florida. pp. 103-120.

Roberts, M. F., and Dennis, E. A. (1989) in *Phosphatidylcholine metabolism* (ed. D.E. Vance) CRC Press, Boca Raton, Florida. pp. 121-142.

Roth, M. (1971) *Anal. Chem.* **43**, 880-882.

Rozek, A., Buchko, G.W., and Cushley, R.J. (1995) *Biochemistry* **34**, 7401-7408.

Rutherford, M. S., Rock, C. O., Jenkins, N. A., Gilbert, D. J., Tessner, T. G., Copeland, N. G., and Jackowski, S. (1993) *Genomics* **18**, 693-701.

Schagger, H., and von Jagow, G. (1987) *Anal. Biochem.* **166**, 368-379.

Scheiber, W., Jahn, R., Doucet, J-P., Rothlein, J., and Greengard, P. (1986) *J. Biol. Chem.* **261**, 8383-8390.

Schneider, W. C. (1963) *J. Biol. Chem.* **238**, 3572.

Segrest, J. P., deLoof, H., Dahlman, J. G., Brouillette, C. G. and Anantharamaiah, G. M. (1990) *Proteins: Structure, Function, and Genetics* **8**, 103-117.

Segrest, J. P., Jackson, R. L., Morrisett, J. D., and Gotto., A. M. (1974) *FEBS Letters* **38**, 247-253.

Segrest, J. P., Jones, M. K., De Loof, H., Broulillette, C. G., Venkatachalapathi, Y., V., and Anantharamaiah, G., M. (1992) *J. Lipid Res.* **33**, 141-166.

Segrest, J. P., Garber, D. W., Brouillette, C. G., Harvey, S. C., and Anantharamaiah, G. M. (1994) *Adv. in Protein Chem.* **45**, 303-369.

Seto-Young, D., Monk, B. C., and Perlin, D. S. (1992) *Biochim. Biophys. Acta* **1102**, 213-219.

Skinner, H. B., McGee, T. P., McMaster, C. R., Fry, M. F., Bell, R. M., and Bankaitis, V. A. (1995) *Proc. Natl. Acad. Sci.* **92**, 112-116.

Slack, B. E., Breu, J., and Wurtman, R. J. (1991) *J. Biol. Chem.* **266**, 24503-24508.

Sleight, R., and Kent, C. (1980) *J. Biol. Chem.* **255**, 10644-10650.

Sleight, R., and Kent, C. (1983a) *J. Biol. Chem.* **258**, 824-830.

Sleight, R., and Kent, C. (1983b) *J. Biol. Chem.* **258**, 831-835.

Sleight, R., and Kent, C. (1983c) *J. Biol. Chem.* **258**, 836-839.

Sohal, P. S., and Cornell, R. B. (1990) *J. Biol. Chem.* **265**, 11746-11750.

Sonnichsen, F. D., Van Eyk, J. E., Hodges, R. S., and Sykes, B. D. (1992) *Biochemistry* **31**, 8790-8798.

Sparrow, J.T., Sparrow, D.A., Culwell, A.R., and Gotto, A.M. (1985) *Biochemistry* **24**, 6984-6988.

Sparrow, J.T., Sparrow, D.A., Fernando, G., Culwell, A.R., Kovar, M., and Gotto, A.M. (1992) *Biochemistry* **31**, 1065-1068.

Stern, W., Kovac, C., and Weinhold, P. A. (1976) *Biochim. Biophys. Acta* **441**, 280-293.

Summers, M. D., and Smith, G. E. (1987) *A Manual of Methods for Baculovirus Vectors and Insect Cell Culture Procedures* Texas Agricultural Experimental Station Bulletin No. 1555.

Sundler, R., and Akesson, B. (1975) *J. Biol. Chem.* **250**, 3359-3367.

Sweitzer, T. D., and Kent, C. (1994) *Arch. Biochem. Biophys.* **311**, 107-116.

Teegarden, D., Taparowsky, E. J., and Kent, C. (1990) *J. Biol. Chem.* **265**, 6042-6047.

Tercé, F., Brun, H., and Vance, D. E. (1994) *J. Lipid Res.* **35**, 2130-2142.

Tercé, F., Record, M., Chap, H., and Douste-Blazy, L. (1988) *J. Biol. Chem.* **263**, 3142-3149.

Terwilliger, T. C., Weissman, L., and Eisenberg., D. (1982) *Biophys. J.* **37**, 353-361.

Tronchère, H., Planat, V., Record, M., Tercé, F., Ribbes, G., and Chap, H. (1995) *J. Biol. Chem.* **270**, 13138-13146.

Tronchère H., Tercé, F., Record, M., Ribbes, G., and Chap, H. (1991) *Biochem. Biophys. Res. Comm.* **176**, 157-165.

Tsukagoshi, Y., Nikawa, J., and Yamashita, S. (1987) *Eur. J. Biochem.* **169**, 477-486.

Tsukagoshi, Y., Nikawa, J., Hosaka, K., and Yamashita, S. (1991) *J. Bacteriol.* **173**, 2134-2136.

Ulbrandt, N. D., London, E., and Oliver, D. B. (1992) *J. Biol. Chem.* **267**, 15184-15192.

Utal, A. K., Jamil, H., and Vance, D E. (1991) *J. Biol. Chem.* **266**, 24084-24091.

Van Ceunebroeck, J. C. L., Krebs, J., Hanssens, I., and Van Cauwelaert, F. (1986) *Biochem. Biophys. Res. Comm.* **138**, 604-610.

van Tilbeurgh, H., Sarda, L., Verger, R., and Cambillau, C. (1992) *Nature* **359**, 159-162.

Vance, D. E., and Choy, P. C. (1979) *Trends Biochem. Sci.* **4**, 145-148.

Vance, D. E., Trip, E. M., and Paddon, H. B. (1980) *J. Biol. Chem.* **255**, 1064-1069.

Vance, D. E., and Pelech, S. L. (1984) *Trends Biochem. Sci.* **9**, 17-20.

Vance, D. E., Choy, P. C., Farren, S. B., Lim, P. H., and Schneider, W. J. (1977) *Nature* **270,** 268-269.

Vance, J. E., and Vance, D. E. (1988) *J. Biol. Chem.* **263**, 5898-5909.

Veitch, D. P., and Cornell, R. B. (1994) *Protein Sci.* **3** (1), 120M.

Walkey, C. J., Kalmar, G. B., and Cornell, R. B. (1994) *J. Biol. Chem.* **269**, 5742-5749.

Wang, Y., and Kent, C. (1995a) *J. Biol. Chem.* **270**, 17843-17849.

Wang, Y., and Kent, C. (1995b) *J. Biol. Chem.* **270**, 18948-18952.

Wang, Y., MacDonald, J. I. S., and Kent, C. (1995) *J. Biol. Chem.* **270**, 354-360.

Wang, Y., MacDonald, J. I. S., and Kent, C. (1993a) *J. Biol. Chem.* **268**, 5512-5518.

Wang, Y., Sweitzer, T. D., Weinhold, P. A., and Kent, C. (1993b) *J. Biol. Chem.* **268**, 5899-5904.

Watkins, J. D., and Kent, C. (1990) *J. Biol. Chem.* **265**, 2190-2197.

Watkins, J. D., and Kent, C. (1991) *J. Biol. Chem.* **266**, 21113-21117.

Watkins, J. D., and Kent, C. (1992) *J. Biol. Chem.* **267**, 5686-5692.

Wedegaertner, P. B., Wilson, P. T., Bourne, H. R. (1995) *J. Biol. Chem.* **270**, 503-506.

Weinhold, P. A., Rounsifer, M. E., Feldman, D. A. (1986) *J. Biol. Chem.* **261**, 5104-5110.

Weinhold, P. A., Skinner, R. S., and Sanders, R. D. (1973) *Biochim. Biophys. Acta* **326**, 43-51.

Weinhold, P. A., Charles, L., Feldman, D. A. (1994) *Biochim. Biophys. Acta* **1210**, 335-347.

Weinhold, P. A., Feldman, D. A., Quade, M. M. Miller, J. C., and Brooks, R. L. (1981) *Biochim. Biophys. Acta* **665**, 134-144.

Weinhold, P. A., Charles, L., Rounsifer, M. E., and Feldman, D. A. (1991) *J. Biol. Chem.* **266**, 6093-6100.

Weinhold, P. A., Rounsifer, M. E., Williams, S. E., Brubaker, P. G., and Feldman, D. A. (1984) *J. Biol. Chem.* **259**, 10315-10321.

Weinhold, P. A., Rounsifer, M. E., Charles, L., and Feldman, D. A. (1989) *Biochim. Biophys. Acta* **1006**, 299-310.

Wetterau, J. R., and Jonas, A. (1982) *J. Biol. Chem.* **257**, 10961-10966.

Whitlon, D.S., Anderson, K. E., and Mueller, G. C. (1985) *Biochim. Biophys. Acta* **835**, 369-377.

Wieder, T., Geilen, C.C., Wieprecht, M., Becker, A., and Orfanos, C. (1994) *FEBS Letters* **345**, 207-210.

Wiener, M. C., and White, S. H. (1991) *Biochemistry* **30**, 6997-7008.

Wilson, J. E. (1978) *Trends Biochem. Sci.* **3**, 124-125.

Wright, P.S., Morand, J.N., and Kent, C. (1985) *J. Biol. Chem.* **260**, 7919-7926.

Yang, W., and Jackowski, S. (1995) *J. Biol. Chem.* **270**, 16503-16506.

Yang, W., Boggs, K.P. and Jackowski, S. (1995) *J. Biol. Chem.* **270**, 23951-23957.

Yao, Z., Jamil, H., and Vance, D.E. (1990) *J. Biol. Chem.* **265**, 4326-4331.

Yoshimura, T., Goto, Y., and Aimoto, S. (1992) *Biochemistry* **31**, 6119-6126.

Yu, S., Harding, P.G.R., Smith, N., and Possmayer, F. (1983) *Lipids* **18**, 522-529.

Zhang, T., and Hager, L.P. (1987) *Arch. Biochem. Biophys.* **255**, 201-204.